Alpha Decay of Superheavy Nuclei with $104 \leq Z \leq 125$

By

MALATHI S

(Reg. No. 21PPH007)

Supervisor

Dr. N. S. Rajeswari

Department of Physics

A Thesis submitted to

Avinashilingam Institute for Home science and Higher Education for Women, Coimbatore- 641043

In partial fulfilment of the requirements for the degree of

MASTER OF SCIENCE IN PHYSICS

MAY 2023

Alpha Decay of Superheavy Nuclei with $104 \leq Z \leq 125$

By

MALATHI S

(Reg. No 21PPH007)

Supervisor

Dr. N. S. Rajeswari

Department of Physics

A Thesis submitted to

Avinashilingam Institute for Home science and Higher Education for Women, Coimbatore- 641043

In partial fulfilment of the requirements for the degree of

MASTER OF SCIENCE IN PHYSICS

MAY 2023

CERTIFIED AS A BONAFIDE RESEARCH WORK

12/05/23

Signature of Head of the Department

Dr. J. SHANTHI, M.Sc., M.Phil., Ph.D.,
Professor and Head
Department of Physics
Avinashilingam Institute for Home Science
and Higher Education For Women
Coimbatore - 641 043.

12/05/2023

Signature of the Supervisor

ACKNOWLEDGEMENT

I owe my sincere thanks to the Lord Almighty and My Parents without whom I would have been nothing and showering their blessings upon me in all my endeavours.

I wish to express my deep sense of reverential gratitude to **Prof. S. P. Thyagarajan**, Chancellor, Avinashilingam Institute for Home Science and Higher Education for Women, Coimbatore for all the good wishes towards the completion of the study.

I extend my sincere thanks to **Dr. (Mrs.) V.Bharathi Harishankar** Chancellor, Avinashilingam Institute for Home Science and Higher Education for Women, Coimbatore for her encouragement towards the academic performance.

I wish to express my deep sense of gratitude to **Dr.(Mrs.) S.Kowsalya**, Registrar, Avinashilingam Institute for Home Science and Higher Education for Women, Coimbatore for her moral support and help for my study.

I wish to express my gratitude to **Dr.(Mrs.) G.Padmavathi**, Dean, School of Physical Sciences and Computational Sciences, Avinashilingam Institute for Home Science and Higher Education for Women, Coimbatore for her positive advice and generous help.

I wish to express my deep sense of gratitude to **Dr.(Mrs.) J.Shanthi**, Professor and Head, Department of Physics, Avinashilingam Institute for Home Science and Higher Education for Women, Coimbatore for her encouragement to complete my study.

I express my sincere gratitude to my guide **Dr.(Mrs.) N.S.Rajeswari**, Assistant Professor, Department of Physics, Avinashilingam Institute for Home Science and Higher Education for Women, Coimbatore for her excellent guidance, constant encouragement, valuable advice and moral support throughout the study.

I sincerely thank **all other staff members** of the **Department of Physics**, Avinashilingam Institute for Home Science and Higher Education for Women, Coimbatore for being supportive on all our activities.

I am thankful to Research Scholar **Ms. P. Mehana** for her constant support for successfully completing the project work.

I would like to express my thanks to **all my friends** and **my family members** for their support throughout my study and help in carrying out this work successfully.

CONTENTS

LIST OF FIGURES

LIST OF TABLES

CHAPTER I

INTRODUCTION

1.1 Introduction

Henri Becquerel discovered radioactivity in 1896, after he got interested in the discovery of X-rays by Roentgen in 1895. So he began the investigation of fluorescent materials. He took potassium uranyl sulfate and placed it on black paper wrapped with a photographic plate. Then he exposed it to sunlight and developed the photographic plate. He saw the darkened in a photographic plate and found that the Uranium salt emitted radiations that could penetrate the black paper. He thought that the sunlight was the reason for uranium radiation to conform to this, he repeated the experiment on 26 Feb 1896. Due to the climate (cloudy), he put the covered uranium sulfate placed on the photographic plate in his drawer. A few days after, he developed the photographic plate and saw the dark in the photographic plate. Initially, Becquerel thought radiations from Uranium (Becquerel rays) were similar to x-rays, and after further experiments, he concluded that the invisible rays are emitted spontaneously and are different from x-rays that are produced by x-ray tubes under special conditions **[1,2]**

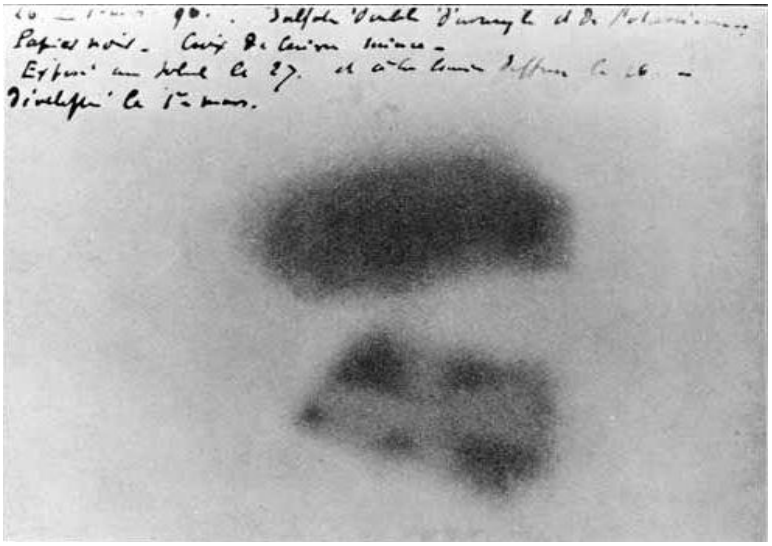

Fig. 1.1 The image obtained while Becquerel using Uranium salt

In Becquerel Laboratory, based on experiments, Marie Curie found thorium salts emit the Becquerel rays, and she also discovered that pitchblende, the ore from which uranium is extracted, emits Becquerel rays with a much stronger intensity than Uranium. In 1898 Marie Curie and her husband, Pierre Curie, discovered two new elements, polonium and radium; from the laborious process of chemical separation Radium is million times more radioactive than uranium. Marie Curie got the Nobel Prize for the discovery of Radium. Radioactive elements are unstable nuclei. They become more stable when the nuclei undergo radioactive decay. In this process, the nuclei give off energy and may emit charged particles of matter.

In 1899, Rutherford discovered two types of radiation such as α rays and β rays, from radioactive material, which are different in their penetrating powers. Villard discovered a third type of radiation which is called gamma-ray. The gamma rays could not be deflected in a magnetic field and affect the photographic plate. The radiations emitted from radioactive sources are known as Becquerel rays **[3]**.

1.2 Nuclear stability

"Nuclear stability denotes that the nucleus of an element is stable and thus it does not decay spontaneously emitting any kind of radioactivity." The nucleus of an atom is extremely small. The radius of the nucleus is around 10^{-15} m. Protons and neutrons are trapped together in such a short space. Because protons are positively charged, they should be repelled; however, the majority of nuclei are stable, indicating that there must be some factors that affect nuclear stability. Some of the factors affecting nuclear stability are as follows: **[4]**

- Binding energy.
- The neutron-to-protonn ratio (N/Z ratio).
- Odd and even number of nucleons.
- Magic Numbers

1.2.1 Binding energy

Mass defect refers to the difference between the calculated mass due to nucleons and the actual observed isotopic mass of the nucleus. " Δm " stands for "mass defect." Consider an Isotope ${}_{Z}X^{A}$. Let A be the mass number, and Z be the atomic number of the element. If the masses of a proton, electron, and neutron are m_p, m_e, and m_n, respectively. $\mathbf{M_i}$ is the observed mass of the Isotope, and $\mathbf{M_{cal} (= Zm_p + Nm_n)}$ is the calculated mass of the Isotope, thus

$$\textbf{Mass defect } (\Delta m) = \textbf{ Calculated mass } - \textbf{ observed mass}$$

$$\Delta m = [\, Zm_p + Nm_n] \; - \; M_i$$

mass of an electron is negligible. Hence it is not considered for the calculation of mass defect. The mass equivalent of mass defect is converted into energy which is given by Einstein's energy equation, $\mathbf{E = \Delta m \times C^2}$. This energy is called nuclear binding energy.

$$BE = \{(Zm_p + Nm_n) - M_i\}c^2$$

Nuclear binding energy is the amount of energy required for dividing the nucleus into its individual nucleons, which is equivalent to mass defect. It is represented by E and is measured in joules or million electron volts (MeV). If Binding Energy is greater than Zero, the nucleus is stable. If Binding Energy is less than zero, the nucleus is unstable **[5]**.

The nucleons are held in the nucleus by binding energy. Nuclear stability is proportional to the nuclear binding energy. The more binding energy, the greater the nuclear stability. A curve can be drawn by plotting the binding energy per nucleon in MeV versus the mass numbers (A) for various nuclei. The curve is called the **binding energy curve**. This curve represents the relative stability of the nuclei of the elements **[4,5]**.

1.2.2 Neutron to proton ratio

The neutron-to-proton ratio is the most important factor in deciding when a nucleus is stable. The nuclei of elements with (Z<20) are smaller, and their nuclei have a ratio of 1:1 preferring to have an equal number of protons and neutrons. Heavy atoms have a different ratio than light elements with atomic numbers ranging from 20 to 83. The difference between the ratios is the repulsive force between protons: the more significant the repulsive force is, the greater the neutrons needed to stabilize the nuclei.

1.2.3 Number of nucleons

The number of nucleons in a nuclear atom determines its stability There is no stable nucleus greater than lead-208. This is because, despite being 100 times stronger proton repulsions, the strong nuclear force only works over relatively small distances **[6]**.

1.2.4 Magic numbers

A **Magic number** is a number of nucleons either protons or neutrons, separately such that they are arranged into complete shells within the atomic nucleus. As a result, atomic nuclei with a 'magic' number of protons or neutrons are much more stable than other nuclei. The seven most widely recognized magic numbers are **2, 8, 20, 28, 50, 82, and 126**. All the stable elements at the end of the decay series have a magic number of protons and neutrons. For example, the nuclei of O-16, He-4, and the Pb-208, having 126 neutrons and 82 protons, contain a magic number of protons and neutrons, equally stable **[7]**.

1.3 Radioactivity

Radioactivity is the spontaneous emission of radiation of particles or high energy photons resulting from a nuclear reaction. The process by which the nucleus of an unstable atom loses energy by emitting radiation such as alpha particles, beta particles, and gamma rays is known as radioactivity**.** It is also known as radioactive decay, nuclear decay, nuclear disintegration, or radioactive disintegration. There are many forms of electromagnetic radiation, but they are not always produced by radioactivity. For example, a light bulb may emit radiation in the forms of heat and light, yet it is not radioactive. A substance that contains unstable atomic nuclei is considered to be radioactive **[8]**.

1.3.1 Natural radioactivity

The elements with a mass number greater than 200 are generally called unstable nuclei. Among the elements in the periodic table, there are three naturally occurring radioactive series. These are known as the uranium, actinium, and thorium series. Each series decays through several unstable nuclei by alpha and beta emission until it reaches a stable lead isotope.

1.3.2 Artificial or Induced radioactivity

Irene Curie and F. Joliot discovered artificial radioactivity or induced radioactivity in 1934. This is also referred to as man-made radioactivity. Artificial radioactivity is the process by which even light elements turn radioactive by artificial or induced methods. Curie and Joliot showed that when lighter elements like boron and aluminum were bombarded with -particles, they continued to emit radioactive radiations even after the alpha source was removed. They showed that the radiation was caused by the emission of a particle with one unit of positive charge and the mass of an electron. This particle is known as a positron and the reaction is

$$_5B^{10} + _2He^4 \rightarrow _7N^{13*} + _0n^1$$

The nitrogen atom is radioactive and decays with a half-life of about 10.1 minutes into a stable isotope of carbon with the emission of a positron **[9]**

$$_7N^{13*} \rightarrow _6C^{13} + _1e^0$$

1.4 Units of radioactivity

SI Unit of Radioactivity is Becquerel. The definition of Becquerel is one disintegration per second. In the laboratory, to measure the convenient size of Radioactive sources, kilo becquerels, and mega becquerels are used. Radioactivity is also measured by Curie. The definition of curie is 3.7×10^{10} disintegration per second. Curie is represented by Ci. For laboratory scale, radioisotope sources are also measured in millicurie and microcurie. One Becquerel is equal to 2.703×10^{-11} Curie ($1Bq = 2.703 \times 10^{-11}$ Ci). Another unit of radioactivity is Rutherford and Roentgen.

1.5 Law of radioactive disintegration

In 1902, Rutherford and Soddy established this law experimentally in Great Britain. According to them, when a radioactive material decays, it is independent of chemical and physical properties and dependent on the number of atoms present at that time. The number of atoms present changes while disintegration takes place continuously. Hence the rate of disintegration will change with time.

The law states that "The rate of radioactive decay of an atom at a given time is directly proportional to the number of nuclei of the elements present at that time." Let N be the number of atoms present in a particular radio element at a given instant time t. The number of dN that will decay during the interval dt (from t to t+dt) must be proportional to N and also proportional to dt.

$$dN \ \alpha \ Ndt$$

$$dN = -\lambda Ndt$$

where λ is a decay constant or disintegration constant of a radioactive element, and the negative sign represents the number of atoms of the radioactive element decreases with respect to time **[10,11]**.

1.5.1 Half-life

The time in which half of the original nuclei decay into daughter nuclei is called the half-life period. $T_{1/2}$ denotes the half-life period. After two half-lives, there will be one-fourth of the originals left. After three half-lives, one-eighth of the original sample is left, and so on.

1.6 Types of radioactive decay

Radioactive decay is classified on its properties. There are three basic types of radioactive decay.

1. Alpha decay
2. Beta decay
3. Gamma decay

1.6.1 Alpha decay

In alpha decay, an atom spontaneously releases a fast-moving particle, and that particle is composed of two protons and two neutrons. An alpha particle is a helium atom with two protons and two neutrons in its nucleus. After an alpha decays, the parent atom loses two protons, so the product that is the daughter atom has to drop back two places in the periodic table. Alpha particles carry a lot of energy, which is converted to heat as the particles collide with their surroundings **[12]**.

$$_{94}Pu^{240} \rightarrow {}_{2}He^{4} + {}_{92}U^{236}$$

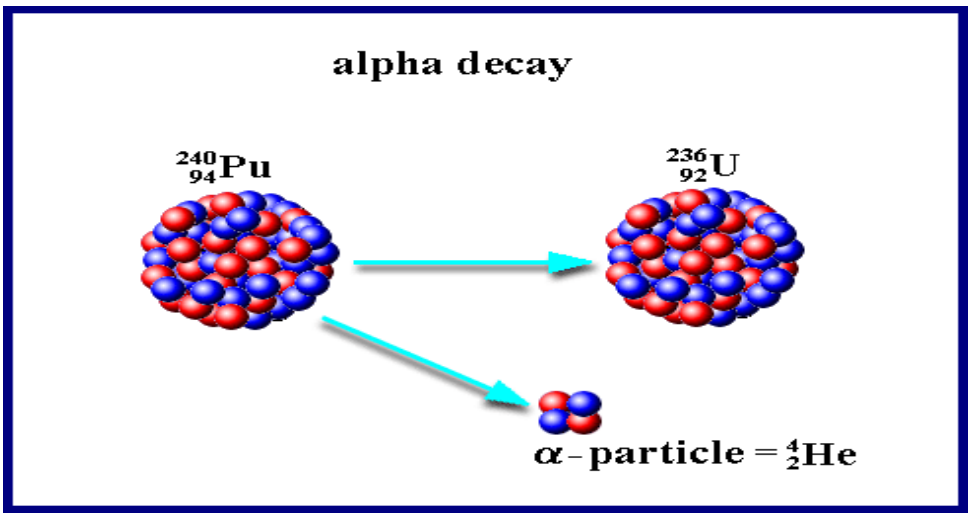

Fig. 1.2 Schematic representation of alpha decay

1.6.1.1 Properties of alpha ray

- Alpha particle carries twice the positive charge of a proton, which is equivalent to the charge on the helium nucleus.
- The mass of an alpha, - particle is approximately four times that of a hydrogen atom, i.e, it is equal to the mass of the helium nucleus.
- Electric and magnetic fields deflect alpha (α) particles.
- The velocity of most of the emitted Alpha particles is within the range ~1.5×10^7m/s and ~2.2×10^7m/s.
- Alpha α particles produce fluorescence in certain substances, like barium – plantinocyanide and zinc-sulfide.
- Alpha rays have less penetrating power compared to other rays.
- Alpha rays affect the photographic plates slightly.
- The range of alpha α particles in air depends upon the radioactive source producing it. At normal pressure in air, the range of α particles varies from 3 to 8 cm.
- Alpha α particles are scattered while passing through thin metal foils. Most of the α particles are scattered at small angles, but a few of them are scattered at an angle of more than 90^0 also.
- Because of large mass and large velocity, α particles have large ionizing power. Each α particle produces thousands of ions before being absorbed **[12]**.

1.6.2 Beta decay

Beta radiation produces high-energy electrons, which are called beta rays which are a much lighter kind of radioactive particle. In this process, a neutron spontaneously changes to a proton, plus this fast-moving electron that speeds away from the atom. Beta rays are identical to an electron, but they can also be a positron. The mass of the beta particle is 1/1836 of the mass of the proton. If the reaction involves electrons, the nucleus sheds out neutrons one by one.

For example,

$$_{90}\mathbf{Th}^{234} \rightarrow \ _{91}\mathbf{Pa}^{234} + \ _{-1}\mathbf{e}^{0}$$

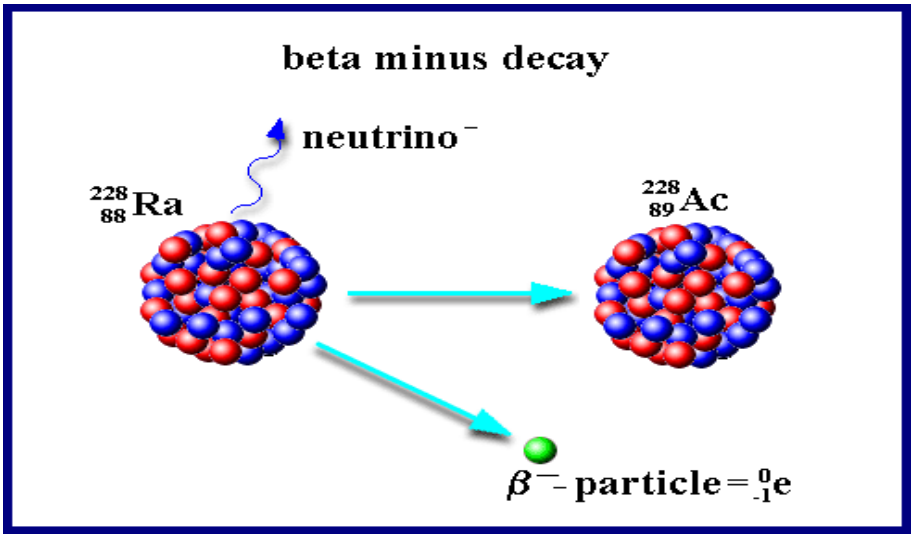

Fig. 1.3 Schematic representation of Beta decay

During beta decay, mass number and charge are conserved, and the occurring daughter product moves one place up in the periodic table and gains of positive charge to the daughter product due to the loss of negative charge by the nucleus. Beta rays are approximately 100 times more penetrating than alpha rays, and they can penetrate a few mm thick through aluminum. These rays have less ionization power in the air. Beta particles are emitted with energies between zero to a certain maximum from a particular beta active element, and this maximum energy is known as endpoint energy.

1.6.3 Gamma decay

When a nucleus is in an excited state and has too much energy, then gamma decay occurs to become stable nuclei. Most of the time, after the alpha or beta decay, the gamma decay has occurred. In **gamma decay**, only energy is emitted in the form of gamma rays so that number of protons remains the same and the atom does not become a different element during this type of decay.

Gamma rays are one of the rays in the electromagnetic spectrum. They have the lowest wavelength in the electromagnetic spectrum and range between ~1.7×10^{-8} cm and ~4×10^{-6} cm. Gamma-ray photons are more energetic than X-ray photons and also have more penetrating power than X-rays. Gamma rays are ~100 times more penetrating power than beta rays **[13]**.

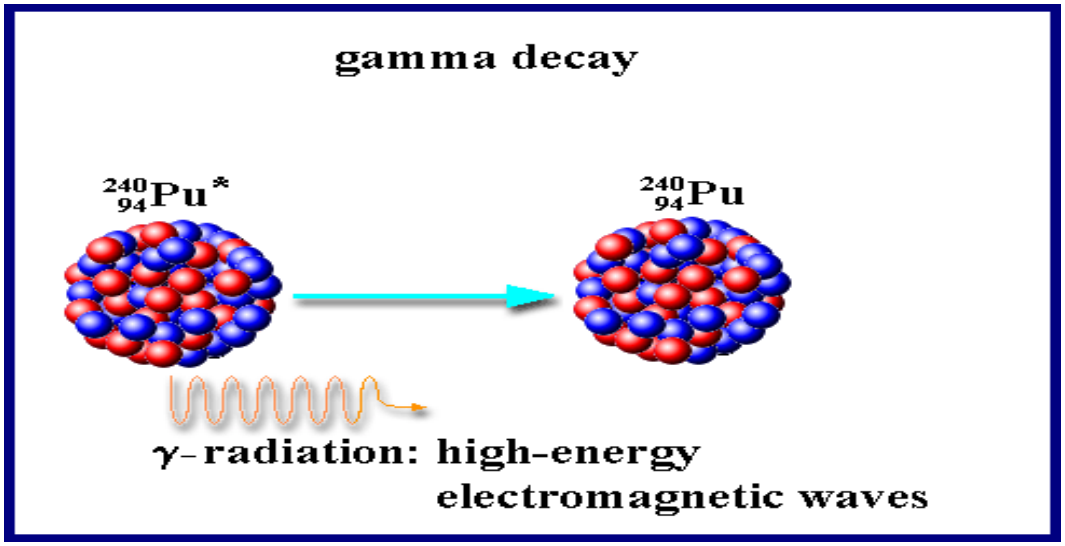

Fig. 1.4 Schematic representation of Gamma decay

1.7 Application of alpha radiation

Alpha particles are large, powerful subatomic particles that are extremely damaging to human cells. However, they lose their energy fast, limiting their ability to penetrate materials. There are numerous methods in which science successfully utilizes alpha radiation to its advantage.

- **Cancer Treatment:** Alpha radiation is used to treat a variety of cancers. This procedure, known as unsealed source radiotherapy, involves injecting tiny amounts of radium-226 into cancerous tumors. The alpha particles destroy cancer cells but lack the penetrating ability to damage the surrounding healthy cells. Radium-226 has generally been replaced by safer, more effective radiation sources like cobalt-60. Radium-223 is still used to treat bone cancer under the brand name Xofigo **[13]**.
- **Heating Devices:** Unlike radioisotope thermoelectric generators, which convert heat to electricity, radioisotope thermal generators make direct use of the heat produced by alpha decay **[13]**.
- **Static Eliminator:** Alpha radiation from polonium-210 is often used in industrial applications to eliminate static electricity. The alpha particles positive charge attracts free electrons, thus lowering the potential for local static electricity. This is a frequent technique in paper mills **[14]**.

- **Smoke Detector:** Alpha radiation can be used as a smoke detector in specific cases. alpha particles from Americium-241 bombard in air molecules which release electrons. These electrons have the ability to generate an electrical current. This current is successfully disrupted by smoke particles **[15]**.
- **Spacecraft Power and Pacemaker Battery:** Radioisotope thermoelectric generators have been used to power a variety of satellites and spacecraft, including Pioneer 10 and 11, as well as Voyager 1 and 2. These devices function similarly to a long-lasting batteries. Plutonium-238 is an incredible fuel source, producing alpha radiation and generating heat, which is then transformed into electricity. Plutonium-238 has an 88-year half-life, which could provide a long lifespan for pacemakers. However, they are no longer utilized due to their toxicity, difficulty with patients traveling, and disposal issues **[15]**.
- **Remote Sensing Stations:** The United States Air Force powers remote sensing stations in Alaska with alpha radiation. The most common fuel source is strontium-90. These alpha-powered systems allow for long periods of unmanned operation without the need for repair, but local opposition to the use of radiation is forcing the air force to replace many of these devices with alternate power sources, such as diesel-solar hybrid generators. The United States Coast Guard powers some of its oceanic buoys with alpha radiation. Alpha radiation is also used to power some offshore equipment in the oil industry **[16]**.

1.8 Objective

The present work has the following objectives:

1. To calculate the alpha decay half-lives ($T_{1/2}$) of the heavy nuclei and superheavy nuclei using Yukawa-plus- exponential Model.
2. To compare the calculated alpha decay half-lives of heavy and superheavy nuclei with other works.

CHAPTER II

REVIEW OF LITERATURE

2.1 Introduction

In 1896, Alpha (α) decay was first observed as an unknown radioactive phenomenon by Becquerel. More than a decade later, it is further described as a process that the parent nucleus emits a ^{4}He particle by Rutherford. Subsequently, this process is successfully explained by Gamow and Condon, and Gurney using the quantum tunnelling effect in 1928. Alpha decay is one of the dominant decay modes for heavy and superheavy nuclei and can provide rich and important nuclear structure information, such as ground-state energies, half-lives, nuclear spins, shell effects, nuclear deformation, and so on. More importantly, observing alpha decay chains is the only effective approach to identify new elements and /or isotopes at present. So far the study of α decay is still a popular field in nuclear physics.

The synthesis of superheavy nuclei (SHN) has become a very attractive subject in recent years. Experimentally, elements with Z = 107–112 have been synthesized in cold-fusion reactions. While, elements with Z = 113–118 have been successfully synthesized in hot-fusion reactions. Currently, the synthesis of new elements Z =119 and 120 are also in progress. A series of synthetic experiments undoubtedly required more accurate theoretical support. Theoretically, numerous models have been proposed to study α-decay process, such as two-potential approach, generalized liquid drop model, effective liquid drop model, unified fission model , the density dependent M3Y effective interaction , etc. There are also lots of empirical formulae developed to study this process, such as Royer formula, Viola-Seaborg-Sobiczewski (VSS) formula, Sobiczewski-Parkhomenko (SP) formula, Horoi formula, Santhosh formula ,Ni-Ren-DongXu formula, Deng-Zhang-Royer formula. These works are in good agreement with the experimental data **[17]**.

Superheavy elements refer to synthesized nuclei with $Z \geq 104$. Alpha decay is the favoured decay mode of such synthesized superheavy nuclei and the decay chain ended with spontaneous fission. Majority of superheavy nuclei are synthesized in laboratories using heavy-ion fusion reactions. Nuclei beyond Z = 118 and many isotopes of the synthesized nuclei need further predictions from theoretical perceptions Half-lives of alpha decay of superheavy nuclei are calculated within Unified Fission Model (UFM) and analytical formula due to Royer's formula **[18]**.

2.2 Theoretical studies of alpha decay of heavy and superheavy nuclei

Akhilesh Yadav *et al* (2023) [19] have studied the nuclear structure systematics of the superheavy nuclei lying at the extreme of mass for Z = 120 and their α-decay half-lives using the relativistic mean-field (RMF) model. The results are obtained using four different point-coupling parameters after analyzing the reliability of these parameter sets for the binding energy of experimentally observed nuclei (Z = 100–118) by comparing them with the available experimental and WS-4 microscopic calculations. The optimal parameter set thus obtained is further used for predicting the Z =120 α-decay chain and decay half-lives.

D.N. Poenaru *et al* (2023) [20] have investigated Superheavy nuclei of interest for the forthcoming synthesis of the isotopes with Z = 119,120. One of the very interesting experiments is performed at the velocity filter SHIP (GSI Darmstadt), trying to produce $^{299}120$ in a fusion reaction $^{258}Cm(54Cr,3n)^{299}120$. They have reported the calculations of α decay half-lives using four models: AKRA (Akrawy), ASAF (Analytical Super-Asymmetric Fission), UNIV (Universal Formula), and semFIS (Semi-empirical formula based on Fission Theory). The released energy, Q, is calculated using the theoretical model of atomic masses WS4. For $^{92,94}Sr$ cluster radioactivity of $^{300,302}120$ they have predicted a branching ratio relative to α decay of –0.10 and 0.49, respectively, which is expected to be measured in a forthcoming experiment.

V. Zanganeh *et al* (2023) [21] have considered the α-decay half-lives of neptunium (ZNp = 93) nuclei in the case of deformed nuclei in the range $219 \leq A \leq 239$ using the generalized liquid-drop model (GLDM) with 1977 nuclear proximity potential suggested by Blocki et al. (1977). Also, They have analyzed the α-decay half-lives of Np isotopes within the WKB method and the Deformed Proximity Potential Model (DPPM) and considered the quadrupole and hexadecapole deformations at θ = 0, θ = 30, θ = 45, and θ = 90 degrees. The calculated half-lives and the alpha decay branching ratios are compared with experimental data and are in good agreement. Comparing the results obtained with the corresponding experimental data and with the models UNIV, UDL, SemFIS, the Coulomb and Proximity Potential Model (CPPM), SLB, and Royer and it is found that they match well over a wide range. The calculated results are in reasonable agreement with the experimental data. DPPM gives reliable and accurate results for favored α-decays in the neptunium mass region.

Chen-Qi L *et al* (2022) [22] have calculated nuclear masses, binding energy, and α-decay half-lives are intractable for heavy nuclei. They took advantage of the powerful nonlinear transformation and feature representation ability of deep neural networks (DNN) to predict the nuclear masses and α-decay half-lives. For the nuclear binding energy prediction problem, they have achieved standard deviation $\sigma = 0.263$ MeV on 10-fold cross-validation on 2149 nuclei. Word vectors which are the high-dimensional representation of nuclei from the hidden layers of mass-regression DNN, help us to calculate α-decay half-lives. They got $\sigma = 0.797$ on 100 times 10-fold cross-validation on 350 nuclei on $\log_{10}T_{1/2}$ and $\sigma = 0.731$ on 486 nuclei. DNN is also used to reduce the residual of the three-parameter Gamow formula on 159 even-even nuclei, from 0.3627 to 0.2297 on $\log_{10}T_{1/2}$, using 100 times 10-fold cross-validation. They have found physical a priori such as a shell structure, magic numbers, and augmented inputs inspired by the finite-range droplet model is important for this small data regression task.

Mayan Ibraheem Khalil and Firas Mohamed Ali (2022) [23] have studied the most important factors in -decay are the Alpha particle preformation factors P_α and the Q_α -value, which provides more information about the nuclear structure. The value, which is retrieved from the cluster formation model (CFM), is carefully explored, whereas the Q_α -value is identified as (firas),(F.H1), (F.H2), and (Buck and Merchant), respectively. Hence it turned out that the alpha decay energy has a significant effect on the accuracy of determining the half-lives of heavy nuclei. Any change in the alpha decay energy, no matter how small, will have a very clear effect on the half-life of any nucleus. The Royer and Brown formulas are used to compute the theoretical alpha decay half-lives. The findings suggest that the and Q_α -decay energies are crucial observable values for conveying information about nuclear shell structure. In addition, Q_α has a good friendship. This has suggested that they could support the Gieger–Nuttal relationship, particularly in the discovery of new non-existent nuclei.

Song Luo *et al* (2022) [24] have considered the blocking effect of unpaired nucleons and the orbital angular momentum taken away by the emitted α particle. They put forward an improved Geiger-Nuttall law to calculate α-decay half-lives of heavy and superheavy nuclei. There are three adjustable parameters in this formula, whose values were obtained by fitting experimental α decay half-lives of 216 nuclei ranging from $Z = 90$ to $Z = 118$ with $N \geq 130$ from the ground state and/or isomeric state. The calculated results are in good agreement with the experimental data. The corresponding root-mean-square (rms) were 0.301, 0.587, and 0.541 for 65 even–even, 116 odd-A, and 35 odd–odd nuclei, respectively. Sobiczewski- Parkhomenko formula

(SP) proposed by A. Parkhomenko et al are also used. This improved formula is extended to predict α-decay half-lives for nuclei with Z = 117, 118, 119, and 120.

N. S. Rajeswari and Vasanthi (2021) [25] have used generalizing liquid drop model in order to describe scattering, fusion, fission, and ground state masses. Krappe and collaborators have developed a unified nuclear potential. They have incorporated phenomenological parameters accounting for the attractive force between two separated fragments. One of the phenomenological parameters involved in this model was the range of folded Yukawa function, which accounts for t surface diffuseness of the potential and short-range attractive interaction. A significant effect of this function was noted in preformation probability which improves the accuracy of half-lives of alpha decay. Half-lives for alpha decay are better obtained for two values of the range of folding function 0.54 and 0.8 fm for heavy and superheavy mass regions, respectively. The study has concluded the associated shell structure N = 126 in heavy nuclei and N = 152, 162, and 184 in superheavy nuclei.

F. Koyuncu (2021) [26] has systematically investigated the experimental α-decay half-lives of the 263 parent nuclei in the range of $52 \leq Z \leq 107$ for the ground state to ground state α-transitions in terms of a molecular potential called the Morse potential by utilizing the Wentzel-Kramers-Brillouin (WKB) approximation and Bohr-Sommerfeld quantization condition. They have found the optimum parameters of the Morse potential to explain the α-decay half-lives of the parent nuclei and compared our results with the unified model for α-decay and α capture (UMADAC) and the Universal Decay Law (UDL). They have achieved better results than the UMADAC and UDL models in terms of a few degrees of freedom in calculations of the α-decay half-lives of the parent nuclei

Jun-Gang Deng and Hong-Fei Zhang (2021) [27] have systematically investigated α-particle preformation factors, one of the most significant quantities in α decay, which are extracted from the ratios between theoretical α-decay half-lives calculated by the generalized liquid drop model and experimental data. The results have indicated both α-particle preformation factors P_α and α decay energy Q_α are important observed quantities for revealing the nuclear shell structure information, and the results show that Z = 82 and N = 126 closed shells play more important roles than Z = 50 and N = 82 shell closures in which the shell effect of N = 126 is stronger than that of Z = 82 in the α decay process. Besides, the unpaired nucleons inhibits the preformation of α-particle. The outstanding precision of this formula in describing the α-particle preformation factors indicates that it can be used to perform accurate calculations for

α decay half-lives as well as provide some general guidance for microscopic study on α-particle preformation factors and nuclear structure.

W. A. Surdoval and D. A. Berry (2021) [28] have presented a new general method for calculating the alpha decay half-life. The method predicted an a priori exact value for the beryllium-8 half-life. Beryllium-8 is an exception to the current alpha decay theory captured in the Geiger-Nuttal law. The new method has predicted the beryllium-8 alpha half-life using only constants and measured isotopic mass. The method also reliably predicted all the heavier isotope alpha decay half-lives consistent with the Geiger-Nuttal law. One result is that given the consistency of the new method presented here for all isotopes, including an exact a priori result for beryllium-8, the evidence strongly has suggested that the beryllium-8 decay is, in fact, an alpha decay; a second result has that the method definitively demonstrates that the entire rest mass of the two helium-4 electrons was converted to energy in the decay process and this energy becomes part of the emitted alpha particle kinetic energy.

Omar Nagib (2020) [29] has calculated the half-life using the Coulomb and proximity potential models with a new semiempirical formula for the diffuseness parameter. The half-life calculations of the present model universal decay law (UDL), generalized liquid-drop model (GLDM) and experimental half-lives in the region Z = 104 - 118 has been compared. Various statistical parameters have shown that the present model was the most accurate in reproducing experimental half-lives, followed by UDL then GLDM. The predicted half-lives of 51 SHN (Superheavy Nuclei) in the Z = 122 - 125 region by the present model has been compared with those of UDL and GLDM. SHN $^{295\text{-}307}122$ and $^{314\text{-}320}125$ are identified as candidates to be detected.

Jun-Gang Deng *et al* (2020) [30] have obtained the original Royer formulas and satisfactory calculations of -decay half-lives for the preferred alpha decay, but when it is expanded to the unfavorable -decay, significant discrepancies between the calculations and experimental results may have arisen. The α-decay half-lives of even-even nuclei and odd-A nuclei with Z =117, 118, 119, and 120 have been predicted using our improved formula and universal decay law. For ^{293}Ts and ^{294}Og, predicted α-decay half-lives by our improved formula have shown better accordance with experimental data, indicating that predictions by our improved formula is more reliable. The features of predicted α-decay energy and half-lives implied that N = 184 is the next neutron magic number after N =126.

O. N. Ghodsi and M. Hassanzad (2020) [31] have calculated α-decay half-lives of a great number of superheavy isotopes with $106 \leq Z \leq 126$ within proximity potentials and Coulomb spherical-deformed potentials. In formalism, they have used Q_α from the WS4 formalism to compute the penetration probability within the WKB approximation and also included the preformation factor within the CFM. Furthermore, they have compared the obtained half-lives with the ones computed from semiempirical relationships, such as Royer, VSS, UDL, and SemFIS2, which has shown a good agreement.

Hong-Ming Liu *et al* (2020) [32] have investigated the decay preformation factors, P, and the Alpha decay half-lives of 152 nuclei around Z=82, N=126 closed shells based on the generalized liquid drop model (GLDM) with P being extracted from the ratio of calculated decay half-life to the experimental one. The results have shown that there is a remarkable linear relationship between P_α and the N_α product of valance protons (holes) and valance neutrons(holes). At the same time, they extracted the alpha decay preformation factor values of the even-even nuclei around the Z=82, N=126 closed shells. Finally, using the formula obtained by fitting the alpha decay preformation factor data calculated by the GLDM, they have calculated the alpha decay half-lives of these nuclei. The calculated results agree with the experimental data well.

Aladdin Abdul-latif and Omar Nagib (2019) [33] have calculated α-decay half-lives of super heavy nuclei (SHN), revealing that the diffuseness parameter is a great bottleneck for achieving accurate results and predictions. In particular, when the universal proximity function is adopted for nuclear potential, the half-life was found to vary significantly and nonlinearly as a function of the diffuseness parameter. To overcome this limiting hurdle, a new semiempirical formula for diffuseness that is dependent on charge and neutron numbers is proposed in this work. calculations of half-lives for 68 SHN are compared against experimental data, and the calculated data is obtained by using a deformed Woods-Saxon, deformed Coulomb potentials model, and six semiempirical formulas. The predictions of 150 SHN are compared against the predictions of seven of the current best semiempirical formulas. They have concluded that more attention should be directed toward obtaining accurate diffuseness parameter values for using it in nuclear calculations.

D. T. Akrawy *et al* (2019) [34] have performed a systematic calculation on the alpha decay half-lives of heavy mass nuclei with $106 \leq Z \leq 118$, within the universal decay law (UDL) and modified universal decay law (MUDL). The calculated half-life values are founded to be in

agreement with the experimental data. The standard deviations of the logarithm of half-lives is found to be the least for MUDL in all cases of even-even, even-odd, odd-even and odd-odd, so the MUDL formula is better than UDL formula for α-decay studies. They have predicted half-lives of some SHN in the region Z = 110 - 118 that are not yet experimentally detected. The decay energies has been computed using three different mass models.

B. R. Sivasankaran *et al* (2019) [35] have used Gamow's theory to systematically compute the alpha decay half-lives of even-even isotopes between the atomic numbers Z = 62 and Z = 118. The decay energy (Q_α) values has been extracted from experimental data and the frequency with which the alpha particle attempts to penetrates the potential barrier of the parent nuclei is calculated using the classical relations. The calculated half-life is compared with available experimental data. The computed values using Gamow's theory are founded to be in close agreement with the experimental data.

D. N. Poenaru and R. A. Gherghescu (2018) [36] have investigated the superheavy nuclei of interest for the forth coming synthesis of the isotopes with Z =119, 120. One of the very interesting latest experiments has been performed at the velocity filter SHIP (GSI Darmstadt) which is trying to produce $^{299}120$ in a fusion reaction ^{248}Cm (^{54}Cr,3n) $^{299}120$. Where port calculations of α-decay half-lives using four models: AKRA (Akrawy), ASAF (analytical super asymmetric fission), UNIV (universal formula), and semFIS (semi-empirical formula based on fission theory). They have predicted a branching ratio relative to α-decay of -0.10 and 0.49 respectively, meaning that it is worth trying to detect such kinds of decay modes in competition with α-decay.

K.P. Santhosh and C. Nithya (2017) [37] have studied the decay modes of 1051 odd Z superheavy nuclei within therange$105 \leq Z \leq 135$, and their daughter nuclei by comparing the alpha decay half-lives with the spontaneous fission half-lives. For a theoretical comparison, the alpha decay half-lives are also computed with the Coulomb and proximity potential model (CPPM), Viola-Seaborg-Sobiczewski semi-empirical relation (VSS), Universal curve of (UNIV), the analytical formula of Royer, and the Universal decay law (UDL). The predicted decay modes and half-lives are compared with the available experimental results.

S. S. Hosseini and H. Hassanabadi (2017) [38] have calculated the half-lives using the experimental Q_α values. The computed half-life is compared with the experimental data and with existing empirical estimates and it is founded to be in good agreement. They also have obtained α-preformation factors from the ratio between theoretical and experimental results for

some superheavy nuclei and has evaluated the standard deviation. Alpha decay half-lives for some superheavy nuclei, such as Rf, Sg, Hs, Ds, Cn, Fl, Lv and Og has been analysed using the Viola-Seaborg, Royer formulae and a new analysis in the Brown formula. The computed half-life values was compared with the experimental data, and it is indicated acceptable agreement with some of the systematic empirical correlations.

S. S. Hosseini *et al* (2017) [39] have studied α- decay half-lives under the Yukawa proximity potential model. A comparison with the existing experimental data has revealed that Yukawa proximity potential showed an acceptable agreement, and they have made an analysis of some isotopes of SHN using the VS and Royer formulae and a new analysis in the Brown formula. They have been calculating the HLs for some SH isotopes of even-even, even-odd, odd-even, and odd-odd nuclei as Po, U, Th, Ra, Fl, Lv, and Og. The computed half-life values are compared with the experimental data, and it is indicated acceptable agreement with some of the 15 systematic empirical correlations. They have depicted some results using empirical and theoretical ways by comparison with experimental data for SHN.

D.T. Akrawy and D.N. Poenaru (2017) [40] have presented a new semi-empirical formula for calculations of α-decay half-lives. It is derived from the Royer relationship by introducing new parameters that have been fixed, to fit a set of experimental data. They have been using three sets: set A with 130 e-e (even-even), 119 e-o (even-odd), 109 o-e, and 96 o- o, set B with 188 e-e, 147 e-o, 131 o-e and 114 o-o, and set C with 136 e-e, 84 e-o, 76 o-e and 48 oo alpha emitters. A comparison of results has been obtained with the new formula (newF) and the following well known relationships: semi-empirical relation based on fission theory (semFIS), analytical super asymmetric fission (ASAF) model and universal formula (UNIV) made in terms of rms standard deviation.

C. Nithya and K. P. Santhosh (2017) [41] have studied the alpha decay chains of isotopes of superheavy nuclei $^{278\text{-}282}$Rg and were using CPPMDN. They have predicted 3α chains from the isotopes $^{278\text{-}280,282}$Rg. The isotope ^{281}Rg decays through spontaneous fission. The obtained predictions are in good agreement with the experimental results. The alpha decay half-lives has been calculated using CPPMDN is compared with five other theoretical models. It is seen that for predicting the decay modes of superheavy nuclei, CPPMDN suits better than the other models. As they are successful in reproducing the experimental results of 278-282Rg, they have been planning to extend our work to predict the decay modes of all the isotopes of Rg within the range $259 \leq A \leq 339$.

Shan Zhang *et al* (2017) [42] have improved semi-empirical relation for α-decay half-lives was proposed by introducing a precise radius formula and an analytic expression for preformation probability. By using the improved relationship, the α-decay half-lives of 421 nuclei has been calculated. It is shown that the accuracy of this semi-empirical relation was improved significantly compared to its predecessor. Further research has shown that it also has reproduced the experimental half-lives of the superheavy nuclei well. Last, with the improved a formula the α-decay half-lives of the Z =118-121 isotopes have been predicted, which are helpful for the future experiments. In addition, there is a prediction of a magic number effect at N =184.

M. Ismail *et al* (2017) [43] have preformed cluster model, a simple method for calculating $T_{1/2}$ of heavy and superheavy nuclei has been derived using the WKB approximation for the penetration of the Coulomb barrier with the Woods-Saxon potential for the nuclear part and the Langer modified centrifugal potential for the centrifugal part. Then, the variation of $\log_{10}T_{1/2}$ with neutron numbers of the daughter nuclei was studied. Consequently, it is founded by simple calculations, for the alpha decay half-lives that N = 126, 152, 162, 178 and 184 are neutron magic numbers and Z = 108, 114, 118 and 120 are proton magic numbers. In fact, these magic numbers are in a good agreement with those which have been predicted in other studies.

H.C. Manjunatha and K.N. Sridhar (2017) [44] have formulated the semiempirical formula for α-decay half-lives of heavy and superheavy nuclei for different isotopes of the wide atomic-number range $94 < Z < 136$. They have considered 2627 isotopes of heavy and superheavy nuclei for the fitting. The value produced by the present formula is compared with that of experiments and other eleven models, i.e. ImSahu, Sahu, Royer10, VS2, UNIV2, SemFIS2, WKB. Sahu16, Densov, VSS and Royer formula. This formula is exclusively for heavy and superheavy nuclei. α-decay is one of the dominant decay modes of superheavy nucleus. By identifying the α-decay mode superheavy nuclei could be detected. This formula helps in predicting the α-decay chains of superheavy nuclei.

B. Gillis Carlssona *et al* (2016) [45] have presented the α-decay of superheavy nuclei. The microscopic modelling of α-decay was a challenging theory. The approach discussed gave an improved description of hindrance factors that are important for predicting decay and half-lives of superheavy elements. Future experiments might have utilized the reactions such as titanium on berkelium that could have led to the creation of element 119. For the ^{98}Cf, ^{100}Fm, ^{102}No and ^{104}Rf chains, it is possible to measure α-decay to several different final states.

K. P. Santhosh and C. Nithya (2016) [46] have investigated superheavy nuclei by comparing the α-decay half-lives with the spontaneous fission half-lives. α-decay half-lives has been calculated using the Coulomb and proximity potential model for deformed nuclei (CPPMDN). The agreement between theoretical and experimental α-decay half-lives have shown the predictability of the CPPMDN in the superheavy region. A modified formula is proposed for calculating the spontaneous fission half-lives including the shell correction. The agreement between theoretical predictions and experimental results of spontaneous fission half-lives is satisfactory for heavy and superheavy nuclei ranging from Th to Fl. A comparison between the spontaneous fission half-lives has been done using eight different formalisms was performed for even-even superheavy nuclei in the range of $108 \leq Z \leq 120$.

Xiao-Dong Sun *et al* (2016) [47] have studied α decay half-lives for even-even nuclei from Z = 62 to Z = 118 are systematically based on the two-potential approach with a quasistationary state approximation. As for the nuclear potential, the isospin effect is considered, which slightly improves the results by 6.8%. To reduce the deviations between experimental half-lives and calculated results due to the nuclear shell structure, the analytic expression of hindrance factors is employed. The results can reproduce the experimental half-lives as good as using the density-dependent cluster model and the generalized liquid drop model.

X J Bao *et al* (2015) [48] have investigated α-decay half-lives of recently synthesized superheavy nuclei (SHN) by employing a unified fission model (UFM) and Royer's analytical formula. The good agreement with the experimental data has indicated the UFM and the analytical formula are useful tools to investigate these α-decays. A modified formula is proposed for determining the spontaneous fission half-lives based on Swiatecki's formula, including the microscopic shell correction and isospin effect. They have calculated spontaneous fission half-lives for heavy and SHN in regions from Th to Fl systematically. Experimental data are well reproduced by the modified Swiatecki formula. They have predicted decay modes for the unknown cases and competition between α-decay and spontaneous fission is analyzed detailly.

Y. Z. Wang *et al* (2015) [49] have calculated Q_α values and α-decay half-lives of the SHN with $Z \geq 100$ by using 20 models and 18 empirical formulas, respectively. By comparisons between the calculated results and experimental data, it was shown that (i) the WS4 mass model was the most accurate one to reproduce the experimental Q_α values of the SHN. (ii) although some nuclear mass models, such as FRDM and SNMF, has higher accuracy in reproducing the

measured nuclear masses, they might have noted to scribe the Qα values of the SHN precisely. (iii) because the parameters in the SemFIS2 formula were from the experimental α emitter data of trans uranium nuclei, including SHN (Z = 92 - 118), it is the best one to predict the α-decay half-lives of the SHN. (iv) The UNIV2 formula with the fewest parameters and the VSS, SP, and NRDX formulas with fewer parameters worked well in predicting the SHN α-decay half-lives. Finally, the α-decay half-lives of Z =110 - 120 were predicted within the SemFIS2, VSS, SP, NRDX, and UNIV2 formulas by inputting the Qα values extracted from the WS4 mass model.

Yibin Qian and Zhongzhou Ren (2014) [50] have studied the α-decay half-lives of superheavy odd-Z nuclei within the density-dependent cluster model, including the nuclear deformation effect. The decay energy Q has been obtained as the difference between the parent and the two decay products plus the electron screen correction, based on two calculated masses, namely the FRDM and KTUY05. The competition between α-decay and spontaneous fission was being performed via an improved phenomenological description of spontaneous fission half-lives. In addition, the heavier cluster decay is supposed to be not competitive with the two decay modes from the empirical estimations. It has been founded that the calculated result was in good agreement with the available experimental data.

N. S. Rajeswari and M. Balasubramaniam (2013) [51] have studied the alpha decay half-lives of 108 even-even isotopes of heavy nuclei within a modified unified fission model for the use of different nuclear surface energy coefficients ($\gamma - MN76$, $\gamma - MN95$, $\gamma - MS67$ and $\gamma - MS00$) entering in the calculation of proximity potential, for the use of two different forms of overlapping potentials, linear and second-order polynomial forms. The exact fitting of the half-lives for the isotopes of Ra, Th, and U is obtained by introducing a parameter R, which extends the touching point radius. A linear relation connecting this parameter ΔR and the Q-value of the decay is obtained with a constraint to have a continuity of the potential in the overlapping and non-overlapping regions. For the use of this linear relation, half-life values are calculated for all 108 even-even isotopes of heavy nuclei. Calculated half-lives for the use of different versions of nuclear surface energy coefficients, using both linear and polynomial overlapping potentials, compared well with the experimental values.

Ren Yuejiao and Ren Zhongzhou (2013) [52] have calculated the half-lives of Z=85- 91 nuclei with new Geiger-Nuttall law and has tested the validity of new Geiger-Nuttall law for odd - Z isotopic chains. It is discovered that the new law could have been applied to odd-Z

nuclei without the additional introduction of new parameters. A new island with abnormally long half-lives manifested itself for Z = 85 - 92 isotopes with N ≤ 126 due to the spherical shell closure. This is the first island with abnormally long half-lives beyond the stable line. The mechanism of the appearance of this island could have been used to explore other long-lifetime islands beyond the stable line. It is also used for investigating the variation of magic numbers for nuclei which is far from stable.

Hiroyuki Koura (2012) [53] have derived a phenomenological formula for alpha decay half-lives with a global parameter set. It has been constructed in a conventional way by considering the penetrability of a charged particle in a spherical Coulomb potential. Parameters 19 in the formula had been fixed because they had been determined by physical constants except for the following three adjustable parameters. The distance between the charge radius and the radius of an inner point of the Coulomb barrier, r_0, and the odd-mass hindrance, h_0. Parameter values are reasonably consistent with physical considerations. The root-mean-square deviations from experimental partial half-lives for even-even, odd-A, and odd-odd nuclei are 0.344, 0.740, and 0.940 (in log10), respectively. The obtained formula has given half-lives that were two or three times longer than those obtained using the Viola-Seaborg formulae in the superheavy nuclear mass region.

H.F. Zhang *et al* (2012) [54] have introduced the term "island of stability" of superheavy nuclei due to shell effects, and the α-decay half-lives of these nuclei are predicted by him. The calculations of the binding energies within a new Macroscopic-Microscopic Model (MMM) are performed, and it is compared with the experimental data for heavy nuclei from Md to the Z = 118 elements. It is an excellent agreement. The data have confirmed that the ^{270}Hs is a deformed double sub-magic nucleus beyond ^{208}Pb. The features of α-decay energies and one-proton-separation energies from the MMM has revealed that the next double magic nucleus after ^{270}Hs should be ^{298}114. The α-decay half-lives are determined using a generalized liquid drop model (GLDM) with the Q_α from the MMM for Hs and Z = 114 isotopes, respectively.

Yuejiao Ren and Zhongzhou Ren (2012) [55] have proposed the new Geiger-Nuttall law for the calculations of α-decay half-lives where the effects of quantum numbers had been naturally taken into account. This approach included the change of the node number of the wave function of the α-core relative motion in the Geiger-Nuttall law. By including the change of quantum numbers, the available data of α-decay half-lives of ground-state transitions in even-even nuclei, both N ≥ 126 and N ≥ 128, are well reproduced. The new Geiger-Nuttall law is an

important development to the original Geiger-Nuttall law or the Viola-Seaborg formula based on quantum theory, and it is an extension of the original Geiger-Nuttall law to α-decay of a broader range of nuclei and transitions. It has been expected that the extension was useful for similar decay processes, such as cluster radioactivity and proton emissions.

Jianmin Dong *et al* (2010) [56] have investigated the half-lives of α-decay for SHN in the framework of the Unified Fission Model (UFM) with a new method for assault frequency. No adjustable parameter is involved in the calculations. The results of the present calculations using the UFM were in excellent agreement with the experimental data. For some nuclei in $^{282}113$, $^{280}111$, and $^{279}111$ α-decay chains, the half-lives from the UFM, together with other models, are underestimated by a few times, possibly from the nonzero angular momentum transfers. They have also found that Q_α value dependence of the α-decay half-life becomes increasingly a new element 117 and the experimental measurements to a certain extent. Finally, they have mentioned that Q_α value and half-life are insufficient to obtain more information about the nuclear structure and other properties of SHN (such as rotational bands, isomeric states, and various deformations) that deserve intensive study.

Ni and Zhongzhou Ren (2010) [57] have presented a new theoretical approach to evaluate the α-decay study of well-deformed even-even nuclei by the multichannel cluster model (MCCM). Based on the axially deformed Woods-Saxon potential, the coupling potential is taken into full account in terms of the general quantum theories, and the decay width is computed by utilizing the quasibound solution of the coupled-channel Schrodinger Equation. This is the first four-channel calculation of α-decay within the framework of the coupled-channel approach. The results that have been shown were very satisfactory. Some predictions of the branching ratios to high-spin daughter states are made for superheavy nuclei.

V. Yu. Denisov and A. A. Khudenko (2010) [58] have estimated the α-decay half-lives of even-even SHEs within the range of proton numbers $104 \leq Z \leq 126$, which might be formed by possible cold and hot fusion reactions, in the framework of various approaches 21 for α-decay half-life evaluation and by using the Q values of α transitions are obtained within different approximations for atomic masses. Spectacular differences between the Q values and half-lives are calculated in the framework of various approaches in the range $Z \geq 118$ and $180 \leq N \leq 192$ could have been used for the discrimination of a correct theoretical approach for atomic masses. Because of this, experimental studies of SHEs with Z =126 and N = 184 are very desirable.

H. F. Zhang *et al* (2009) [59] have investigated Experimental α decay energies and half-lives systematically to extract α particle preformation in heavy nuclei. Formulas for the preformation factors are proposed that can be used to guide microscopic studies on preformation factors and perform accurate calculations of the α decay half-lives. There is little evidence for the existence of an island of long stability of superheavy nuclei.

H. F. Zhang and G. Royer (2008) [60] have presented the even-even nuclei from Z = 52 to Z = 118. The decay constants have been obtained from the experimental half-lives. The penetration probabilities have been calculated from the WKB approximation, and the penetration barriers are constructed with the GLDM. The preformation factors are not constant for these nuclei and have shown regular law for the studied isotopes. The penetrability is determined mainly by the behavior of the decay constant. The study has been extended to the even-even superheavy nuclei. The penetration probabilities were relatively very large, and its range is narrow for the heaviest nuclei. So, it was easy for the α-particle to escape from these nuclei as soon as they were formed, confirming that the superheavy nuclei are weakly bound.

G. Royer and H.F. Zhang (2008) [61] have compared the α-decay half-lives with the results obtained from previously proposed formulas, which depended only on the mass, charge numbers of the α emitter, and the Q_α value. For the heaviest nuclei, they have compared with calculations using the density-dependent M3Y (DDM3Y) effective interaction and the ViolaSeaborg-Sobiczewski (VSS) formulas. The correct agreement have allowed them to make predictions for the α-decay half-lives of other still unknown superheavy nuclei from those analytic formulas using the extrapolated Q_α of G. A. Audi et al. mass table.

Zhongzhou Ren and Chang Xu (2008) [62] have investigated the α-decay half-lives of superheavy nuclei (Z=115→113→111) by the density-dependent cluster model. The theoretical α-decay half-lives have been calculated by using the renewed experimental α-decay energies. The agreement between theory and experiment is generally reasonable for those odd-Z superheavy nuclei. The deviations between experimental and calculated half-lives are within a factor of 5 for most nuclei by taking into account, and influence of the non-zero angular momentum.

D. N. Poenaru *et al* (2007) [63] have produced the potential barrier for the ^{20}O radioactivity of ^{228}Th for the first time by adding the shell and pairing corrections to the phenomenological deformation energy. The analytical super-asymmetric fission (ASAF) model predictions have been confirmed. The fine structure of the emitted cluster is not detected till now. The strong

shell effects of the daughter ^{208}Pb are not fully exploited. New experimental searches could be performed. The expected half-lives could have been estimated by using the universal curves. The ASAF model and the universal curves might be used to calculate the half-lives against the α-decay of superheavy nuclei.

Chang Xu1 and Zhongzhou Ren (2007) [64] have systematically analyzed the α-transitions to ground and first excited 0+ states in neutron-deficient Pb and Po isotopes by the density-dependent cluster model. The magnitude of nuclear deformation of the coexisting 0^+_1 and 0^+_2 states is extracted directly from the experimental α-decay energies and half-lives. They clearly demonstrated the phenomenon of shape coexistence around the Z = 82 shell closure in this analysis. The obtained deformation values from Rn → Po → Pb decay chains are generally consistent with both the available experimental and theoretical studies.

Chang Xu and Zhongzhou Ren (2007) [65] have systematically studied the α-decay half-lives of the exotic N = 125, 126, and 127 isotones (Po, Rn, Ra, Th, and U) by the density-dependent cluster model (DDCM). The influence of the neutron shell closure N = 126 on the α-cluster formation and penetration probabilities are analyzed and discussed in detail. By combining the DDCM and a two-level microscopic model together, the experimental half-lives of α transitions to both the ground state and the excited state in the daughter nuclei are reproduced very well.

Chang Xu and Zhongzhou Ren (2008) [66] have investigated the α-decay half-lives of ground and isomeric states of exotic nuclei around the shell closures Z = 82 and N = 82 by the density-dependent cluster model (DDCM). The calculations have concentrated on four kinds of favored α transitions: (1) ground state to ground state, (2) ground state to isomeric state, (3) isomeric state to ground state, and (4) isomeric state to isomeric state. The calculated α-decay half-lives of both ground and isomeric states are found to be in good agreement with the experimental data. Useful predictions on the partial half-lives of several α emitters are made for future experiments.

Chang Xu and Zhongzhou Ren (2006) [67] have calculated the α-decay half-lives of ground-state transitions of even-even nuclei with Z = 52 - 104. The double-folding potentials between the spherical α-particle and the deformed daughter nucleus have been evaluated by the multipole expansion method. The nuclear and Coulomb potentials are fully microscopic and well-grounded in physics because the popular M3Y nucleon-nucleon interaction is used for calculations. It is found that the nuclear deformations significantly affect the barrier penetration

probabilities, and the reason has been explained. The theoretical α-decay half-lives are found to be in excellent agreement with the experimental data.

Xu and Zhongzhou Ren (2006) [68] have carried out a global calculation of favored α-decay half-lives of both even-A and odd-A deformed nuclei in the framework of a deformed version of the density-dependent cluster model (DDCM). The influence of nuclear deformation on α-decay half-lives is taken into account in the deformed DDCM. The microscopic potential between the spherical α particle and the deformed daughter nucleus is evaluated numerically from the double-folding model by the multipole expansion method. The deformation and orientation dependence of the α-core potential was analyzed and discussed. The 485 total number of α emitters is calculated in this article, and this covers the nuclei with Z = 52–110. This study showed α-decay half-lives on both even-A and odd-A nuclei with deformed microscopic potentials. The numerical results obtained by the deformed DDCM were in good agreement with the experimental data.

Chang Xu1 and Zhongzhou Ren (2006) [69] have investigated the half-lives of newly observed α-emitters ^{105}Te and ^{109}Xe by the density-dependent cluster model. The half-lives of α-emitters close to the N = Z line are also studied in a unified framework where the influence of the nuclear deformation was properly taken into account. Good agreement between the model and data was obtained, and some possible α-emitters are suggested for future experiments.

M. M. Sharma and A. R. Farhan (2005) [70] have investigated the properties of α-decay chains of recently produced superheavy elements Z = 115 and Z = 113 using the new Lagrangian model NL-SV1 with the inclusion of the vector self-coupling of the ω meson in the framework of relativistic mean-field theory. It has been shown experimentally that the observed α-decay energies and half-lives are reproduced well by this Lagrangian model. Further calculations for the heavier elements with Z =117 - 125 have shown that these nuclei are super deformed with a prolate shape in the ground state. A super-deformed shell closure at Z = 118 lends additional binding and extra stability to nuclei in this region. Consequently, it is predicted that the corresponding Q_α values provide α-decay half-lives for heavier superheavy nuclei within experimentally feasible conditions. The results are compared with those of macroscopic-microscopic approaches.

V. Yu. Denisov and H. Ikezoe (2005) [71] have derived the set of parameters for α-nucleus potential by using the data for both the α-decay half-lives and the fusion cross sections around

the barrier for reactions α + ^{40}Ca, α + ^{59}Co, and α + ^{208}Pb. The α-decay half-lives are obtained in the framework of a cluster model using the WKB approximation. The evaluated α-decay half-lives and the fusion cross sections agrees well with the data. Fusion reactions between α particles and heavy nuclei can be used for both the formation of very heavy nuclei and spectroscopic studies of the formed compound nuclei.

Chang Xu and Zhongzhou Ren (2005) [72] have done a systematic calculation on α-decay half-lives of medium mass nuclei by the improved version of the density-dependent cluster model, in which the nuclear potential between α-particle and daughter nucleus is obtained from the double-folding integral of the renormalized M3Y nucleon–nucleon interaction with the matter density distributions of α-particle and daughter nucleus, and the Coulomb potential is obtained from the double-folding integral of the proton–proton Coulomb interaction with the charge density distributions of α-particle and daughter nucleus. For the favored transitions from nuclear ground states, the theoretical partial half-lives of α-decay are in good agreement with experimental ones. On average, the density-dependent cluster model can reproduce the experimental α-decay half-lives of nuclei with Z = 52–80 to within a factor of 3 or better. Therefore, DDCM gives reliable and accurate results for favored α-decays in the medium mass region.

Y. K. Gambhir *et al* (2005) [73] have studied systematic and comprehensive study of the decay half-lives of nuclei appearing in the observed α-decay chains of superheavy elements (Z =108 - 118). The ground-state properties of the relevant nuclei have been calculated within the framework of the Relativistic Mean-field (RMF) theory. The calculation proceeded in three steps. First, the relativistic mean-field equations have been solved in the axially symmetric deformed oscillator basis to obtain ground-state properties such as binding energies, radii, deformations, and densities. The results are in good agreement with the available experimental systematics, as expected.

D. S. Delion *et al* (2004) [74] have analyzed the alpha decay between ground states along N−Z chains in deformed heavy and superheavy nuclei by using the pairing approach. They have shown that the derivative of the preformation amplitude is practically a constant along any chain, while that of the outgoing wave function changes exponentially upon the Coulomb parameter. This lead to the breakdown of the continuity equation and, therefore, to wrong decay widths. The behavior cannot be explained within the standard shell model, and significantly correct this deficiency by considering an a-cluster factor in the preformation amplitude,

depending exponentially upon the Coulomb parameter. Thus, four-body correlations, connected with the radial shape of the preformation factor, are directly evidenced by the a-decay systematics. Moreover, this procedure, in principle, fully determines the Q value and is an important development in the a-decay theory. It also has allowed analyzing the relative a-clustering structure of the emitter.

Zhongzhou Ren (2002) [75] has investigated the structure of even-even superheavy nuclei with proton number Z=100 - 116 in the RMF model. This is the first systematic comparison between the theoretical binding energies of the RMF model and available data. The calculated binding energy have agreed well with the data. The calculations also set an upper limit and a lower limit for the binding energy based on the comparison with the present data. This is useful for guiding future experiments on superheavy nuclei. The RMF results have shown that there is shape coexistence in superheavy nuclei, and deformations could have appeared for many superheavy nuclei. In some cases, the superdeformed configuration is the ground state of superheavy nuclei, especially for nuclei around Z = 114 and N = 174. The RMF result is in good agreement with the experimental alpha decay energies and lifetimes.

G Royer (2000) [76] has determined the potential energy governing α emission within a liquid drop model, including proximity effects between the α particle and the daughter nucleus, and adjusted to reproduce the experimental Q_α. The α emission half-lives have been deduced from the WKB barrier penetration probability for spontaneous asymmetric fission. The RMS deviation between the theoretical and experimental values of $\log_{10}[T_{1/2}(s)]$ is only 0.63 for a recent data set of 373 α emitters and 0.35 for the subset of even–even nuclides. Predictions for the heaviest and superheavy elements are presented, as well as simple analytical formulae for $\log_{10}[T_{1/2}(s)]$.

D. N. Poenaru and M. Ivascu (1983) [77] have improved up-to-date versions of the known alpha decay half-lives formulae are obtained by changing the additive parameters in order to have a vanishing mean value of the absolute errors. A new semiempirical relationship is derived on the grounds of the fission theory of alpha decay. It has taken into consideration explicitly the dependence on the difference from magicity both of the neutron and proton numbers and to obtain better agreement with experimental data.

D N Poenaru *et al* (1979) [78] have computed Q values and half-lives in the two-center parametrization by using the liquid-drop-model generalization, replacing the surface energy with a folded Yukawa plus exponential potential. Alpha decay is considered to be a very

asymmetric fission process with fragments of different charge densities. An empirical shell correction is introduced to obtain the experimental Q values exactly. The experimental half-lives for the alpha decay of Ra, Th, U, Pu, Cm, Cf, Fm, and No even-even isotopes are well reproduced.

D. N. Poenaru and M. Ivascu (1983) [79] have estimated that alpha decay partial half-life could be made by using semiempirical relationship. After changing the additive parameters of the examined formulae in such a way that the mean n value of the errors (1/n) (Ti/Tiexp) vanishes in each group of the nuclei (e-e, o-e, e-o, and o-o), the standard deviation, 0' of log T values is usually reduced. In this way, an up-to-date version of the known formulae has been obtained. The Keller-Miinzel relationship was the best of all formulae, but even this has an increased error in the vicinity of the magic number of neutrons N = 126. This is practically smoothed by the present formula for e-e nuclei.

2.3 Experimental studies of alpha decay of heavy and superheavy nuclei

Wuenschel et al (2018) [80] have explored the production of alpha particle decaying heavy nuclei in reactions $^{238}U + ^{232}Th$ of 7.5 - 6.1 MeV/nucleon using an in-beam detection array composed of YAP scintillators and gas ionization chamber-Si telescopes. They have compared the alpha energies and half-lives for the observed products with those of the previously known isotopes, and that comparison indicates the observation of a number of previously unreported alpha emitters. They have even observed decay energies of alpha particles reaching as high as 12 MeV. Many of these are expected to be from the decay of previously unseen relatively neutron-rich products.

Vladimir Utyonkov *et al* (2016) [81] have studied the discovery and investigation of the "Island of stability" of superheavy nuclei at the separator DGFRS in the ^{238}U - $^{249}Cf + ^{48}Ca$ reactions. The results are compared with the data obtained in chemistry experiments and at the separators SHIP, BGS, TASCA, and GARIS. The synthesis of the heaviest nuclei, their decay properties, and methods of identification is discussed. The role of shell effects in the stability of superheavy nuclei is demonstrated by a comparison of the experimental results and theoretical data.

J. Khuyagbaatar *et al* (2014) [82] have produced the superheavy element with atomic number Z = 117 as an evaporation residue in the $^{48}Ca + ^{249}Bk$ fusion reaction at the gas-filled recoil separator TASCA at GSI Darmstadt. The radioactive decay of evaporation residues and their

α-decay products is studied using a detection setup that allowed measuring decays of single atomic nuclei with half-lives between sub-μs. Two decay chains comprising seven α decays and spontaneous fission each was identified and assigned to the isotope ^{294}117 and its decay products. A hitherto unknown α-decay branch in ^{270}Db (Z = 105) is observed, which populated the new isotope ^{266}Lr (Z = 103). The identification of the long-lived ($T_{1/2}$ = 1.0−0.9 +1.9 h) α-emitter ^{270} Db marks an important step towards the observation of even more long-lived nuclei of superheavy elements located on an "island of stability."

Yu. Ts. Oganessian *et al* (2013) [83] have studied the superheavy nuclei produced in the ^{249}Bk + ^{48}Ca reaction performed using the Dubna Gas Filled Recoil Separator. It has been corroborated through the observation in a total of 11 additional decay chains originating from the 4n evaporation product, ^{293}117, and three decay chains of the 3n channel, ^{294}117, of the reaction ^{249}Bk + ^{48}Ca. The radioactive decay properties of the twelve ^{293,294} 117, ^{289,290}115, ^{285,286}113, ^{281,282}Rg, ^{277,278} Mt, ^{274}Bh, and ^{270}Db isotopes measured in this work are in full agreement with the results of the first experiment as well as with the decay data determined for ^{289}115, ^{285}113, and ^{281}Rg measured in the cross-bombardment ^{243}Am(^{48}Ca,2n) ^{289}115 reaction. The decay properties of odd-Z nuclei produced in the 249Bk + 48Ca reaction are in good agreement.

Yu. Ts. Oganessian (2012) [84] has reported the discovery of a new chemical element with atomic number 117, corroborated through the observation of five additional decay chains originating from the 4n evaporation product, ^{293}117, and two decay chains of the 3n channel, ^{294}117, of the reaction ^{249}Bk + ^{48}Ca. The radioactive decay properties of the 11 isotopes ^{293,294}117, ^{289,290}115, ^{285,286}113, ^{281,282} Rg, ^{278}Mt, ^{274}Bh, and ^{270}Db measured in this work are in full agreement with the results of the first experiment as well as with the decay data determined for ^{289}115, ^{285}113, and ^{281}Rg measured in the cross-bombardment reaction ^{243}Am(^{48}Ca, 2n)^{289}115. The decay properties of the heaviest nuclei are determined more 25 accurately and demonstrated once more the decisive role of nuclear shell effects in the stability of superheavy nuclei.

Yu. Ts. Oganessian *et al* (2011) [85] have identified the heaviest isotopes of elements Z = 117 to Z = 105, ^{294} 117, ^{293}117, ^{290}115, ^{289}115, ^{286}113, ^{285}113, ^{282}Rg, ^{281}Rg, ^{278}Mt, ^{274}Bh and ^{270}Db, by means of the Dubna gas-filled recoil separator among the products of the ^{249}Bk + ^{48}Ca reaction. In the fusion reaction of the radioactive target nuclei ^{249}Bk and the doubly magic ^{48}Ca ions, a new chemical element with the atomic number Z = 117 was synthesized. In the

experiments at E* = 35 and 39 MeV that correspond to the expected maximum cross sections of the channels associated with the evaporation of three and four neutrons, the production of two isotopes of element 117 with similar properties is observed. These correspond to ^{294}117 and ^{293}117. Decay characteristics of the eleven new isotopes produced in the reaction ^{249}Bk + ^{48}Ca are in good agreement with those expected based on the properties of the neighboring even-Z and odd-Z nuclei.

J. M. Gates *et al* (2011) [86] have performed experiments with the new recoil separator, Transactinide Separator, and Chemistry Apparatus (TASCA) at the GSI by using beams of ^{48}Ca to irradiate targets of $^{206-208}$ Pb, which led to the production of $^{252-254}$No isotopes. The isotopes of element 114 ($^{288-291}$ 114) are produced in irradiations of ^{244}Pu targets with ^{48}Ca beams at compound nucleus excitation energies around 41.7 and 37.5 MeV, demonstrating TASCA's ability to perform experiments with picobarn-level cross sections. A total of 15 decay chains are observed and are assigned to the decay of $^{288-291}$114. A new α-decay branch in ^{281} Ds is observed, leading to the new nucleus ^{277}Hs.

P.A. Ellison *et al* (2010) [87] have produced the new, neutron-deficient, superheavy element isotope ^{285}114 in ^{48}Ca irradiations of ^{242}Pu, which targets at a beam energy of 256 MeV (E* = 50 MeV). The α-decay of ^{285}114 was followed by the sequential α-decay of four daughter nuclides, ^{281}Cn, ^{277}Ds, ^{273}Hs, and ^{269}Sg. ^{265}Rf is observed to decay by spontaneous fission. The measured α-decay Q values are compared with those from a macroscopic-microscopic nuclear mass model to give insight into superheavy element shell effects.

Yu. Ts. Oganessian *et al* (2010) [88] have reported the discovery of a new chemical element with atomic number Z = 117. The isotopes ^{293}117 and ^{294}117 are produced in fusion reactions between ^{48}Ca and ^{249}Bk. Decay chains involving 11 new nuclei are identified by means of the Dubna gas-filled recoil separator. The measured decay properties have shown a strong rise of stability for heavier isotopes with $Z \geq 111$, validating the concept of the long-sought island of enhanced stability for superheavy nuclei.

H. F. Zhang *et al* (2009) [89] have investigated the experimental α-decay energies and half-lives systematically. The neutron magic number N = 126 is crucial for long α-decay half-lives. There is little evidence for the existence of an island of stability of superheavy nuclei with half-lives as long as the half-lives of elements observed in nature. The half-lives should be several or several tens of seconds or minutes in the case in which this island of stability had existed. A

formula for the preformation factors is proposed, which could be used to provide general guidance for microscopic study on preformation factors and nuclear structure.

L. Stavsetra *et al* (2009) [90] have presented the independent verification of the production of element Z=114 in the reaction of 244-MeV ^{48}Ca with ^{242}Pu. Two chains of time and position-correlated decays have been assigned to ^{286}114 and ^{287}114. The observed decay modes, half-lives, and decay energies agree with the published results. The measured cross sections at a center-of-target energy of 244 MeV for the ^{242} Pu (^{48}Ca, 3–4n) ^{287,286} 114 reactions are $1.4^{+32}_{-1.2}$ pb each, which are lower than the reported values.

Yu. Ts. Oganessian *et al* (2007) [91] have measured the decay properties of the new isotope ^{282}113 and its daughter nuclei in the ^{237}Np (^{48}Ca, 3n) ^{282}113 reaction. During irradiation with a beam dose of 1.1×10^{19} 244-MeV ^{48}Ca projectiles, two decay chains originating from the odd-odd isotope ^{282} 113 (E_α = 10.63 ± 0.08 MeV, $T_\alpha = 73_{-29}{}^{+134}$ ms) are produced in the complete fusion reaction with a cross-section of $0.9^{+0.6}_{-0.6}$ pb, these properties are all in agreement.

Yu. Ts. Oganessian *et al* (2006) [92] have synthesized the new element with atomic number 118 for the first time in the ^{249}Cf + ^{48}Ca reaction. The isotope of the element Z = 116 daughters was studied in the ^{245}Cm (^{48}Ca, 3n) ^{290}116 reaction, and the isotope of the element Z=114 granddaughters was studied in the ^{242} Pu (^{48}Ca, 4n) ^{286}114 reaction. The even-even ^{294}118 nuclide undergoes consecutive decays, α1 → α2 →SF/α3 →SF. The decay chains are terminated by the spontaneous fission of the granddaughter or great-granddaughter nuclei, ^{286}114 or ^{282}112, respectively. The α-decay energy of ^{294}118 is Q_α = 11.81 ± 0.06 MeV, and the half-life is $T_\alpha = 0.89_{-0.31}{}^{+1.07}$ ms. These decay properties are in agreement with that one can expect for the ground-to-ground state α transition of an element Z=118 isotope from the systematic behavior of Tα vs Qα for even-even isotopes. The measured Q_α, T_α, and TSF values of the ^{294}118, ^{290} 116, ^{286}114, and ^{282}112 nuclei agree well with the properties of other previously synthesized isotopes and with the theoretically predicted properties of the superheavy nuclei in the region of Z = 110 - 118 and N = 169 - 177.

P. Roy Chowdhury *et al* (2006) [93] have analyzed the half-lives for alpha radioactivity with microscopic nuclear potentials. They have obtained it by the double folding procedure by using the DDM3Y effective interaction. The results of the present calculations have been made with DDM3Y and are in good agreement with the published experimental data for the half-lives of the α decays from the isotopes of elements Z = 112, 114, 116, and ^{294}118 and from some decay products. The released energies Q, to which the calculations were quite sensitive when

calculated from the microscopic-macroscopic model, masses do not provide excellent agreement with those observed for super heavies. Nevertheless, the positive decay Q values have supported these α-decay modes.

Yu. Ts. Oganessian *et al* (2004) [94] have presented the synthesized element Z=115 isotopes in the ^{243}Am + ^{48}Ca reaction. With a beam dose of 4.33×10^{18} 248-MeV ^{48}Ca projectiles, they have observed three similar decay chains consisting of five consecutive α decays, all have been detected in time intervals of about 20 s and is terminated at a later time by spontaneous fission with a high-energy release (total kinetic energy, 220 MeV). The decay properties of these synthesized nuclei are consistent with consecutive α decays originating from the parent isotopes of the new element Z=115, ^{288}115, and ^{287}115, produced in the 3n- and 4n-evaporation channels with cross sections of about 3 pb and 1 pb, respectively.

V. Barci *et al* (2003) [95] have produced the level structure of ^{229}Th by alpha particle decay of ^{233}U, which is studied with γ- ray spectroscopy measurements. The sources continuously separated the daughters from ion-exchange chromatography methods. Energies and intensities of about 220 γ rays were accurately determined. About 70 transitions are reported for the first time, especially in the 300-700 keV energy range. A ^{229}Th level scheme is proposed, accounting for 220 transitions among 47 excited states. The agreement with experimental data that has been shown was to be satisfactory.

Yu. Ts. Oganessian *et al* (2001) [96] have produced the first decay event of the new nuclide ^{292}116 in an experiment devoted to synthesizing Z = 116 nuclei in the ^{248}Cm + ^{48}Ca reaction. The implantation of a heavy recoil in the focal-plane detector was followed at 46.9 ms by an α particle with E_α = 10.56 MeV. The energies and decay times of the descendant nuclei are in agreement with those observed in the decay chains of the even-even isotope ^{288}114, previously produced in the ^{244}Pu + ^{48}Ca reaction. Thus, the first alpha decay should be attributed to the parent nuclide ^{292}116 produced via the evaporation of four neutrons in the complete fusion of ^{248}Cm and ^{48}Ca.

S. Hofmann and G. Munzenberg (2000) [97] have predicted the nuclear shell model that the next doubly magic shell closure beyond ^{208}Pb was at a proton number between Z = 114 and 126 and at a neutron number N = 184. The outstanding aim of experimental investigations is the exploration of this region of spherical superheavy elements (SHE's). This work has described the experimental methods that led to the identification of elements Z = 107 to 112 at GSI, Darmstadt. In a study of the reaction ^{86}Kr + ^{208}Pb, ^{294}118, three decay chains are measured

and is assigned to the superheavy nucleus $^{293}118$. The decay data revealed that, for the heaviest elements, the dominant decay mode is alpha emission, not fission. At a higher sensitivity, the exploration of the region of spherical SHE's seemed to be feasible more than 30 years after it is predicted.

Yu. Ts. Oganessian *et al* (1999) [98] have observed the decay sequence consisting of an implanted heavy atom in the bombardment of ^{244}Pu with ^{48}Ca with three subsequent alpha decay and spontaneous fission (SF) all correlated in time and position. The measured alpha energies and corresponding time intervals were E_α = 9.71 MeV ($\triangle$t = 30.4 s), 8.67 MeV ($\triangle$t = 15.4 min), and 8.83 MeV ($\triangle$t = 1.6 min) for the SF ($\triangle$t =16.5 min), the total deposited energy was approximately 190 MeV. The α-particle energies, together with the decay times and SF terminating the chain, offer evidence of the decay of nuclei with high atomic numbers. This decay chain is a good candidate for originating from the α-decay of the parent nucleus $^{289}114$, produced with a cross-section of about 1 pb.

Yu. A. Lazarev *et al* (1995) [99] have discovered the n-decaying nuclide $^{267}108$ with a half-life of 19^{+29}_{-10}ms, E = 9.74 to 9.87 MeV, and the production cross-section of about 2.5 pb in bombardments of ^{238}U targets with 186-MeV ^{34}S projectiles. The new nuclide have been identified by measuring correlations in energy, time, and position to establish genetic links between its implantation in a position-sensitive silicon detector and subsequent α-decay followed by α decays of known descendant nuclides.

CHAPTER III

METHODOLOGY

3.1 Introduction

Alpha decay is energetically preferred and is a spontaneous decay mode of naturally occurring heavy and artificially produced superheavy nuclei, when the disintegration energy is positive. Initially, quantum tunnelling theory was applied to explain alpha emission **[100]**. Later alpha emission was interpreted as a very asymmetric fission and it was suggested that models used to explain fission could be applied to alpha decay **[101]**. Nuclear spectroscopic studies on alpha decay of heavy and superheavy nuclei act as a probe to obtain spin and parity of nuclear energy levels. Numerous studies have been carried out to obtain half-lives of alpha decay. These studies, generally, are classified under fission model and cluster model. These models differ in expression for decay constant through preformation probability

The present study aims to find half-lives of alpha decay. Further, the influence of the preformation probability is studied in deciding the accuracy of half-lives of alpha decay. Shanmugam and Kamalaharan **[101]** have calculated the life-time of alpha emission and their branching ratio relative to cluster decay, by using Yukawa-plus-exponential potential in post-scission region. Yukawa-plus-exponential potential for the post-touching region and a third-order polynomial potential for the over-lapping region is explained in this chapter **[102]**.

In order to describe large-scale collective nuclear motion and obtain the satisfactory experimental data, Krappe et al **[103]** developed a unified nuclear potential by generalizing liquid drop model and incorporating phenomenological parameters which account for attractive nuclear interaction energy between two separated fragments. The parameter a which is the range of folded Yukawa function accounts for both short range nuclear force and diffuseness of the surface. Yukawa interaction is supposed to contain the combined effect of two interacting diffuse matter distributions and some short range interaction.

3.2 Yukawa- plus-exponential Model

If the Q value of the reaction is taken as the origin, then the potential as a function of r (which is the distance of mass centers of the fragments) for the post-scission region is given by

$$V(\mathrm{r}) = \frac{Z_1 Z_2}{r} e^2 + V_n(r) - Q, \qquad r > r_t \tag{3.1}$$

where

$$V_n(r) = -D\left[F + \frac{r-r_t}{a}\right]\frac{r_t}{r}\exp[(r_t - r)/a] \quad (3.2)$$

$V_n(r)$ is the nuclear potential, $V_c = \frac{Z_1 Z_2}{r}e^2$ is the Coulomb potential and $r_t = R_{1+}R_2$ is the sum of their equivalent sharp surface radii.

The depth constant D is given by

$$D = \frac{4a^3 g_1 g_2\, e^{r_t/a}\,[C_s(1)C_s(2)]^{1/2}}{r_0^2\, r_t} \quad (3.3)$$

The constant F is given by

$$F = 4 + \frac{r_t}{a} - \frac{f_1}{g_1} - \frac{f_2}{g_2}, \quad (3.4)$$

where

$$g_j = (R_j/a)cosh(R_j/a) - sinh(R_j/a), \quad (3.5)$$

$$f_j = (R_j/a)^2 sinh\,(R_j/a\,), \quad (3.6)$$

$$C_s(j) = a_s(1 - K_s I_j^2), \quad (3.7)$$

$$I_j = \frac{N_j - Z_j}{A_j}, \quad (j = 1,2) \quad (3.8)$$

I_j is the neutron excess. Here, r_o =1. 16 fm; a=0.68 fm; a_s =21.13 MeV, and K_s,=2.3.

The interaction barrier of the two fragments can be easily computed in this one-dimensional parametrization as the maximum of the interaction potential energy. For spherical fragments, this maximum V(R,) occurs at a distance of R, from the origin in the LDM. But, in the Yukawa-plus-exponential model (YEM), the maximum V(r), occurs at a distance of r that can be calculated by using the relation

$$\left[\frac{dV(r)}{dr}\right]_{r=r_m} = 0 \quad (3.9)$$

Q values are computed as

$$Q = [M(A,Z) - M(A_1,Z_1) - M(A_2,Z_2)] \times 931.501MeV, \quad (3.10)$$

$$A = A_1 + A_2,\ Z = Z_1 + Z_2 \tag{3.11}$$

For the overlapping region, we approximate the barrier by a third-order polynomial in r having the form with Q value being taken as origin. Cubic barrier is given as

$$V(r) = -E_v + [V(r_t) + E_v]\left[s_1\left[\frac{r-r_i}{r_t-r_i}\right]^2 - s_2\left[\frac{r-r_i}{r_t-r_i}\right]^3\right], r_i < r < r_t, \tag{3.12}$$

where r_i is the distance between the centers of mass of two portions of a sphere (cut by a plane) in two pieces with volume asymmetry of the decay. For r_i, the expression is given by

$$r_i = \frac{3}{4}\left[\frac{h_1^2}{R_0 + h_1} + \frac{h_2^2}{R_0 + h_2}\right], \tag{3.13}$$

where h_1 and h_2 are the heights of the spherical segments. For symmetric case, it reduces to

$r_i = \frac{3}{4} R_0$, since $h_1 = h_2 = R_0$.

When one wants to include E, in the calculation of the lifetimes, one has to be careful to see that the conservation of energy is preserved. In order to accomplish this, the cubic part of the barrier is not set to zero at r =r_i, but to —E_v. For calculating the half-life of the system, we use the formula

$$T_{1/2} = \frac{1.4333 \times 10^{-21}}{E_v P_o P_{nov}} \tag{3.14}$$

P_{ov} (or P_0) indicates pre-formation probability which is the penetrability for pre-touching region and P_{nov} is the penetrability for post-touching region; both are calculated using WKB method.

$$P_0 = P_{OV} = exp\left[-\frac{2}{\hbar}\int_{r_a}^{r_t}\{2\mu V(r)\}^{1/2}dr\right] \tag{3.15}$$

$$P = P_{nov} = exp\left[-\frac{2}{\hbar}\int_{r_a}^{r_t}\{2\mu V(r)\}^{1/2}dr\right] \tag{3.16}$$

r_a and r_b are turning points such that V (r_a) = V (r_b) = 0.

Zero-point vibration energy is incorporated in the potential and at r = r_i, potential is equated to $-E_v$, in spite of 0. Zero-point vibration energy is given by

$$E_v = \frac{\pi\hbar}{2}\frac{(2Q/\mu)^{1/2}}{(C_1 + C_2)} \tag{3.17}$$

with the Sùsmann central radii, given by

$$C_i = R_i\left(1 - \frac{b^2}{R_i^2}\right) fm, \tag{3.18}$$

with i = 0, 1, 2 are the central radii, respectively, for the parent, daughter nuclei and particle emitted and b is the nuclear surface width given by b = 1 fm. The sharp radii are given by the expression

$$R_i = r_0 A_i^{1/3} fm, \tag{3.19}$$

with r_0 = 1.16 fm and i = 0, 1, 2, respectively, represents parent, daughter and particle emitted. In order to compare the calculated half-lives with the experimental values, the standard deviation (SD) is calculated as

$$\sigma = \sqrt{\frac{1}{n}\sum_{i=1}^{n}\left[log_{10}\left(\frac{T_{i1/2}^{cal}}{T_{i1/2}^{expt}}\right)\right]^2} \tag{3.20}$$

Here, $T_{i1/2}^{exp}$ and $T_{i1/2}^{cal}$ represent the experimental and calculated half-lives, respectively, and n is the number of nuclei under consideration **[102]**.

CHAPTER IV

RESULTS AND DISCUSSION

4.1 Introduction

The alpha decay is an important point in both theoretical and experimental nuclear physics research. This mechanism of nuclear decay is important in describing the structure of nuclei. Furthermore, alpha decay is the most significant component in obtaining information regarding identification of new superheavy elements. As a result, alpha decay is significant in theoretical and experimental nuclear physics studies.

The alpha decay mechanism is described quantum mechanically by quantum mechanical tunnelling through the potential barrier generated by the Coulomb interaction between the alpha particle and daughter nucleus. This potential is essential in calculating the penetration probability, which is needed to determine the theoretical half-life of alpha decay.

Therefore, various theoretical models were used to analyse alpha decay, including density dependent M3Y effective interaction, unified fission model, generalised liquid drop model, cluster model, Coulomb potential, and proximity potential model. The proximity potential is widely used for determining alpha decay half-life. Since heavy and superheavy nuclei are deformed the role of nuclear deformation, for both parent and daughter nuclei, is very important in the potential barrier between alpha particle and daughter nucleus **[104]**. However for the present study, only spherical nuclei are considered.

In this present work, we are calculating the preformation probability and alpha decay half-life of heavy and superheavy nuclei using the Yukawa-plus-exponential Model. Further we have plotted the graphs between logarithmic preformation probability value against daughter neutron number for heavy nuclei with Z= 82 to 102 and super heavy nuclei with Z= 104 to 125.The half-lives of 1140 nuclei for alpha decay are predicted in super heavy with $104 \leq Z \leq 125$.

4.2 Preformation probability of alpha in heavy nuclei

Fig.4.1 to Fig.4.11 represents the logarithmic preformation probability values against daughter neutron number, N_1 for Pb, Po, Rn, Ra, Th, U, Pu, Cm, Cf, Fm and No isotopes. In Fig.4.1 the logarithmic preformation probability value reduces monotonously as N_1 increases, for Pb isotopes.

In case of Po isotopes, Fig.4.2 the logarithmic preformation probability value decreases and reaches minimum at N_1 =122 and then increases. It is maximum at N_1=126. Probability for formation of alpha particle is maximum when daughter neutron number, N_1=126. Shell closure happens for daughter neutron number at 126, and preformation probability is high for two neutrons outside the closed shell to form an α-particle by combining with two protons

In Fig.4.3, the logarithmic preformation probability values of Rn isotopes slowly decreases and reaches minimum at N_1=122. Sudden rise in $\log_{10}P_0$ value for the daughter neutron number is 126, confirms the role of shell structure since the shell closure occurs at N_1 = 126.

In Fig. 4.4 the logarithmic preformation probability values decreases as N_1 increases for Ra isotopes, reaches minimum at N_1= 123. Then increases and reaches maximum at N_1 = 126, which is a magic number.

In case of Th isotopes, Fig 4.5 the logarithmic preformation probability values decreases as N_1 increases and reaches minimum at N_1 =122. Then it increases and reaches maximum at N_1 = 126. Shell closure happens for daughter neutron number 126, and preformation probability is high for two neutrons outside the closed shell to form an α-particle by combining with two protons.

Fig.4.6 represents the logarithmic preformation probability values against daughter neutron number, N_1 for U isotopes, Sudden rise in $\log_{10}P_0$ value the daughter neutron number is 126 confirms the role of shell structure since the shell closure occurs at N_1 = 126.Then it slowly decreases and reaches minimum at N_1 =144.

For Pu, Cm, Cf, Fm and No isotopes, the logarithmic preformation probability is depicted in Fig. 4.7 to Fig.4.11 respectively. Here also the preformation probability is found to be maximum at N_1=152 for Cf isotopes and Fm isotopes. In other cases the preformation probability decreases and reaches minimum and an increase is noted N_1=152 which confirms the predicted neutron magic number 152.

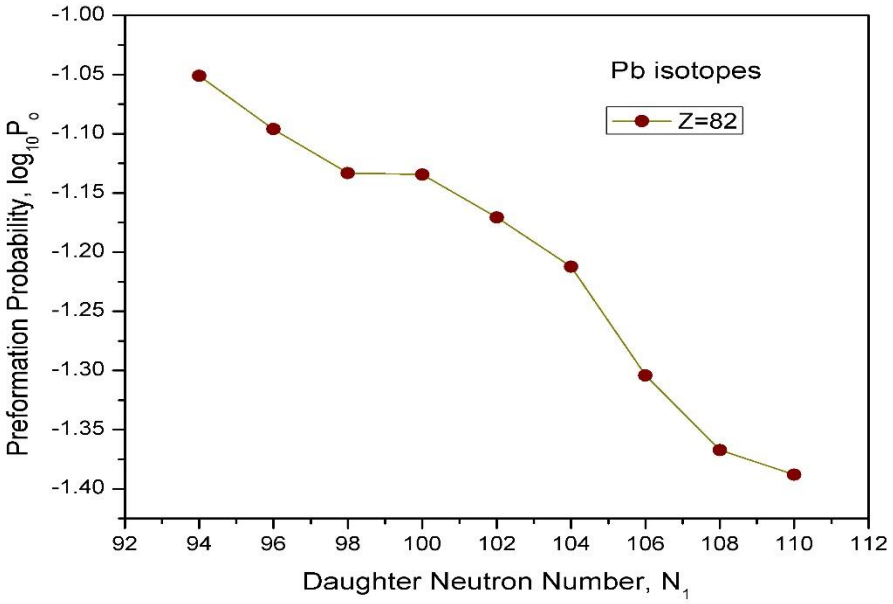

Fig. 4.1 Logarithmic preformation probability values against daughter neutron number, N_1, for Pb isotopes (9 isotopes).

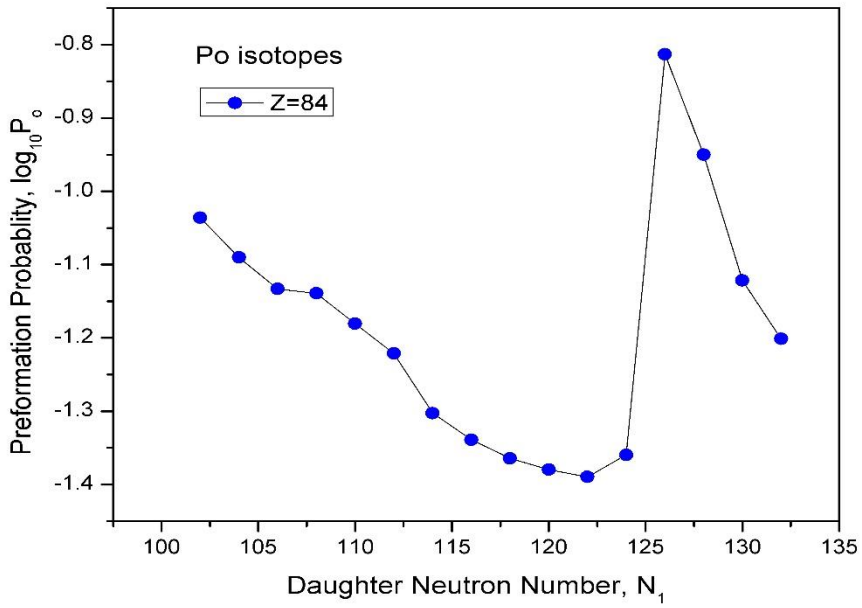

Fig. 4.2 Logarithmic preformation probability values against daughter neutron number, N_1, for Po isotopes (16 isotopes).

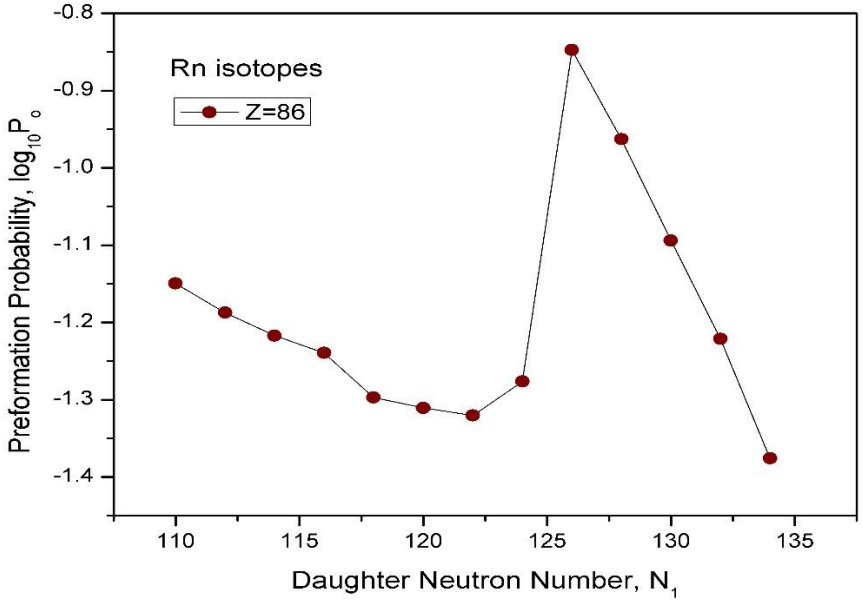

Fig. 4.3 Logarithmic preformation probability values against daughter neutron number, N_1, for Rn isotopes (13 isotopes).

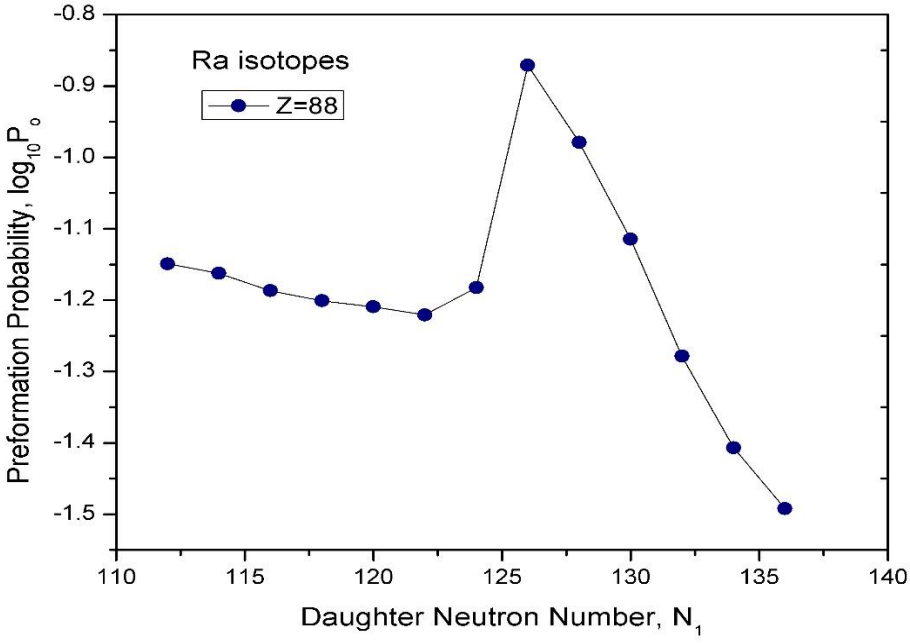

Fig. 4.4 Logarithmic preformation probability values against daughter neutron number, N_1, for Ra isotopes (13 isotopes).

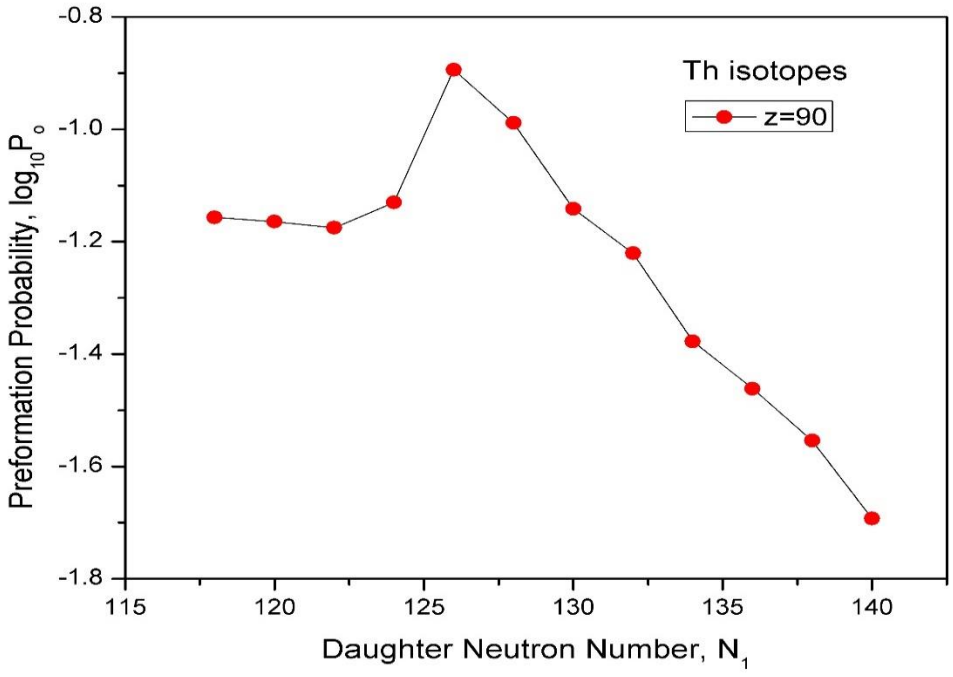

Fig. 4.5 Logarithmic preformation probability values against daughter neutron number, N_1, for Th isotopes (12 isotopes).

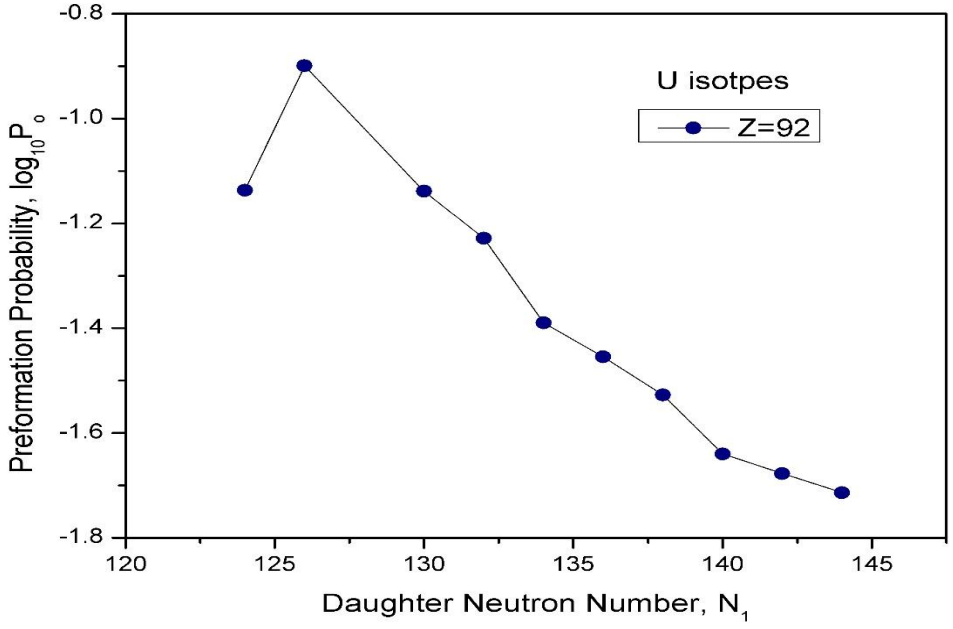

Fig. 4.6 Logarithmic preformation probability values against daughter neutron number, N_1, for U isotopes (10 isotopes).

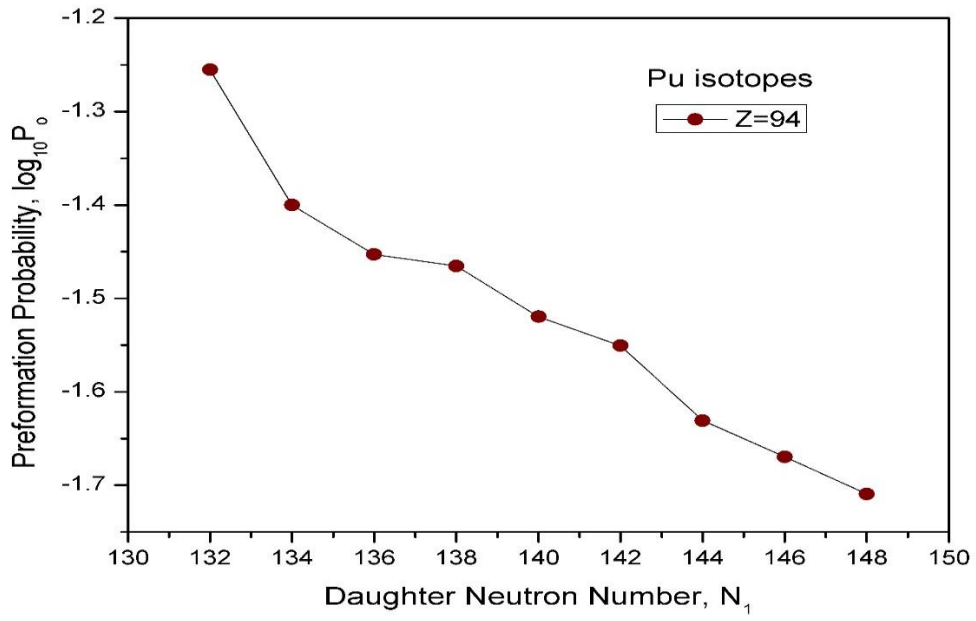

Fig. 4.7 Logarithmic preformation probability values against daughter neutron number, N_1, for Pu isotopes (9 isotopes).

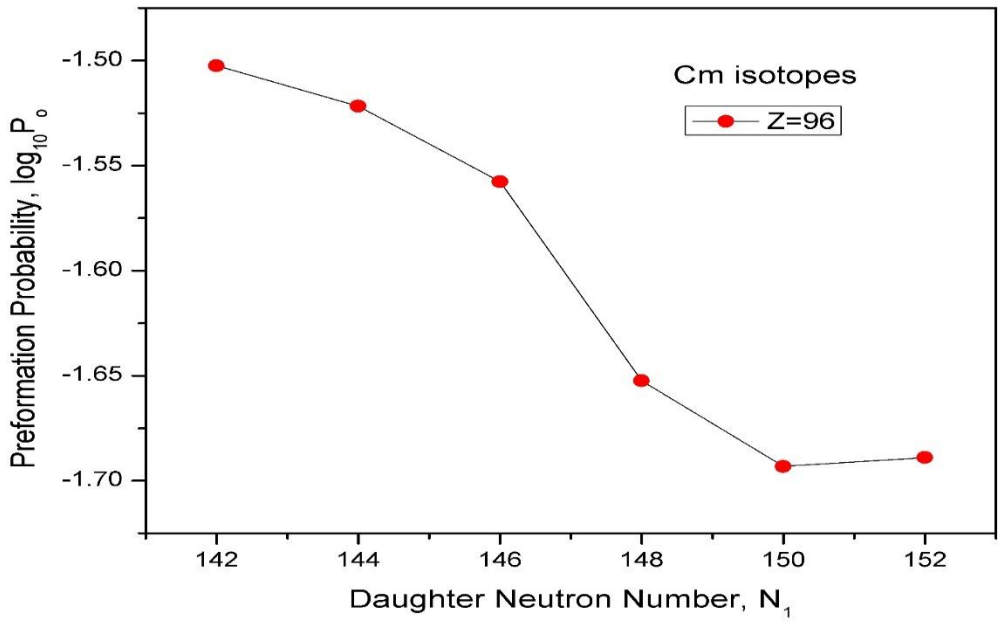

Fig. 4.8 Logarithmic preformation probability values against daughter neutron number, N_1, for Cm isotopes (6 isotopes).

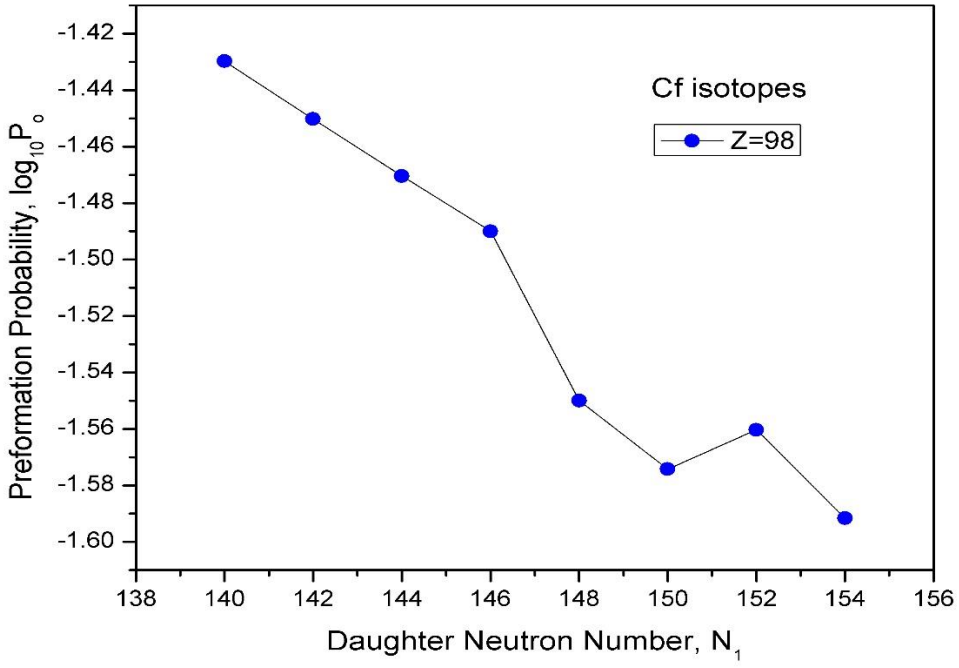

Fig. 4.9 Logarithmic preformation probability values against daughter neutron number, N_1, for Cf isotopes (8 isotopes).

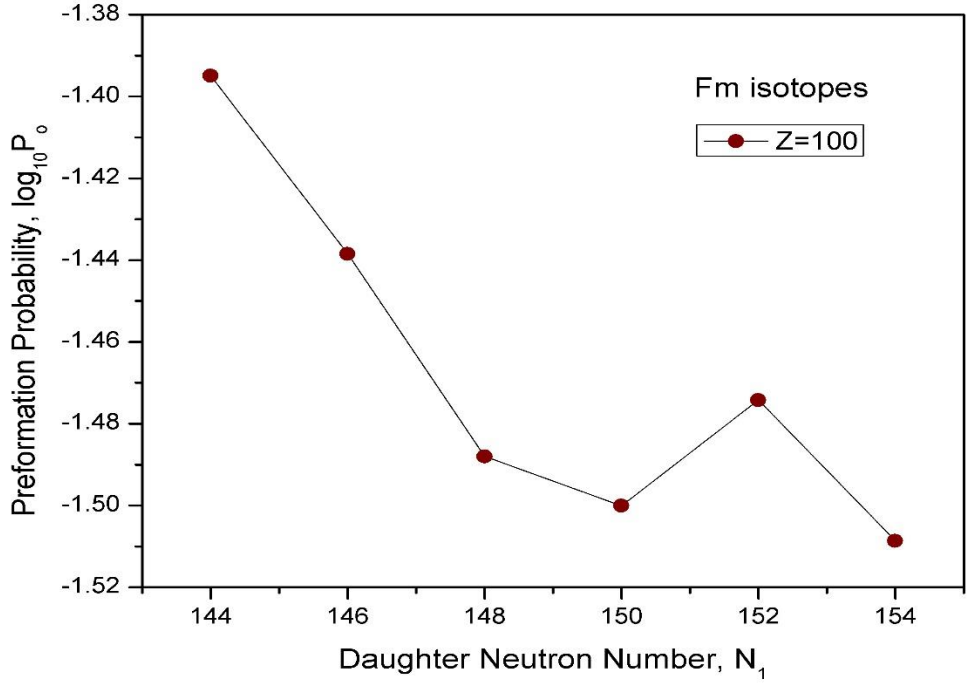

Fig. 4.10 Logarithmic preformation probability values against daughter neutron number, N_1, for Fm isotopes (6 isotopes).

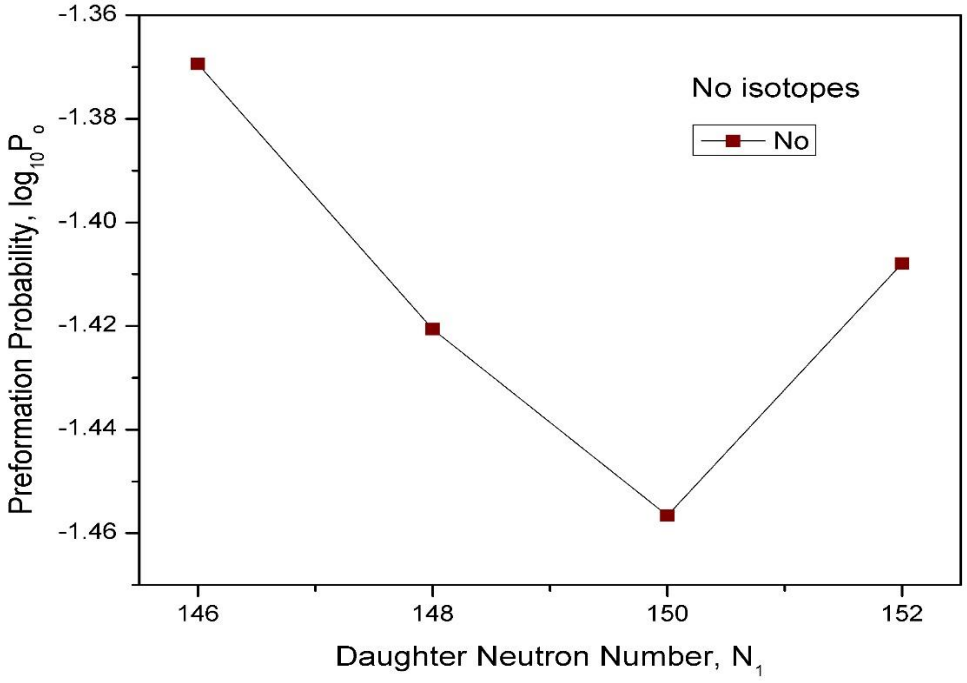

Fig. 4.11 Logarithmic preformation probability values against daughter neutron number, N_1, for No isotope (4 isotopes).

4.3 Half-lives of alpha decay for even-even heavy nuclei with Z=82 to 102

Table 4.1 represents the characteristics half-lives of alpha decay of heavy nuclei with Z=82 to 102. First column represents the parent nuclei with 108 even-even isotopes of heavy elements such as Pb, Po, Rn, Ra, Th, U, Pu, Cm, Cf, Fm and No. The second column represents the daughter nuclei. The third and fourth column represents the Q-values and experimental logarithmic half-lives. The logarithmic half-lives calculated using Cubic-plus- Coulomb- plus-Yukawa-plus exponential model are listed in fifth column. P_o is the penetrability for pre-touching region and P_{nov} is the penetrability for post-touching region are listed in sixth and seventh column respectively.

In this table, the penetrability of the overlapping region varies from 9.50×10^{-03} to 19.72×10^{-02}. The penetration probability of the non-overlapping region ranges from 3.27×10^{-40} to 1.14×10^{-10}. The calculated half-lives ranges from -7.04 $T_{1/2}$ in s to 19.34 $T_{1/2}$ in s. The calculated logarithmic half-lives matches well with the experimental half-lives but a very slight difference is noted and calculated logarithmic half-lives are compared with other works $\boldsymbol{log_{10}T_{1/2}^{NSR}}$.

Table 4.1 Calculated logarithmic half -lives of 106 cases of alpha decay of heavy nuclei are compared with the experimental half-lives. Experimental Q-values and $\log_{10}T_{1/2}$ values of heavy nuclei are taken from Ref **[102]**.

Parent Nuclei	**Daughter Nuclei**	**Q**	$log_{10}T_{1/2}^{exp}$	$log_{10}T_{1/2}^{cal}$	**P_o**	**P_{nov}**	$log_{10}T_{1/2}^{NSR}$
		MeV	**$T_{1/2}$ in s**	**$T_{1/2}$ in s**			**$T_{1/2}$ in s**
Z=82							
^{178}Pb	^{174}Hg	7.79	-3.64	-3.41	8.89×10^{-02}	1.56×10^{-17}	-3.88
^{180}Pb	^{176}Hg	7.42	-2.30	-2.26	8.01×10^{-02}	1.27×10^{-18}	-2.80
^{182}Pb	^{178}Hg	7.08	-1.26	-1.14	7.36×10^{-02}	1.07×10^{-19}	-1.82
^{184}Pb	^{180}Hg	6.77	-0.21	-0.07	7.34×10^{-02}	9.35×10^{-21}	-0.82
^{186}Pb	^{182}Hg	6.47	1.08	1.07	6.75×10^{-02}	7.52×10^{-22}	0.29
^{188}Pb	^{184}Hg	6.11	2.43	2.58	6.13×10^{-02}	2.69×10^{-23}	1.66
^{190}Pb	^{186}Hg	5.70	4.26	4.51	4.96×10^{-02}	4.04×10^{-25}	3.44
^{192}Pb	^{188}Hg	5.22	6.56	7.02	4.29×10^{-02}	1.50×10^{-27}	5.73
^{194}Pb	^{190}Hg	4.74	9.99	9.87	4.09×10^{-02}	2.33×10^{-30}	–
Z=84							
^{188}Po	^{184}Pb	8.09	-3.40	-3.71	9.20×10^{-02}	2.98×10^{-17}	-4.17
^{190}Po	^{186}Pb	7.69	-2.60	-2.50	8.12×10^{-02}	2.14×10^{-18}	-3.06
^{192}Po	^{188}Pb	7.32	-1.54	-1.30	7.36×10^{-02}	1.55×10^{-19}	-1.88
^{194}Po	^{190}Pb	6.99	-0.41	-0.18	7.26×10^{-02}	1.23×10^{-20}	-0.87
^{196}Po	^{192}Pb	6.66	0.76	1.06	6.60×10^{-02}	7.98×10^{-22}	0.29
^{198}Po	^{194}Pb	6.31	2.18	2.48	6.01×10^{-02}	3.40×10^{-23}	1.58
^{200}Po	^{196}Pb	5.98	3.79	3.99	4.98×10^{-02}	1.32×10^{-24}	2.98
^{202}Po	^{198}Pb	5.70	5.13	5.33	4.58×10^{-02}	6.77×10^{-26}	4.22
^{204}Po	^{200}Pb	5.48	6.28	6.44	4.32×10^{-02}	5.65×10^{-27}	5.26
^{206}Po	^{202}Pb	5.33	7.15	7.23	4.17×10^{-02}	9.67×10^{-28}	5.94
^{208}Po	^{204}Pb	5.22	7.97	7.82	4.08×10^{-02}	2.59×10^{-28}	6.46
^{210}Po	^{206}Pb	5.41	7.08	6.70	4.37×10^{-02}	3.10×10^{-27}	5.44
^{212}Po	^{208}Pb	8.95	-6.52	-6.61	1.54×10^{-01}	1.42×10^{-14}	-6.87
^{214}Po	^{210}Pb	7.83	-3.87	-3.48	1.12×10^{-01}	1.55×10^{-17}	-4.00
^{216}Po	^{212}Pb	6.90	-0.82	-0.26	7.56×10^{-02}	1.46×10^{-20}	-1.09
^{218}Po	^{214}Pb	6.11	2.27	2.98	6.29×10^{-02}	1.07×10^{-23}	1.90
Z=86							
^{198}Rn	^{194}Po	7.35	-1.19	-0.66	7.08×10^{-02}	3.72×10^{-20}	-1.22
^{200}Rn	^{196}Po	7.04	0.00	0.43	6.50×10^{-02}	3.34×10^{-21}	-0.25
^{202}Rn	^{198}Po	6.77	1.06	1.45	6.07×10^{-02}	3.54×10^{-22}	0.69

Table 4.1 continued

Parent Nuclei	Daughter Nuclei	Q	$log_{10}T_{1/2}^{exp}$	$log_{10}T_{1/2}^{cal}$	Po	Pnov	$log_{10}T_{1/2}^{NSR}$
		MeV	$T_{1/2}$ in s	$T_{1/2}$ in s			$T_{1/2}$ in s
^{204}Rn	^{200}Po	6.55	2.00	2.31	5.76×10^{-02}	5.18×10^{-23}	1.52
^{206}Rn	^{202}Po	6.38	2.71	3.05	5.05×10^{-02}	1.12×10^{-23}	2.18
^{208}Rn	^{204}Po	6.26	3.34	3.54	4.89×10^{-02}	3.72×10^{-24}	2.57
^{210}Rn	^{206}Po	6.16	3.96	3.96	4.78×10^{-02}	1.46×10^{-24}	2.97
^{212}Rn	^{208}Po	6.38	3.17	2.92	5.29×10^{-02}	1.43×10^{-23}	2.02
^{214}Rn	^{210}Po	9.21	-6.57	-6.54	1.42×10^{-01}	1.28×10^{-14}	-6.69
^{216}Rn	^{212}Po	8.20	-4.35	-3.82	1.09×10^{-01}	3.40×10^{-17}	-4.30
^{218}Rn	^{214} Po	7.26	-1.45	-0.76	8.05×10^{-02}	4.21×10^{-20}	-1.39
^{220}Rn	^{216} Po	6.40	1.75	2.64	6.01×10^{-02}	2.43×10^{-23}	1.74
^{222}Rn	^{218}Po	5.59	5.52	6.59	4.21×10^{-02}	4.22×10^{-27}	5.35
Z=88							
^{202}Ra	^{198}Rn	8.02	-2.58	-2.09	7.09×10^{-02}	9.54×10^{-19}	-2.60
^{204}Ra	^{200}Rn	7.64	-1.23	-0.91	6.88×10^{-02}	6.70×10^{-20}	-1.45
^{206}Ra	^{202}Rn	7.42	-0.62	-0.17	6.50×10^{-02}	1.33×10^{-20}	-0.75
^{208}Ra	^{204} Rn	7.27	0.15	0.33	6.30×10^{-02}	4.41×10^{-21}	-0.27
^{210}Ra	^{206} Rn	7.16	0.56	0.70	6.18×10^{-02}	1.93×10^{-21}	-0.01
^{212}Ra	^{208} Rn	7.03	1.15	1.16	6.02×10^{-02}	6.95×10^{-22}	0.43
^{214}Ra	^{210} Rn	7.27	0.40	0.21	6.57×10^{-02}	5.61×10^{-21}	-0.41
^{216}Ra	^{212} Rn	9.53	-6.74	-6.61	1.35×10^{-01}	1.56×10^{-14}	-6.78
^{218}Ra	^{214} Rn	8.55	-4.59	-4.07	1.05×10^{-01}	6.19×10^{-17}	-4.43
^{220}Ra	^{216} Rn	7.60	-1.74	-1.10	7.68×10^{-02}	9.62×10^{-20}	-1.70
^{222}Ra	^{218} Rn	6.68	1.59	2.41	5.27×10^{-02}	4.60×10^{-23}	1.54
^{224}Ra	^{220} Rn	5.79	5.53	6.55	3.92×10^{-02}	4.80×10^{-27}	5.43
^{226}Ra	^{222}Rn	4.87	10.73	11.95	3.22×10^{-02}	2.54×10^{-32}	10.59
Z=90							
^{210}Th	^{206}Ra	8.05	-1.77	-1.53	6.97×10^{-02}	2.74×10^{-19}	-2.05
^{212}Th	^{208} Ra	7.95	-1.44	-1.25	6.85×10^{-02}	1.45×10^{-19}	-1.77
^{214}Th	^{210} Ra	7.83	-1.00	-0.88	6.68×10^{-02}	6.50×10^{-20}	-1.41
^{216}Th	^{212} Ra	8.07	-1.55	-1.72	7.41×10^{-02}	4.02×10^{-19}	-2.24
^{218}Th	^{214} Ra	9.85	-7.00	-6.68	1.28×10^{-01}	1.92×10^{-14}	-6.82
^{220}Th	^{216} Ra	8.95	-5.01	-4.44	1.03×10^{-01}	1.43×10^{-16}	-4.75

Table 4.1 continued

Parent Nuclei	Daughter Nuclei	Q (MeV)	$log_{10}T_{1/2}^{exp}$ $T_{1/2}$ in s	$log_{10}T_{1/2}^{cal}$ $T_{1/2}$ in s	Po	Pnov	$log_{10}T_{1/2}^{NSR}$ $T_{1/2}$ in s
^{222}Th	^{218}Ra	8.13	-2.55	-2.00	7.22×10^{-02}	7.85×10^{-19}	-2.56
^{224}Th	^{220}Ra	7.30	0.11	0.81	6.01×10^{-02}	1.55×10^{-21}	0.17
^{226}Th	^{222}Ra	6.45	3.39	4.33	4.20×10^{-02}	7.17×10^{-25}	3.42
^{228}Th	^{224}Ra	5.52	7.92	9.00	3.46×10^{-02}	2.01×10^{-29}	7.90
^{230}Th	^{226}Ra	4.77	12.51	13.77	2.79×10^{-02}	4.54×10^{-34}	12.45
^{232}Th	^{228}Ra	4.08	17.76	19.34	2.03×10^{-02}	1.81×10^{-39}	–
Z=92							
^{218}U	^{214}Th	8.77	-3.29	-3.05	7.30×10^{-02}	8.26×10^{-18}	-3.31
^{220}U	^{216}Th	10.30	-7.22	-7.04	1.26×10^{-01}	4.36×10^{-14}	-6.81
^{224}U	^{220}Th	8.62	-3.15	-2.72	7.27×10^{-02}	3.97×10^{-18}	-3.30
^{226}U	^{222}Th	7.70	-0.30	0.20	5.91×10^{-02}	6.27×10^{-21}	-0.32
^{228}U	^{224}Th	6.80	2.76	3.72	4.08×10^{-02}	2.94×10^{-24}	-0.32
^{230}U	^{226}Th	5.99	6.43	7.46	3.51×10^{-02}	6.63×10^{-28}	2.88
^{232}U	^{228}Th	5.41	9.52	10.67	2.97×10^{-02}	5.04×10^{-31}	6.51
^{234}U	^{230}Th	4.86	13.02	14.29	2.29×10^{-02}	1.66×10^{-34}	9.58
^{236}U	^{232}Th	4.57	14.99	16.43	2.10×10^{-02}	1.37×10^{-36}	13.09
^{238}U	^{234}Th	4.27	17.27	18.86	1.93×10^{-02}	5.69×10^{-39}	15.14
Z=94							
^{228}Pu	^{224}U	7.95	-0.70	0.16	5.56×10^{-02}	7.19×10^{-21}	17.52
^{230}Pu	^{226}U	7.17	2.30	3.08	3.98×10^{-02}	1.27×10^{-23}	-0.31
^{232}Pu	^{228}U	6.72	4.20	4.95	3.52×10^{-02}	2.01×10^{-25}	2.42
^{234}Pu	^{230}U	6.31	5.72	6.79	3.43×10^{-02}	3.08×10^{-27}	4.12
^{236}Pu	^{232}U	5.87	8.11	9.03	3.02×10^{-02}	2.09×10^{-29}	5.95
^{238}Pu	^{234}U	5.59	9.59	10.59	2.81×10^{-02}	6.41×10^{-31}	8.10
^{240}Pu	^{236}U	5.26	11.50	12.63	2.34×10^{-02}	7.30×10^{-33}	9.61
^{242}Pu	^{238}U	4.98	13.20	14.48	2.14×10^{-02}	1.15×10^{-34}	11.48
^{244}Pu	^{240}U	4.66	15.50	16.81	1.95×10^{-02}	6.08×10^{-37}	13.30
Z=96							
^{240}Cm	^{236}Pu	6.40	6.52	7.24	3.14×10^{-02}	1.20×10^{-27}	15.55
^{242}Cm	^{238}Pu	6.22	7.28	8.10	3.01×10^{-02}	1.74×10^{-28}	6.42
^{242}Cm	^{240}Pu	5.90	8.88	9.77	2.77×10^{-02}	4.16×10^{-30}	7.26

Table 4.1 continued

Parent Nuclei	Daughter Nuclei	Q (MeV)	$log_{10}T_{1/2}^{exp}$ $T_{1/2}$ in s	$log_{10}T_{1/2}^{cal}$ $T_{1/2}$ in s	Po	Pnov	$log_{10}T_{1/2}^{NSR}$ $T_{1/2}$ in s
^{246}Cm	^{242}Pu	5.47	11.26	12.31	2.23×10^{-02}	1.57×10^{-32}	8.84
^{248}Cm	^{244}Pu	5.16	13.15	14.29	2.03×10^{-02}	1.86×10^{-34}	11.28
^{250}Cm	^{246}Pu	5.17	12.45	14.19	2.05×10^{-02}	2.33×10^{-34}	13.14
Z=98							
^{240}Cf	^{236}Cm	7.73	1.81	2.51	3.72×10^{-02}	4.93×10^{-23}	13.03
^{242}Cf	^{238}Cm	7.53	2.41	3.24	3.55×10^{-02}	9.82×10^{-24}	1.99
^{244}Cf	^{240}Cm	7.33	3.18	4.00	3.39×10^{-02}	1.81×10^{-24}	2.62
^{246}Cf	^{242}Cm	6.86	5.20	5.94	3.24×10^{-02}	2.24×10^{-26}	3.36
^{248}Cf	^{244}Cm	6.36	7.54	8.29	2.82×10^{-02}	1.21×10^{-28}	5.29
^{250}Cf	^{246}Cm	6.13	8.69	9.45	2.67×10^{-02}	9.07×10^{-30}	7.47
^{252}Cf	^{248}Cm	6.22	8.00	8.94	2.75×10^{-02}	2.81×10^{-29}	8.55
^{254}Cf	^{250}Cm	5.93	9.30	10.47	2.56×10^{-02}	9.08×10^{-31}	8.08
Z=100							
^{246}Fm	^{242}Cf	8.37	0.08	0.97	4.03×10^{-02}	1.53×10^{-21}	9.53
^{248}Fm	^{244}Cf	8.00	1.65	2.23	3.64×10^{-02}	9.52×10^{-23}	1.72
^{250}Fm	^{246}Cf	7.56	3.25	3.87	3.25×10^{-02}	2.53×10^{-24}	3.31
^{252}Fm	^{248}Cf	7.15	5.04	5.49	3.16×10^{-02}	6.39×10^{-26}	4.87
^{254}Fm	^{250}Cf	7.31	4.15	4.78	3.36×10^{-02}	3.11×10^{-25}	4.15
^{256}Fm	^{252}Cf	7.03	5.15	5.94	3.10×10^{-02}	2.33×10^{-26}	5.29
Z=102							
^{250}No	^{246}Fm	8.96	-0.30	-0.21	4.27×10^{-02}	2.13×10^{-20}	-0.41
^{252}No	^{248}Fm	8.55	0.62	1.08	3.80×10^{-02}	1.26×10^{-21}	0.77
^{254}No	^{250}Fm	8.23	1.86	2.15	3.49×10^{-02}	1.18×10^{-22}	1.81
^{256}No	^{252}Fm	8.58	0.56	0.90	3.91×10^{-02}	1.84×10^{-21}	0.58

4.4 Preformation probability of alpha in superheavy nuclei with Z= 104 to 125

Fig.4.12 to Fig. 4.33 represents the logarithmic preformation probability values against the daughter neutron number, N_1 for superheavy nuclei with Z=104 to 125 respectively.

In Fig. 4.12 $log_{10}P_o$ values od Rf isotopes are presented, against daughter neutron number, N_1. Generally $log_{10}P_o$ decreases as N_1 increases. However small peaks are observed at N_1=140, 152, 164, 176. In case of Db isotopes, presented in Fig.4.13, a sharp rise is noted at N_1=184, apart from decreases in $log_{10}P_o$ value as N_1 increases.

Similar behaviour as that of Rf isotopes is observed in $log_{10}P_o$ values of isotopes of Sg, Bh, Mt, Rg, CN, Fl isotopes in Figures 4.14, 4.15, 4.17, 4.19, 4.20 and 4.22 respectively.

In case of Hs isotopes, an odd-even structure is noted in $log_{10}P_o$ values, as seen in Fig. 4.16. A similar behaviour noted in Ds isotopes in Fig. 4.18. Consistently, high value of $log_{10}P_o$ is noted for isotopes of Ts, Og, Z=119, 120, 121, 122, 123, 124, 125, at N_1=184, which is a predicted magic number, in Figures 4.25 to 4.33 respectively.

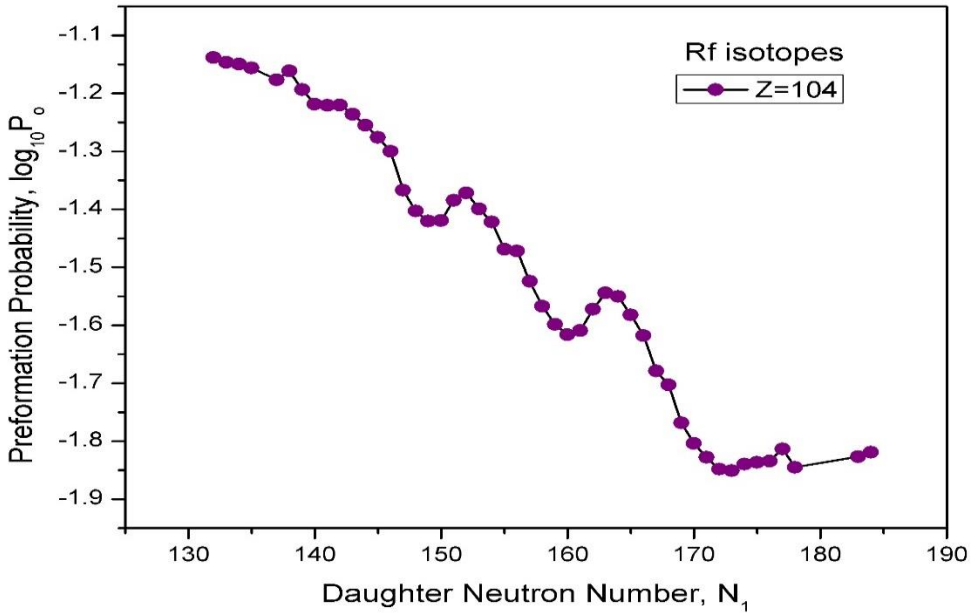

Fig. 4.12 Logarithmic preformation probability values against daughter neutron number, N_1, for Rf isotopes (48 isotopes).

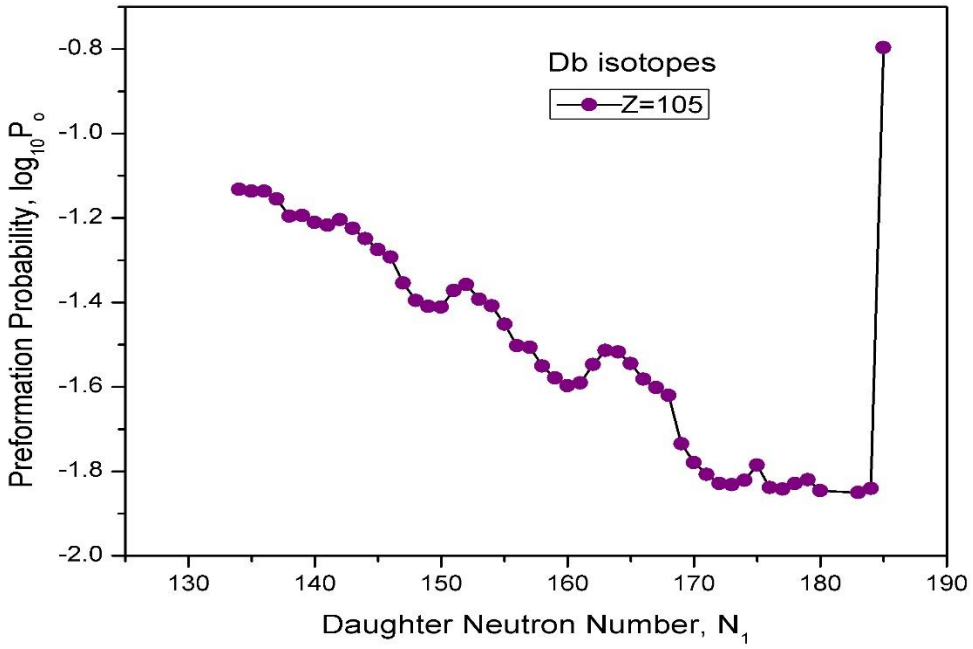

Fig. 4.13 Logarithmic preformation probability values against daughter neutron number, N_1, for Db isotopes (50 isotopes).

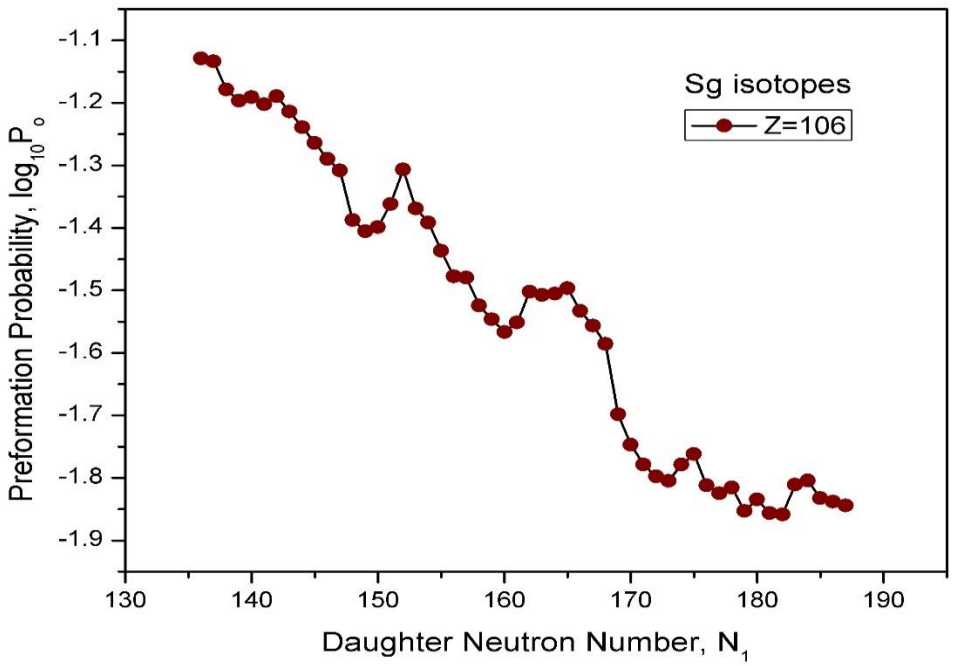

Fig. 4.14 Logarithmic preformation probability values against daughter neutron number, N_1, for Sg isotopes (52 isotopes).

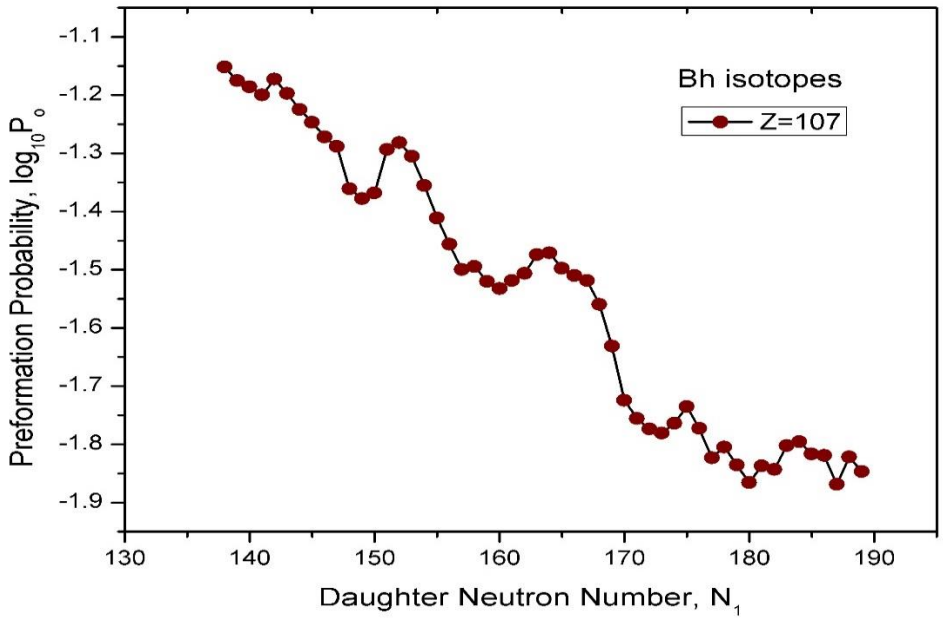

Fig. 4.15 Logarithmic preformation probability values against daughter neutron number, N_1, for Bh isotopes (52 isotopes).

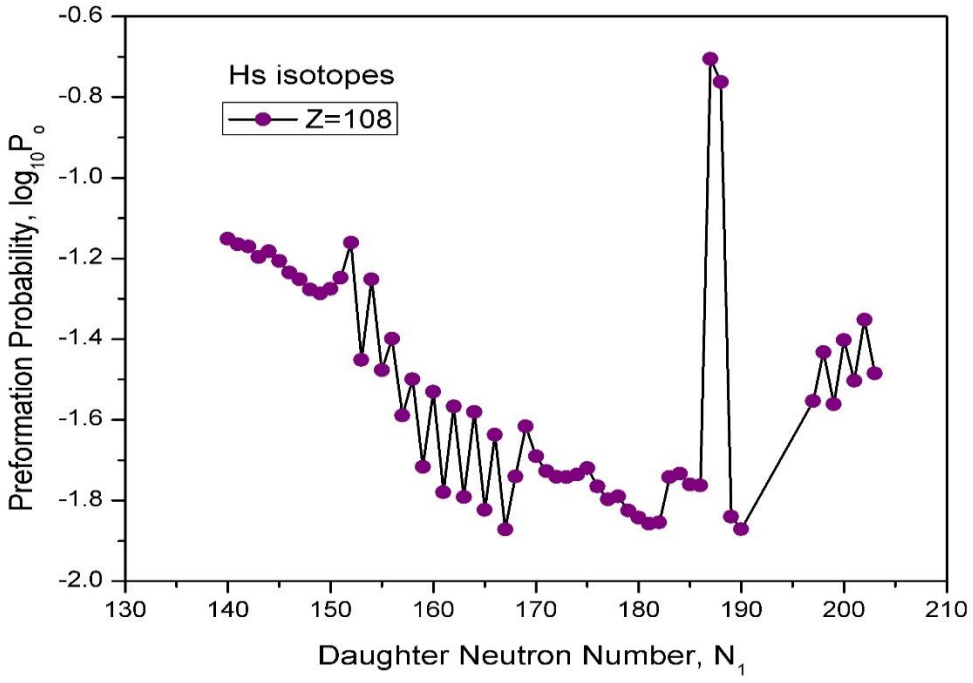

Fig. 4.16 Logarithmic preformation probability values against daughter neutron number, N_1, for Hs isotopes (58 isotopes).

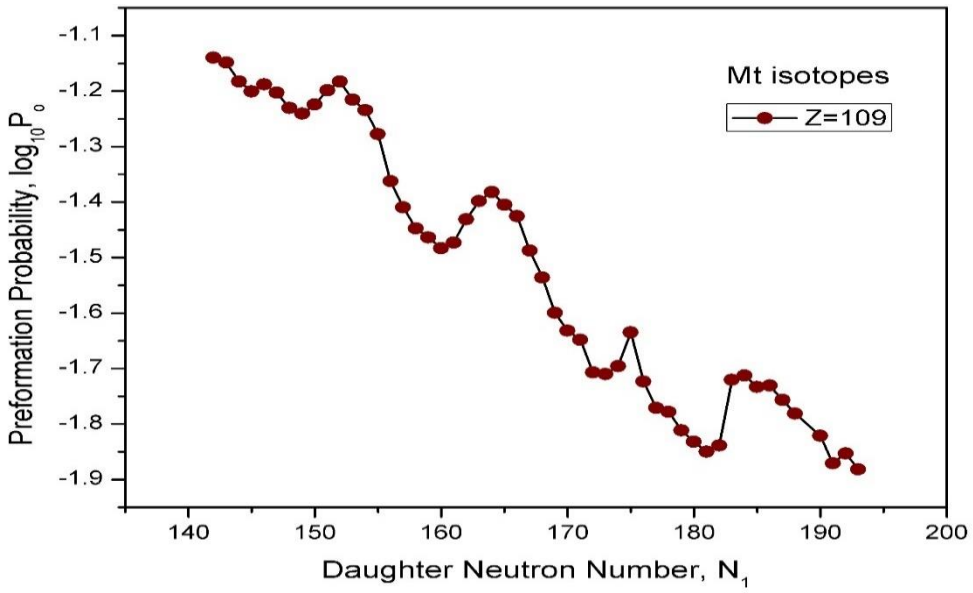

Fig. 4.17 Logarithmic preformation values against daughter neutron number, N_1, for Mt isotopes (51 isotopes).

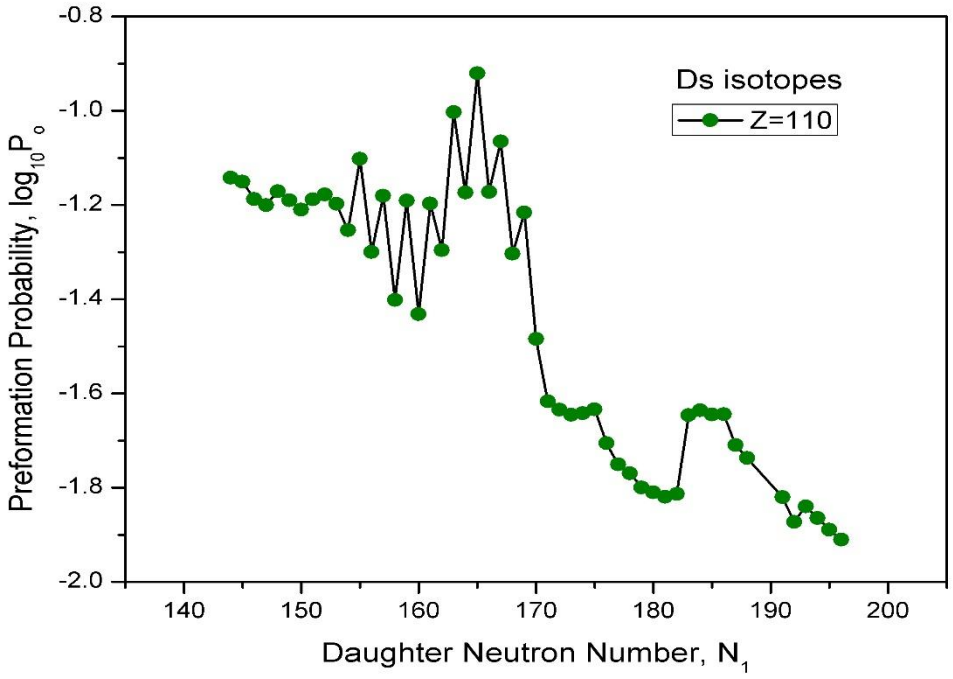

Fig. 4.18 Logarithmic preformation probability values against daughter neutron number, N_1, for Ds isotopes (51 isotopes).

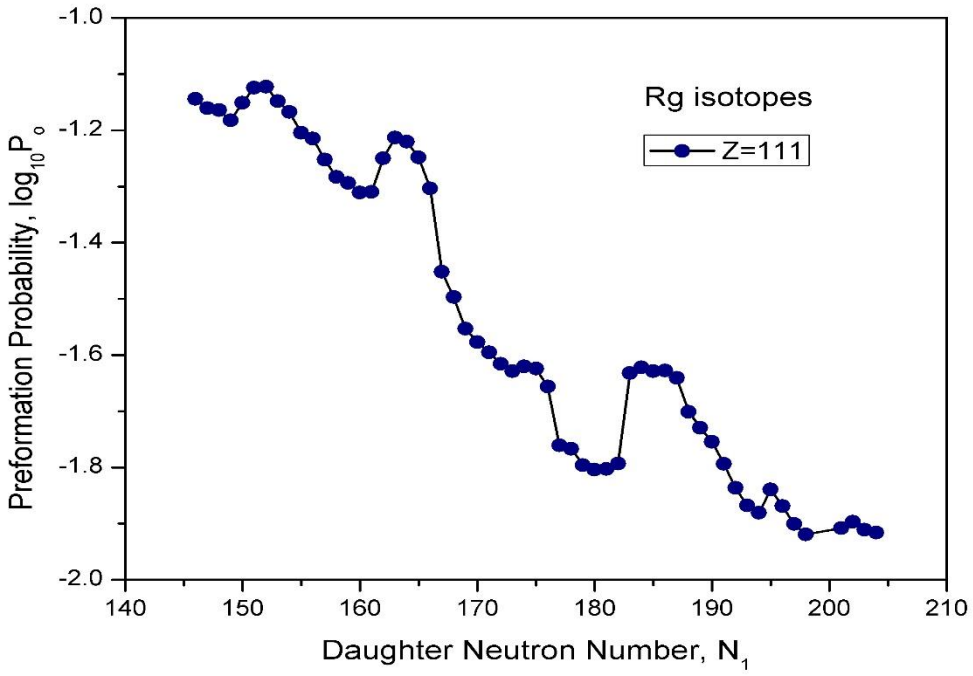

Fig. 4.19 Logarithmic preformation probability values against daughter neutron number, N_1, for Rg isotopes (57 isotopes).

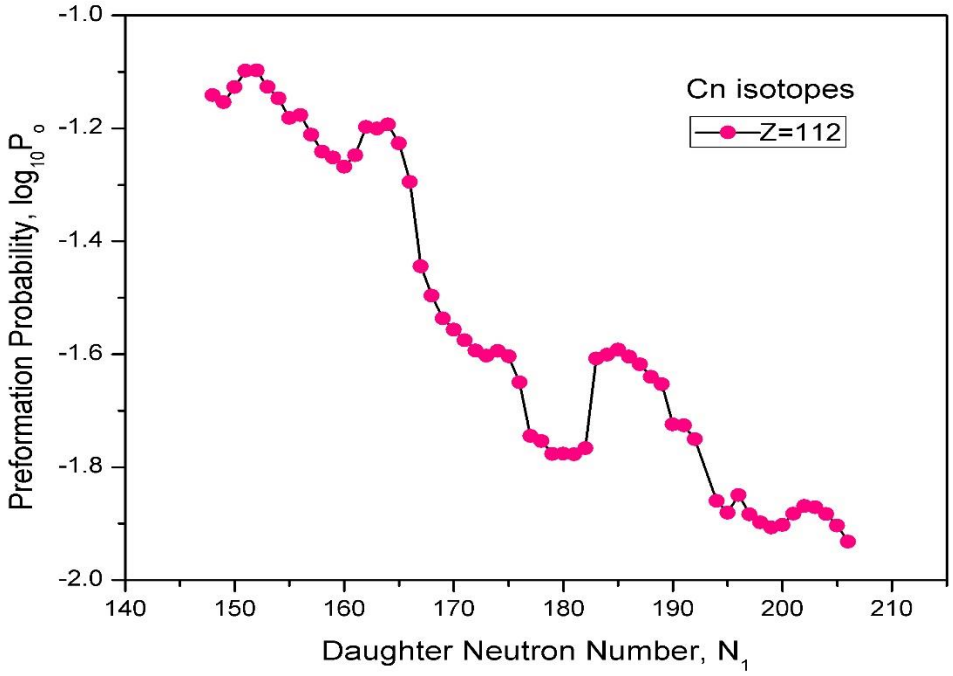

Fig. 4.20 Logarithmic preformation probability values against daughter neutron number, N_1, for Cn isotopes (58 isotopes).

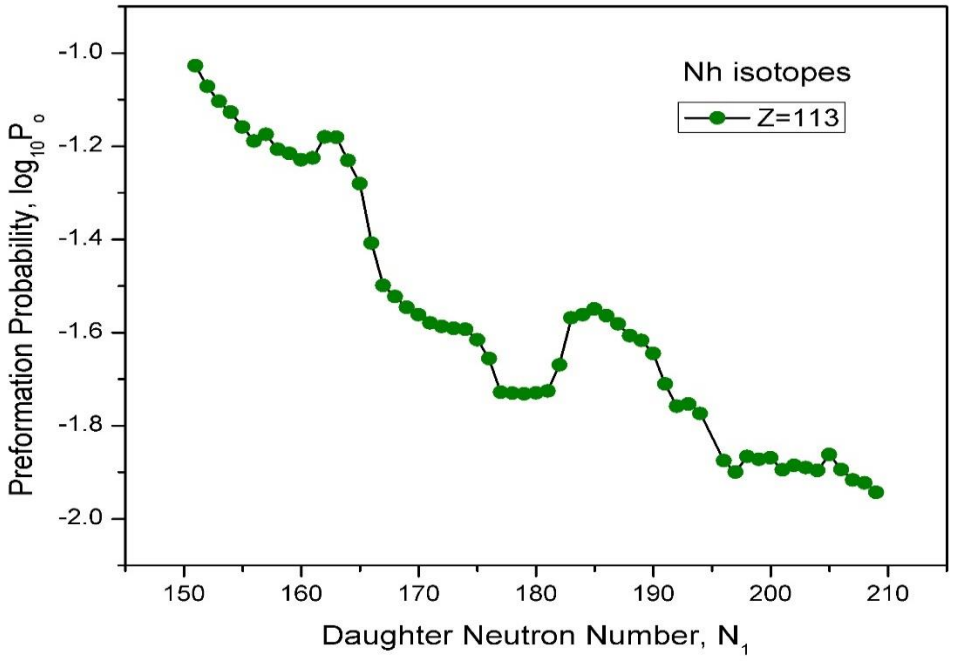

Fig. 4.21 Logarithmic preformation probability values against daughter neutron number, N_1, for Nh isotopes (58 isotopes).

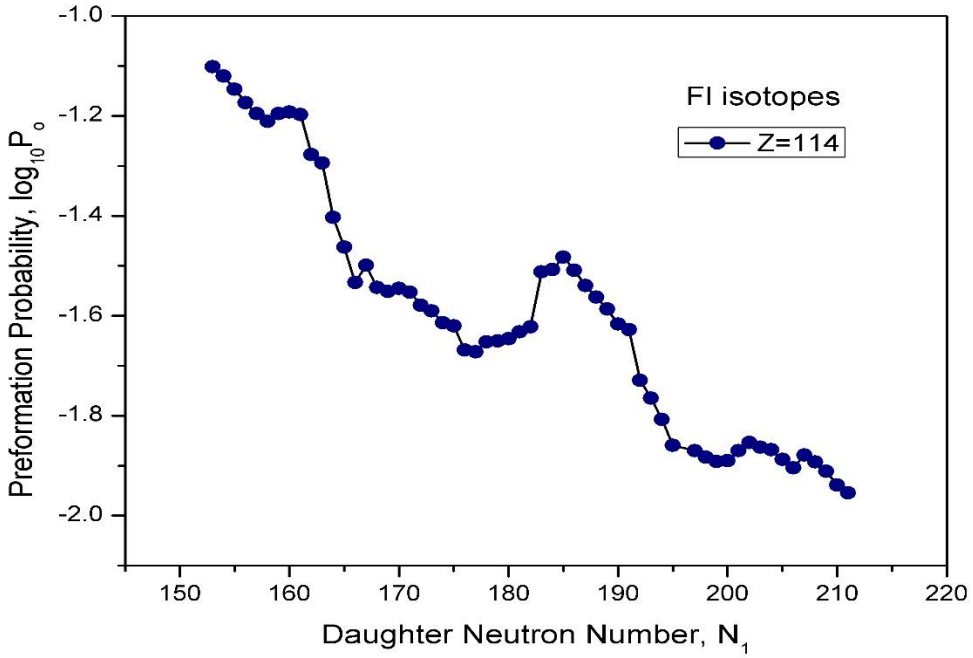

Fig. 4.22 Logarithmic preformation probability values against daughter neutron number, N_1, for Fl isotopes (58 isotopes).

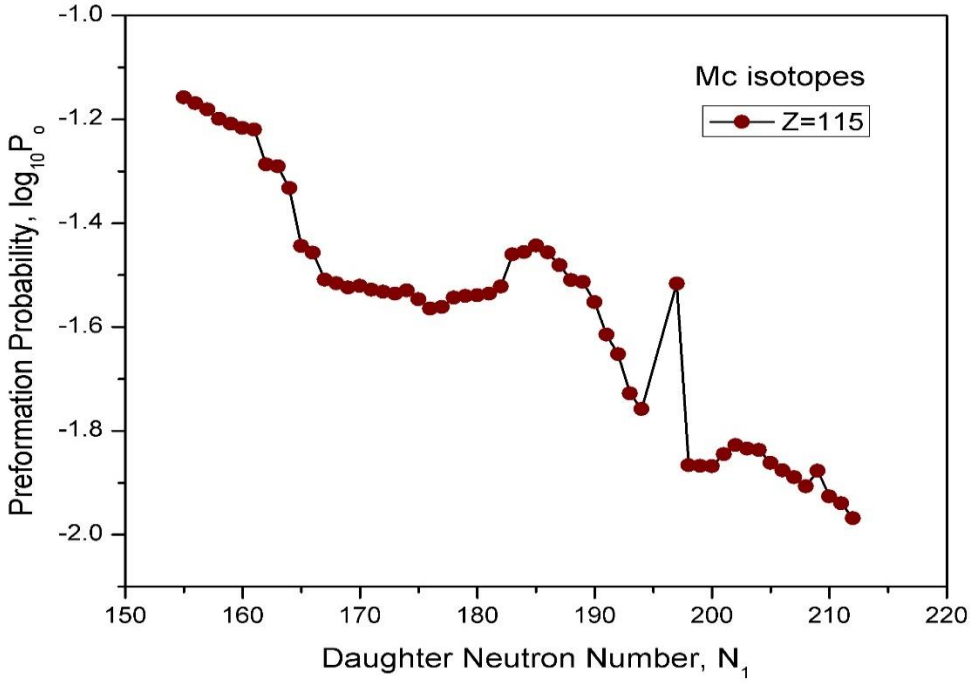

Fig. 4.23 Logarithmic preformation probability values against daughter neutron number, N_1, for Mc isotopes (56 isotopes).

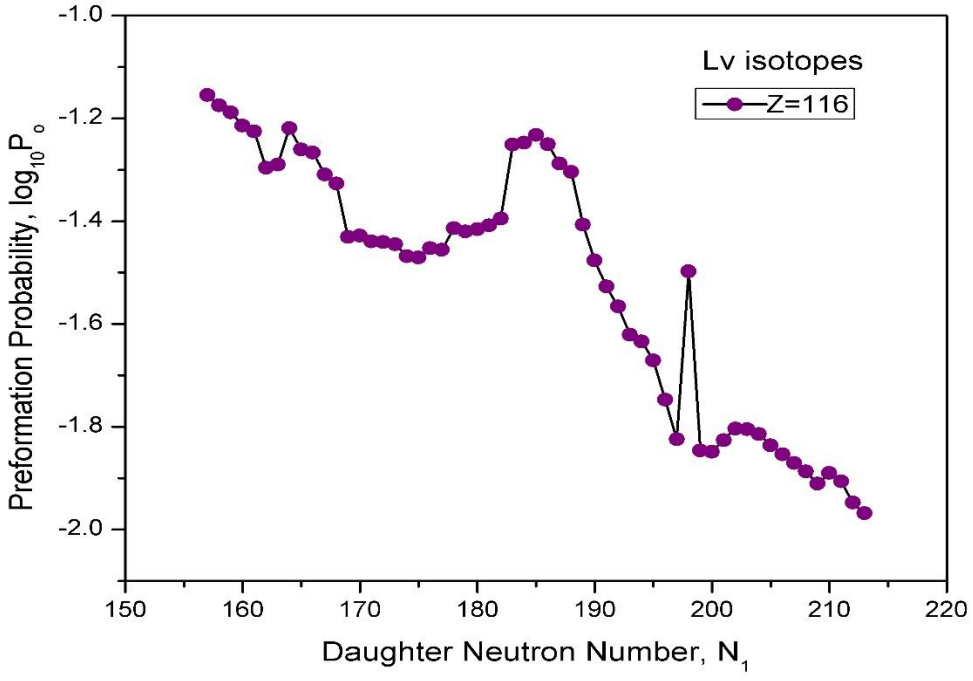

Fig. 4.24 Logarithmic preformation probability values against daughter neutron number, N_1, for Lv isotopes (57 isotopes).

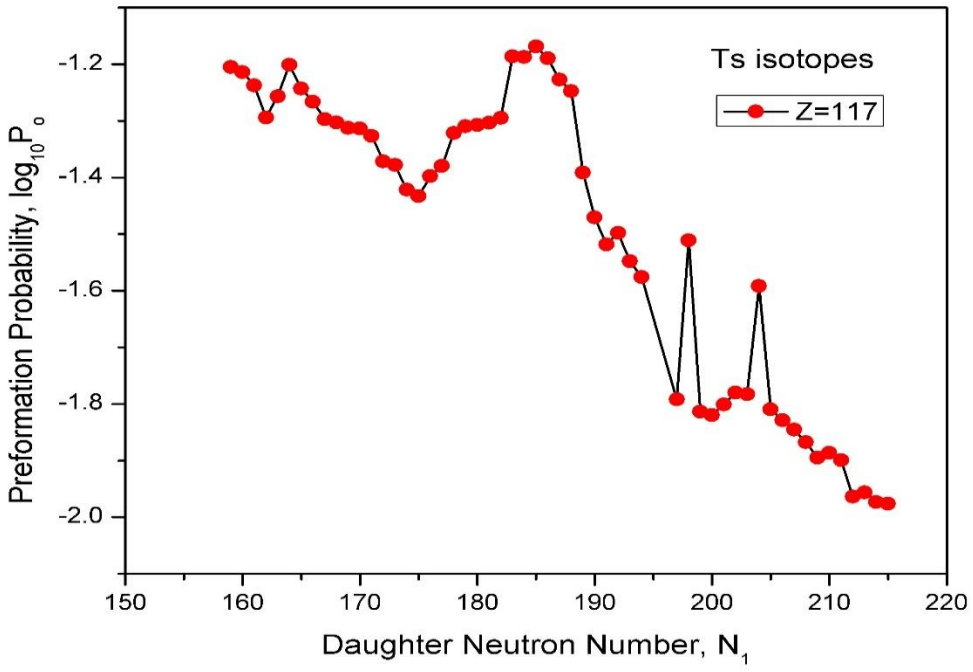

Fig. 4.25 Logarithmic preformation probability values against daughter neutron number, N_1, for Ts isotopes (55 isotopes).

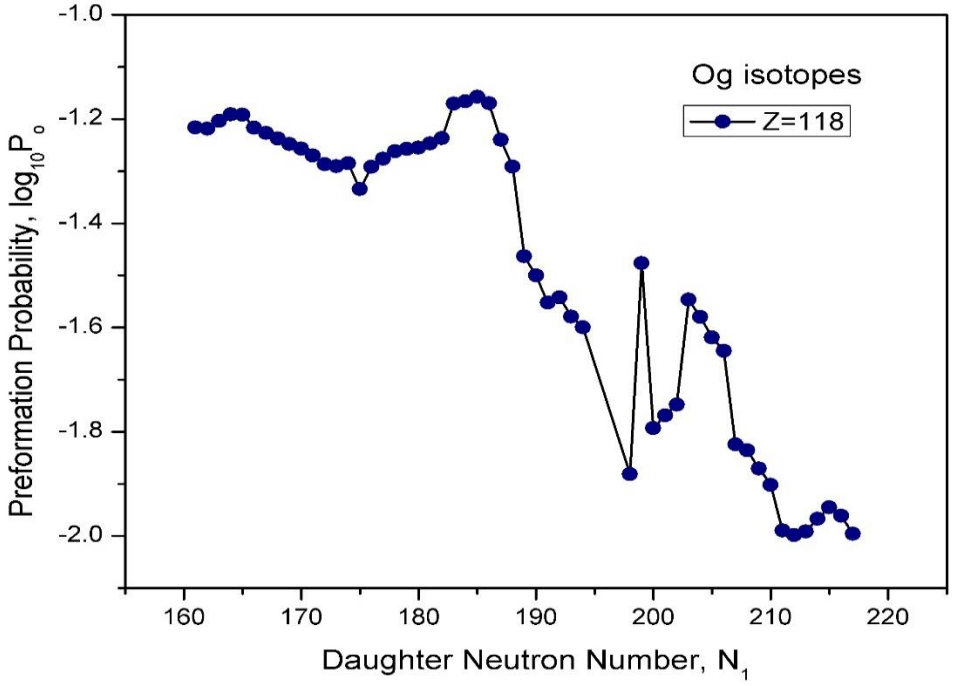

Fig. 4.26 Logarithmic preformation probability values against daughter neutron number, N_1, for Og isotopes (54 isotopes).

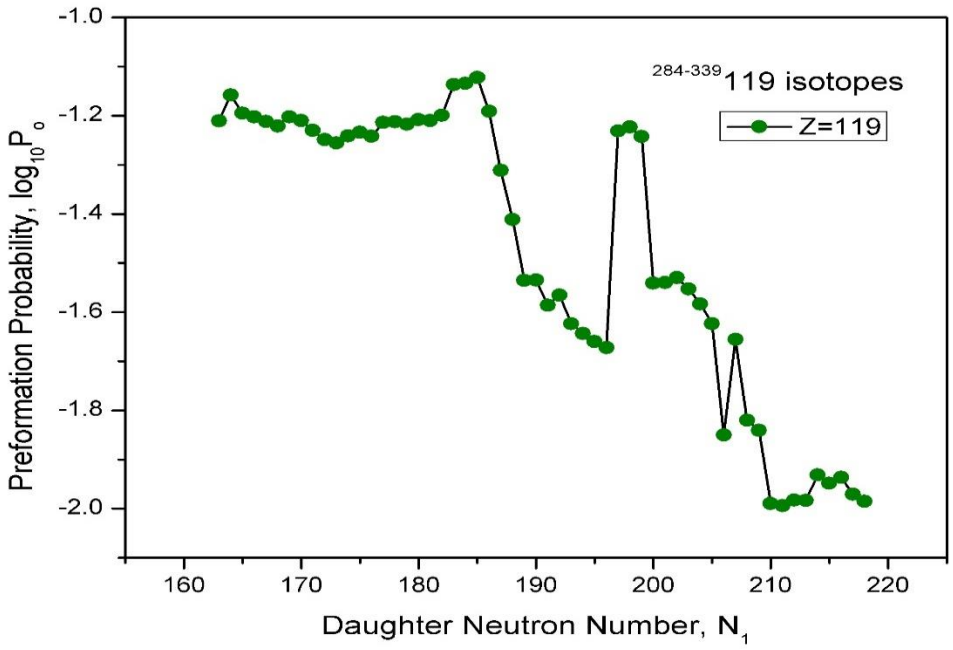

Fig. 4.27 Logarithmic preformation probability values against daughter neutron number, N_1, for $^{284\text{-}339}$ 119 isotopes (56 isotopes).

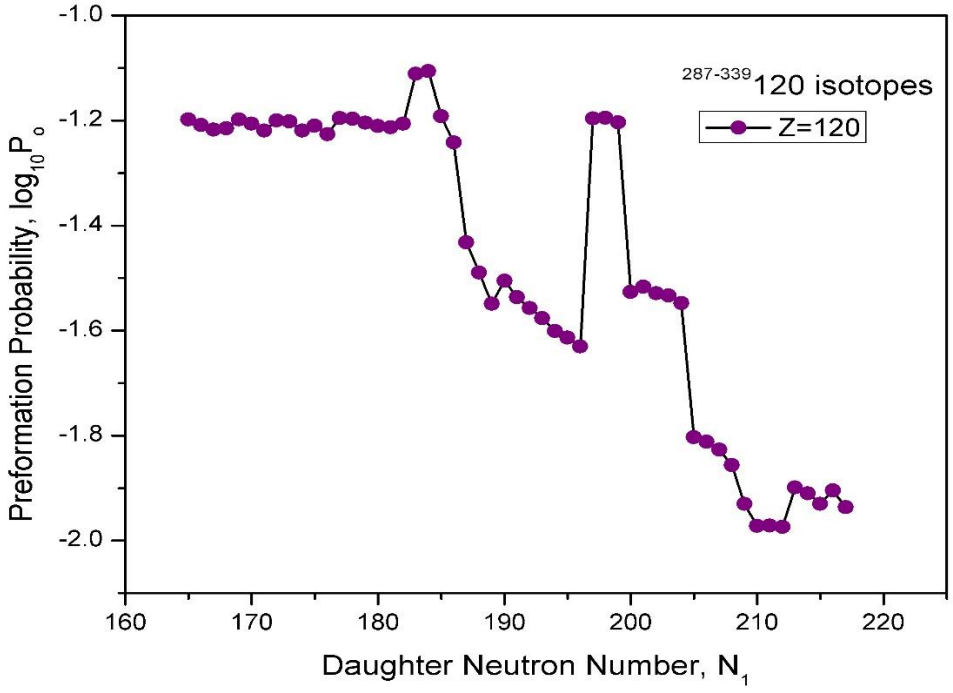

Fig. 4.28 Logarithmic preformation probability values against daughter neutron number, N_1, for $^{287\text{-}339}$ 120 isotopes(53 isotopes).

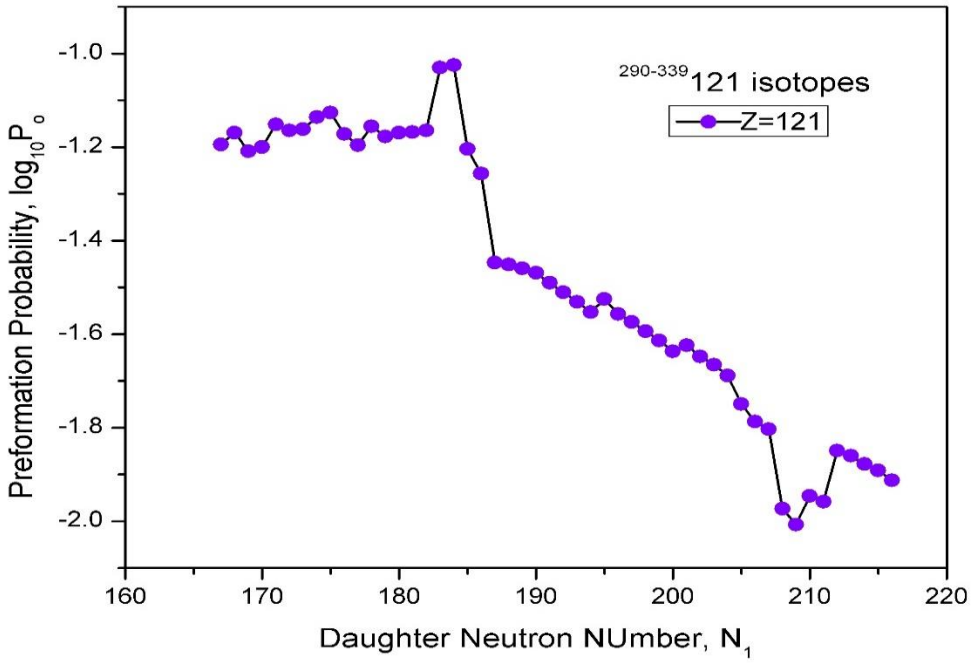

Fig. 4.29 Logarithmic preformation probability values against daughter neutron number, N_1, for $^{290\text{-}339}121$ isotopes (50).

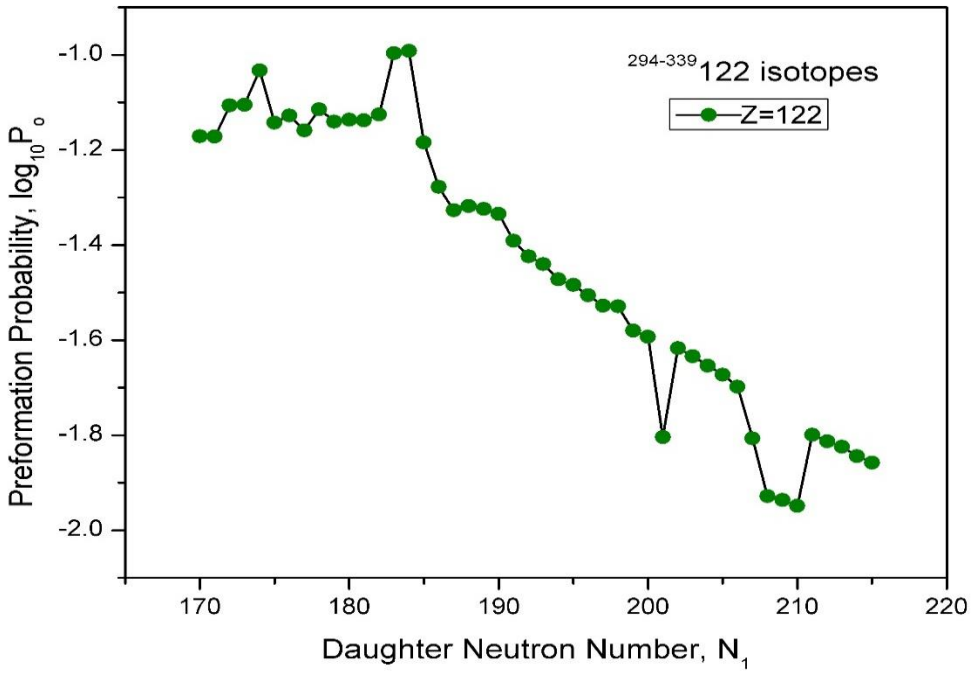

Fig. 4.30 Logarithmic preformation probability values against daughter neutron number, N_1, for $^{294\text{-}339}122$ isotopes (46 isotopes).

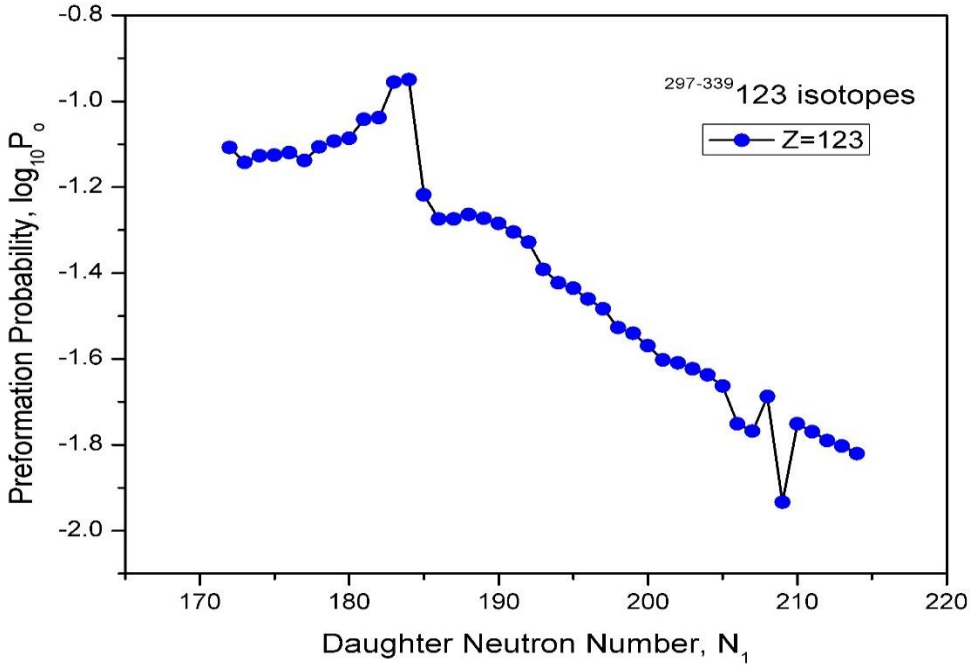

Fig. 4.31 Logarithmic preformation probability values against daughter neutron number, N_1, for $^{297-339}$123 isotopes (43 isotopes).

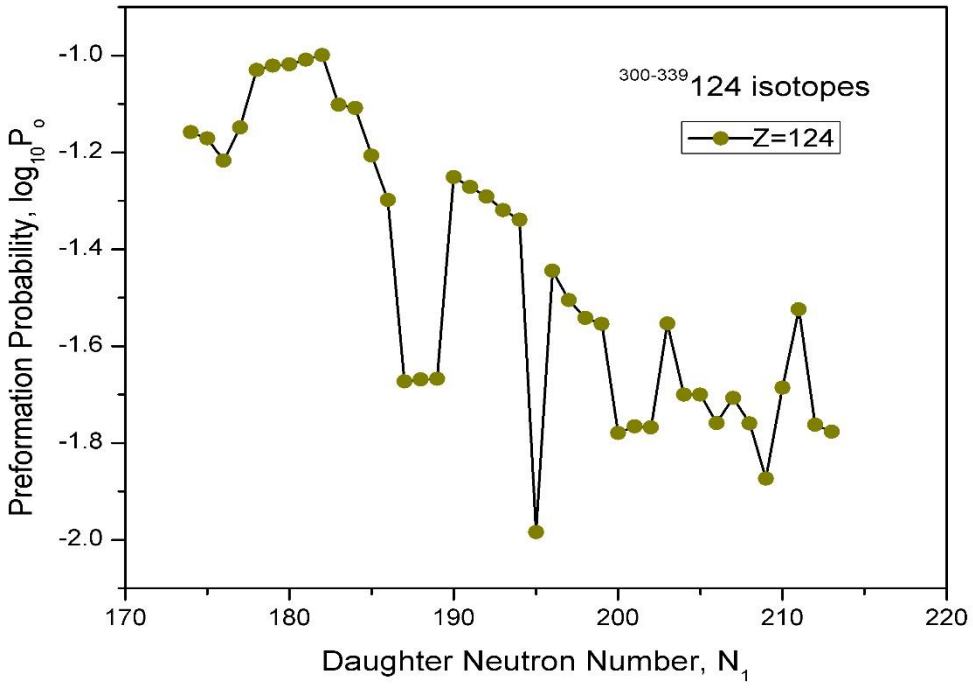

Fig. 4.32 Logarithmic preformation probability values against daughter neutron number, N_1, for $^{300-339}$124 isotopes (40 isotopes).

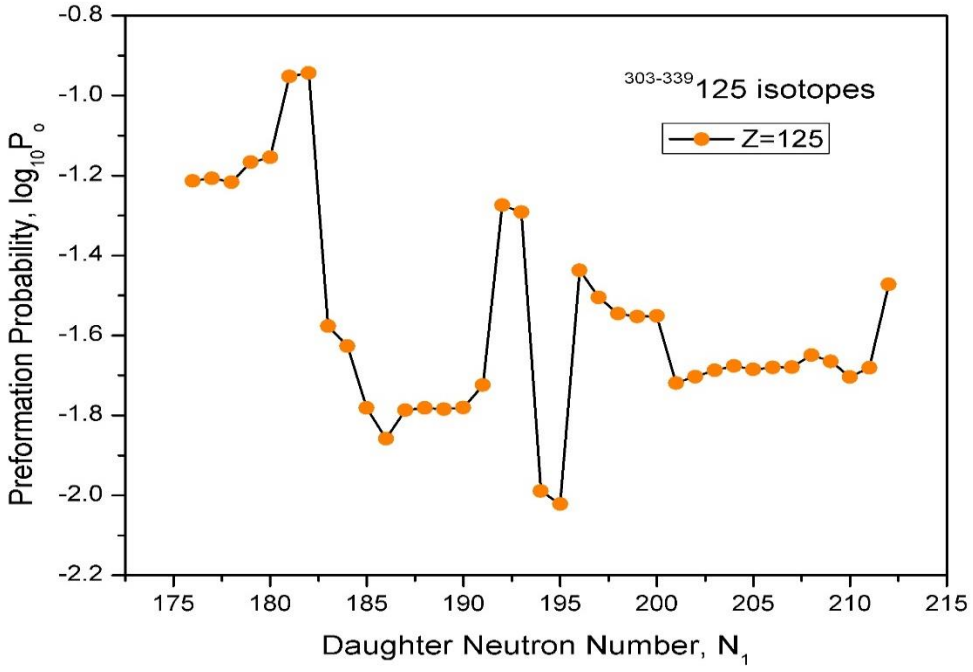

Fig. 4.33 Logarithmic preformation probability values against daughter neutron number, N_1, for $^{303\text{-}339}125$ isotopes (37 isotopes).

4.4 Half-lives of alpha decay of superheavy nuclei with Z= 104 to 125

Table 4.2 represents the half-lives of alpha decay of 1140 cases of superheavy nuclei with Z=104 to 125. First and sixth column represents the parent nuclus, the second and seventh column represent the daughter nuclei. The third and eighth column represents the Q value. Fourth and ninth column represent the calculate half-lives of superheavy nuclei. The calculated half-lives of superheavy nuclei are compared with other work **[104,105]**. The calculated logarithmic half-lives match well with the experimental half-lives.

Fig.4.34 is a contour map of half-lives of nearly 1140 cases of superheavy nuclei. Half-life is calculated for the experimentally synthesized superheavy nuclei with the atomic number ranges from $104 \leq Z \leq 125$ with the mass number ranges from $238 \leq A \leq 331$ and is represented as a contour plot in Fig. 4.34. This plot shows that the nuclei which are having half-life values below 10^4 s are prone to one-proton emission. And the nuclei having half-life greater than 10^4 s are said to have a larger half-life and it will take longer time for its decay. This plot is represented as $log_{10}T_{1/2}$ values. Hence nuclei with half-life greater than 7 are highly stable.

Table 4.2 Calculated logarithmic half- lives of super heavy nuclei with Z=104 to 125. Calculated logarithmic half -lives of 1140 cases of alpha decay of heavy nuclei are compared with other work **[105, 106]**.

Parent nuclei	Daughter Nuclei	Q	$\log_{10}T_{1/2}$	$log_{10}T_{1/2}^{Om}$	Parent nuclei	Daughter nuclei	Q	$\log_{10}T_{1/2}$	$log_{10}T_{1/2}^{Om}$
		MeV	$T_{1/2}$ in s	$T_{1/2}$ in s			MeV	$T_{1/2}$ in s	$T_{1/2}$ in s
Z=104									
^{238}Rf	^{234}No	11.46	-5.77	–	^{268}Rf	^{264}No	7.25	6.62	–
^{239}Rf	^{235}No	11.37	-5.59	–	^{269}Rf	^{265}No	7.47	5.66	–
^{240}Rf	^{236}No	11.32	-5.51	–	^{270}Rf	^{266}No	7.41	5.90	–
^{241}Rf	^{237}No	11.24	-5.35	–	^{271}Rf	^{267}No	7.13	7.10	–
^{243}Rf	^{239}No	11.03	-4.91	–	^{272}Rf	^{268}No	6.81	8.58	–
^{244}Rf	^{240}No	10.8	-4.43	–	^{273}Rf	^{269}No	6.65	9.40	–
^{245}Rf	^{241}No	10.59	-3.93	–	^{274}Rf	^{270}No	6.48	10.25	–
^{246}Rf	^{242}No	10.39	-3.44	–	^{275}Rf	^{271}No	5.96	13.13	–
^{247}Rf	^{243}No	10.35	-3.36	–	^{276}Rf	^{272}No	5.65	15.03	–
^{248}Rf	^{244}No	10.33	-3.33	–	^{277}Rf	^{273}No	5.43	16.47	–
^{249}Rf	^{245}No	10.19	-2.99	–	^{278}Rf	^{274}No	5.24	17.78	–
^{250}Rf	^{246}No	10.02	-2.55	–	^{279}Rf	^{275}No	5.21	17.98	–
^{251}Rf	^{247}No	9.83	-2.06	–	^{280}Rf	^{276}No	5.3	17.32	–
^{252}Rf	^{248}No	9.61	-1.46	–	^{281}Rf	^{277}No	5.32	17.17	–
^{253}Rf	^{249}No	9.4	-0.82	–	^{282}Rf	^{278}No	4.95	19.86	–
^{254}Rf	^{250}No	9.13	-0.02	–	^{283}Rf	^{279}No	5.09	18.76	–
^{255}Rf	^{251}No	8.98	0.43	–	^{284}Rf	^{280}No	5.22	17.83	–
^{256}Rf	^{252}No	8.97	0.44	1.09	^{289}Rf	^{285}No	4.97	19.59	–
^{257}Rf	^{253}No	9.21	-0.32	–	^{290}Rf	^{286}No	5.02	19.18	–
^{258}Rf	^{254}No	9.28	-0.55	-0.39	**Z=105**				
^{259}Rf	^{255}No	9.07	0.07	–	^{241}Db	^{237}Lr	11.69	-6.00	–
^{260}Rf	^{256}No	8.88	0.66	–	^{242}Db	^{238}Lr	11.63	-5.89	–
^{261}Rf	^{257}No	8.49	1.95	–	^{243}Db	^{239}Lr	11.6	-5.84	–
^{262}Rf	^{258}No	8.1	3.29	–	^{244}Db	^{240}Lr	11.44	-5.51	–
^{263}Rf	^{259}No	7.71	4.78	3.30	^{245}Db	^{241}Lr	11.09	-4.74	–
^{264}Rf	^{260}No	7.35	6.26	–	^{246}Db	^{242}Lr	10.82	-4.15	–
^{265}Rf	^{261}No	7.07	7.48	–	^{247}Db	^{243}Lr	10.68	-3.83	–
^{266}Rf	^{262}No	6.9	8.26	–	^{248}Db	^{244}Lr	10.61	-3.68	–
^{267}Rf	^{263}No	6.95	8.00	–	^{249}Db	^{245}Lr	10.68	-3.87	–

Table 4.2 continued

Parent nuclei	Daughter nuclei	Q MeV	$\log_{10}T_{1/2}$ $T_{1/2}$ in s	$log_{10}T_{1/2}^{Om}$ $T_{1/2}$ in s	Parent nuclei	Daughter nuclei	Q MeV	$\log_{10}T_{1/2}$ $T_{1/2}$ in s	$log_{10}T_{1/2}^{Om}$ $T_{1/2}$ in s
^{250}Db	^{246}Lr	10.51	-3.46	–	^{282}Db	^{278}Lr	5.96	13.54	–
^{251}Db	^{247}Lr	10.3	-2.95	–	^{283}Db	^{279}Lr	5.49	16.52	–
^{252}Db	^{248}Lr	10.07	-2.36	–	^{284}Db	^{280}Lr	5.45	16.77	–
^{253}Db	^{249}Lr	9.9	-1.91	–	^{285}Db	^{281}Lr	5.56	16.01	–
^{254}Db	^{250}Lr	9.7	-1.33	–	^{286}Db	^{282}Lr	5.21	18.39	–
^{255}Db	^{251}Lr	9.41	-0.50	–	^{287}Db	^{283}Lr	5.02	19.82	–
^{256}Db	^{252}Lr	9.29	-0.15	–	^{288}Db	^{284}Lr	5.33	17.51	–
^{257}Db	^{253}Lr	9.26	-0.08	1.04	^{289}Db	^{285}Lr	5.41	16.93	–
^{258}Db	^{254}Lr	9.52	-0.88	0.78	^{290}Db	^{286}Lr	13.07	-9.62	–
^{259}Db	^{255}Lr	9.59	-1.11	-0.101	**Z=106**				
^{260}Db	^{256}Lr	9.34	-0.38	–	^{244}Sg	^{240}Rf	11.9	-6.17	–
^{261}Db	^{257}Lr	9.21	0.00	–	^{245}Sg	^{241}Rf	11.84	-6.06	–
^{262}Db	^{258}Lr	8.85	1.13	–	^{246}Sg	^{242}Rf	11.47	-5.28	–
^{263}Db	^{259}Lr	8.41	2.61	1.62	^{247}Sg	^{243}Rf	11.3	-4.91	–
^{264}Db	^{260}Lr	8.06	3.83	1.10	^{248}Sg	^{244}Rf	11.05	-4.39	–
^{265}Db	^{261}Lr	7.7	5.23	–	^{249}Sg	^{245}Rf	10.95	-4.17	–
^{266}Db	^{262}Lr	7.45	6.25	–	^{250}Sg	^{246}Rf	11.01	-4.34	–
^{267}Db	^{263}Lr	7.28	6.97	–	^{251}Sg	^{247}Rf	10.82	-3.90	–
^{268}Db	^{264}Lr	7.32	6.78	–	^{252}Sg	^{248}Rf	10.61	-3.39	–
^{269}Db	^{265}Lr	7.67	5.28	–	^{253}Sg	^{249}Rf	10.39	-2.85	–
^{270}Db	^{266}Lr	7.92	4.26	–	^{254}Sg	^{250}Rf	10.16	-2.27	–
^{271}Db	^{267}Lr	7.88	4.40	–	^{255}Sg	^{251}Rf	9.98	-1.80	–
^{272}Db	^{268}Lr	7.65	5.31	–	^{256}Sg	^{252}Rf	9.69	-0.95	–
^{273}Db	^{269}Lr	7.33	6.64	–	^{257}Sg	^{253}Rf	9.54	-0.53	–
^{274}Db	^{270}Lr	7.15	7.43	–	^{258}Sg	^{254}Rf	9.57	-0.64	–
^{275}Db	^{271}Lr	6.97	8.24	–	^{259}Sg	^{255}Rf	9.8	-1.33	-0.04
^{276}Db	^{272}Lr	6.43	10.98	–	^{260}Sg	^{256}Rf	9.89	-1.64	-1.00
^{277}Db	^{273}Lr	6.06	13.03	–	^{261}Sg	^{257}Rf	9.72	-1.14	-0.27
^{278}Db	^{274}Lr	5.81	14.52	–	^{262}Sg	^{258}Rf	9.55	-0.66	-0.86
^{279}Db	^{275}Lr	5.61	15.78	–	^{263}Sg	^{259}Rf	9.19	0.42	–
^{280}Db	^{276}Lr	5.58	15.96	–	^{264}Sg	^{260}Rf	8.84	1.53	–
^{281}Db	^{277}Lr	5.66	15.43	–	^{265}Sg	^{261}Rf	8.45	2.80	–

Table 4.2 continued

Parent nuclei	Daughter nuclei	Q (MeV)	$\log_{10}T_{1/2}$ $T_{1/2}$ in s	$log_{10}T_{1/2}^{Om}$ $T_{1/2}$ in s	Parent nuclei	Daughter nuclei	Q (MeV)	$\log_{10}T_{1/2}$ $T_{1/2}$ in s	$log_{10}T_{1/2}^{Om}$ $T_{1/2}$ in s
^{266}Sg	^{262}Rf	8.12	4.00	–	^{248}Bh	^{244}Db	11.71	-5.51	–
^{267}Sg	^{263}Rf	7.93	4.71	0.79	^{249}Bh	^{245}Db	11.6	-5.29	–
^{268}Sg	^{264}Rf	7.75	5.41	–	^{250}Bh	^{246}Db	11.46	-5.00	–
^{269}Sg	^{265}Rf	7.86	4.96	1.785	^{251}Bh	^{247}Db	11.34	-4.78	–
^{270}Sg	^{266}Rf	8.23	3.52	1.775	^{252}Bh	^{248}Db	11.17	-4.40	–
^{271}Sg	^{267}Rf	8.48	2.64	–	^{253}Bh	^{249}Db	10.95	-3.90	–
^{272}Sg	^{268}Rf	8.48	2.62	–	^{254}Bh	^{250}Db	10.76	-3.45	–
^{273}Sg	^{269}Rf	8.23	3.47	3.49	^{255}Bh	^{251}Db	10.54	-2.92	–
^{274}Sg	^{270}Rf	7.94	4.55	–	^{256}Bh	^{252}Db	10.38	-2.52	–
^{275}Sg	^{271}Rf	7.74	5.33	–	^{257}Bh	^{253}Db	10.08	-1.70	–
^{276}Sg	^{272}Rf	7.48	6.40	–	^{258}Bh	^{254}Db	9.96	-1.39	–
^{277}Sg	^{273}Rf	6.89	9.11	–	^{259}Bh	^{255}Db	10	-1.51	–
^{278}Sg	^{274}Rf	6.52	10.97	–	^{260}Bh	^{256}Db	10.25	-2.26	-0.97
^{279}Sg	^{275}Rf	6.25	12.42	–	^{261}Bh	^{257}Db	10.33	-2.48	-1.46
^{280}Sg	^{276}Rf	6.08	13.38	–	^{262}Bh	^{258}Db	10.11	-1.92	–
^{281}Sg	^{277}Rf	6.01	13.78	–	^{263}Bh	^{259}Db	10.00	-1.59	–
^{282}Sg	^{278}Rf	6.22	12.54	–	^{264}Bh	^{260}Db	9.61	-0.48	-0.39
^{283}Sg	^{279}Rf	6.35	11.80	–	^{265}Bh	^{261}Db	9.24	0.62	–
^{284}Sg	^{280}Rf	5.92	14.27	–	^{266}Bh	^{262}Db	8.86	1.83	0.29
^{285}Sg	^{281}Rf	5.8	15.00	–	^{267}Bh	^{263}Db	8.55	2.83	1.02
^{286}Sg	^{282}Rf	5.87	14.55	–	^{268}Bh	^{264}Db	8.35	3.54	–
^{287}Sg	^{283}Rf	5.53	16.73	–	^{269}Bh	^{265}Db	8.24	3.93	–
^{288}Sg	^{284}Rf	5.28	18.42	–	^{270}Bh	^{266}Db	8.33	3.58	1.36
^{289}Sg	^{285}Rf	5.11	19.67	–	^{271}Bh	^{267}Db	8.72	2.21	–
^{290}Sg	^{286}Rf	5.09	19.81	–	^{272}Bh	^{268}Db	8.98	1.33	0.47
^{291}Sg	^{287}Rf	5.87	14.47	–	^{273}Bh	^{269}Db	8.99	1.28	–
^{292}Sg	^{288}Rf	5.92	14.14	–	^{274}Bh	^{270}Db	8.75	2.06	1.22
^{293}Sg	^{289}Rf	5.67	15.70	–	^{275}Bh	^{271}Db	8.63	2.45	–
^{294}Sg	^{290}Rf	5.61	16.08	–	^{276}Bh	^{272}Db	8.25	3.76	–
^{295}Sg	^{291}Rf	5.17	19.12	–	^{277}Bh	^{273}Db	7.91	5.05	–
Z=107					^{278}Bh	^{274}Db	7.28	7.69	–
^{247}Bh	^{243}Db	11.92	-5.94	–	^{279}Bh	^{275}Db	6.89	9.56	–

Table 4.2 continued

Parent nuclei	Daughter nuclei	Q	$\log_{10}T_{1/2}$	$log_{10}T_{1/2}^{Om}$ $T_{1/2}$ in s	Parent nuclei	Daughter nuclei	Q	$\log_{10}T_{1/2}$	$log_{10}T_{1/2}^{Om}$ $T_{1/2}$ in s
		MeV	$T_{1/2}$ in s				MeV	$T_{1/2}$ in s	
^{280}Bh	^{276}Db	6.64	10.80	–	^{262}Hs	^{258}Sg	11.41	-4.82	–
^{281}Bh	^{277}Db	6.48	11.63	–	^{263}Hs	^{259}Sg	9.56	0.06	–
^{282}Bh	^{278}Db	6.41	11.99	–	^{264}Hs	^{260}Sg	10.76	-3.29	-2.22
^{283}Bh	^{279}Db	6.54	11.28	–	^{265}Hs	^{261}Sg	8.89	2.10	-2.12
^{284}Bh	^{280}Db	6.76	10.12	–	^{266}Hs	^{262}Sg	9.9	-0.99	-2.09
^{285}Bh	^{281}Db	6.45	11.73	–	^{267}Hs	^{263}Sg	8.04	5.15	-0.96
^{286}Bh	^{282}Db	6.01	14.22	–	^{268}Hs	^{264}Sg	9.07	1.50	–
^{287}Bh	^{283}Db	6.16	13.32	–	^{269}Hs	^{265}Sg	7.28	8.36	–
^{288}Bh	^{284}Db	5.88	14.98	–	^{270}Hs	^{266}Sg	8.47	3.48	0.81
^{289}Bh	^{285}Db	5.6	16.77	–	^{271}Hs	^{267}Sg	6.78	10.73	–
^{290}Bh	^{286}Db	5.43	17.88	–	^{272}Hs	^{268}Sg	8.14	4.67	–
^{291}Bh	^{287}Db	5.38	18.22	–	^{273}Hs	^{269}Sg	6.65	11.36	-0.49
^{292}Bh	^{288}Db	6.14	13.35	–	^{274}Hs	^{270}Sg	8.00	5.19	–
^{293}Bh	^{289}Db	6.19	13.04	–	^{275}Hs	^{271}Sg	6.35	12.95	–
^{294}Bh	^{290}Db	6.00	14.15	–	^{276}Hs	^{272}Sg	7.48	7.30	–
^{295}Bh	^{291}Db	5.97	14.32	–	^{277}Hs	^{273}Sg	5.89	15.64	–
^{296}Bh	^{292}Db	5.52	17.20	–	^{278}Hs	^{274}Sg	6.99	9.56	–
^{297}Bh	^{293}Db	5.49	17.34	–	^{279}Hs	^{275}Sg	7.62	6.65	–
^{298}Bh	^{294}Db	5.32	18.54	–	^{280}Hs	^{276}Sg	7.29	8.11	–
Z=108					^{281}Hs	^{277}Sg	7.06	9.18	–
^{250}Hs	^{246}Sg	12.11	-6.07	–	^{282}Hs	^{278}Sg	6.94	9.74	–
^{251}Hs	^{247}Sg	11.98	-5.82	–	^{283}Hs	^{279}Sg	6.92	9.82	–
^{252}Hs	^{248}Sg	11.91	-5.69	–	^{284}Hs	^{280}Sg	6.96	9.61	–
^{253}Hs	^{249}Sg	11.67	-5.18	–	^{285}Hs	^{281}Sg	7.07	9.06	–
^{254}Hs	^{250}Sg	11.47	-4.80	–	^{286}Hs	^{282}Sg	6.71	10.83	–
^{255}Hs	^{251}Sg	11.29	-4.40	–	^{287}Hs	^{283}Sg	6.43	12.30	–
^{256}Hs	^{252}Sg	11.06	-3.87	–	^{288}Hs	^{284}Sg	6.48	12.01	–
^{257}Hs	^{253}Sg	10.91	-3.52	–	^{289}Hs	^{285}Sg	6.17	13.74	–
^{258}Hs	^{254}Sg	10.68	-2.98	–	^{290}Hs	^{286}Sg	6.01	14.68	–
^{259}Hs	^{255}Sg	10.58	-2.74	–	^{291}Hs	^{287}Sg	5.86	15.59	–
^{260}Hs	^{256}Sg	10.65	-2.93	–	^{292}Hs	^{288}Sg	5.88	15.45	–
^{261}Hs	^{257}Sg	10.85	-3.45	-2.40	^{293}Hs	^{289}Sg	6.83	10.10	–

Table 4.2 continued

Parent nuclei	Daughter nuclei	Q MeV	$\log_{10}T_{1/2}$ $T_{1/2}$ in s	$log_{10}T_{1/2}^{Om}$ $T_{1/2}$ in s	Parent nuclei	Daughter nuclei	Q MeV	$\log_{10}T_{1/2}$ $T_{1/2}$ in s	$log_{10}T_{1/2}^{Om}$ $T_{1/2}$ in s
^{294}Hs	^{290}Sg	6.89	9.78	–	^{270}Mt	^{266}Bh	9.57	0.29	–
^{295}Hs	^{291}Sg	6.67	10.89	–	^{271}Mt	^{267}Bh	9.39	0.83	–
^{296}Hs	^{292}Sg	6.64	11.03	–	^{272}Mt	^{268}Bh	9.46	0.59	–
^{297}Hs	^{293}Sg	14.14	-10.68	–	^{273}Mt	^{269}Bh	9.78	-0.39	–
^{298}Hs	^{294}Sg	13.73	-10.01	–	^{274}Mt	^{270}Bh	10.01	-1.07	-0.97
^{299}Hs	^{295}Sg	5.96	14.84	–	^{275}Mt	^{271}Bh	10.11	-1.37	-2.09
^{300}Hs	^{296}Sg	5.67	16.67	–	^{276}Mt	^{272}Bh	9.93	-0.87	-0.85
^{307}Hs	^{303}Sg	7.92	4.97	–	^{277}Mt	^{273}Bh	9.76	-0.39	–
^{308}Hs	^{304}Sg	9.2	0.44	–	^{278}Mt	^{274}Bh	9.24	1.17	0.11
^{309}Hs	^{305}Sg	7.85	5.22	–	^{279}Mt	^{275}Bh	8.52	3.56	–
^{310}Hs	^{306}Sg	9.43	-0.31	–	^{280}Mt	^{276}Bh	7.98	5.59	–
^{311}Hs	^{307}Sg	8.31	3.41	–	^{281}Mt	^{277}Bh	7.68	6.81	–
^{312}Hs	^{308}Sg	9.79	-1.40	–	^{282}Mt	^{278}Bh	7.52	7.47	–
^{313}Hs	^{309}Sg	8.74	1.88	–	^{283}Mt	^{279}Bh	7.38	8.12	–
Z=109					^{284}Mt	^{280}Bh	7.35	8.24	–
^{253}Mt	^{249}Bh	12.38	-6.37	–	^{285}Mt	^{281}Bh	7.42	7.90	–
^{254}Mt	^{250}Bh	12.29	-6.20	–	^{286}Mt	^{282}Bh	7.59	7.10	–
^{255}Mt	^{251}Bh	12	-5.61	–	^{287}Mt	^{283}Bh	7.23	8.74	–
^{256}Mt	^{252}Bh	11.83	-5.26	–	^{288}Mt	^{284}Bh	6.85	10.57	–
^{257}Mt	^{253}Bh	11.62	-4.85	–	^{289}Mt	^{285}Bh	6.78	10.90	–
^{258}Mt	^{254}Bh	11.5	-4.59	–	^{290}Mt	^{286}Bh	6.49	12.42	–
^{259}Mt	^{255}Bh	11.28	-4.10	–	^{291}Mt	^{287}Bh	6.3	13.47	–
^{260}Mt	^{256}Bh	11.18	-3.89	–	^{292}Mt	^{288}Bh	6.13	14.44	–
^{261}Mt	^{257}Bh	11.28	-4.14	–	^{293}Mt	^{289}Bh	6.22	13.89	–
^{262}Mt	^{258}Bh	11.44	-4.53	–	^{294}Mt	^{290}Bh	7.19	8.81	–
^{263}Mt	^{259}Bh	11.52	-4.74	–	^{295}Mt	^{291}Bh	7.24	8.56	–
^{264}Mt	^{260}Bh	11.28	-4.20	–	^{296}Mt	^{292}Bh	7.08	9.30	–
^{265}Mt	^{261}Bh	11.12	-3.84	–	^{297}Mt	^{293}Bh	7.09	9.24	–
^{266}Mt	^{262}Bh	10.76	-2.97	–	^{298}Mt	^{294}Bh	6.88	10.25	–
^{267}Mt	^{263}Bh	10.36	-1.91	–	^{299}Mt	^{295}Bh	6.67	11.31	–
^{268}Mt	^{264}Bh	10.03	-1.01	-1.68	^{301}Mt	^{297}Bh	6.31	13.25	–
^{269}Mt	^{265}Bh	9.72	-0.13	–	^{302}Mt	^{298}Bh	5.86	15.94	–

Table 4.2 continued

Parent nuclei	Daughter nuclei	Q MeV	$\log_{10}T_{1/2}$ $T_{1/2}$ in s	$log_{10}T_{1/2}^{Om}$ $T_{1/2}$ in s	Parent nuclei	Daughter nuclei	Q MeV	$\log_{10}T_{1/2}$ $T_{1/2}$ in s	$log_{10}T_{1/2}^{Om}$ $T_{1/2}$ in s
^{303}Mt	^{299}Bh	5.61	17.53	–	^{285}Ds	^{281}Hs	7.73	6.97	–
^{304}Mt	^{300}Bh	5.38	19.13	–	^{286}Ds	^{282}Hs	7.75	6.87	–
Z=110					^{287}Ds	^{283}Hs	7.81	6.60	–
^{256}Ds	^{252}Hs	12.55	-6.44	–	^{288}Ds	^{284}Hs	7.54	7.78	–
^{257}Ds	^{253}Hs	12.46	-6.29	–	^{289}Ds	^{285}Hs	7.21	9.27	–
^{258}Ds	^{254}Hs	12.15	-5.65	–	^{290}Ds	^{286}Hs	7.05	10.02	–
^{259}Ds	^{255}Hs	12.02	-5.40	–	^{291}Ds	^{287}Hs	6.79	11.30	–
^{260}Ds	^{256}Hs	11.89	-5.18	–	^{292}Ds	^{288}Hs	6.69	11.80	–
^{261}Ds	^{257}Hs	11.77	-4.93	–	^{293}Ds	^{289}Hs	6.6	12.27	–
^{262}Ds	^{258}Hs	11.87	-5.14	–	^{294}Ds	^{290}Hs	6.64	12.04	–
^{263}Ds	^{259}Hs	12.02	-5.48	–	^{295}Ds	^{291}Hs	7.61	7.31	–
^{264}Ds	^{260}Hs	12.08	-5.62	–	^{296}Ds	^{292}Hs	7.69	6.96	–
^{265}Ds	^{261}Hs	11.9	-5.26	–	^{297}Ds	^{293}Hs	7.6	7.32	–
^{266}Ds	^{262}Hs	11.2	-3.70	–	^{298}Ds	^{294}Hs	7.6	7.31	–
^{267}Ds	^{263}Hs	12.57	-6.70	-4.63	^{299}Ds	^{295}Hs	7.43	8.09	–
^{268}Ds	^{264}Hs	10.78	-2.71	–	^{300}Ds	^{296}Hs	7.22	9.04	–
^{269}Ds	^{265}Hs	11.95	-5.44	-3.48	^{303}Ds	^{299}Hs	6.51	12.59	–
^{270}Ds	^{266}Hs	10.29	-1.40	-3.46	^{304}Ds	^{300}Hs	6.03	15.37	–
^{271}Ds	^{267}Hs	11.56	-4.64	-2.47	^{305}Ds	^{301}Hs	5.86	16.37	–
^{272}Ds	^{268}Hs	10.03	-0.72	–	^{306}Ds	^{302}Hs	5.69	17.48	–
^{273}Ds	^{269}Hs	11.74	-5.05	-3.89	^{307}Ds	^{303}Hs	5.49	18.86	–
^{274}Ds	^{270}Hs	10.7	-2.61	–	^{308}Ds	^{304}Hs	5.31	20.15	–
^{275}Ds	^{271}Hs	12.85	-7.43	-1.63	**Z=111**				
^{276}Ds	^{272}Hs	11.87	-5.38	-1.31	^{259}Rg	^{255}Mt	12.72	-6.53	–
^{277}Ds	^{273}Hs	13.4	-8.50	-2.52	^{260}Rg	^{256}Mt	12.57	-6.25	–
^{278}Ds	^{274}Hs	11.85	-5.38	-0.65	^{261}Rg	^{257}Mt	12.52	-6.16	–
^{279}Ds	^{275}Hs	12.58	-6.93	–	^{262}Rg	^{258}Mt	12.35	-5.84	–
^{280}Ds	^{276}Hs	10.54	-2.29	–	^{263}Rg	^{259}Mt	12.57	-6.30	–
^{281}Ds	^{277}Hs	11.22	-4.01	1.40	^{264}Rg	^{260}Mt	12.74	-6.67	–
^{282}Ds	^{278}Hs	9.44	0.86	–	^{265}Rg	^{261}Mt	12.73	-6.66	–
^{283}Ds	^{279}Hs	8.01	5.86	–	^{266}Rg	^{262}Mt	12.52	-6.25	–
^{284}Ds	^{280}Hs	7.84	6.53	–	^{267}Rg	^{263}Mt	12.35	-5.93	–

Table 4.2 continued

Parent nuclei	Daughter nuclei	Q MeV	$\log_{10}T_{1/2}$ $T_{1/2}$ in s	$log_{10}T_{1/2}^{Om}$ $T_{1/2}$ in s	Parent nuclei	Daughter nuclei	Q MeV	$\log_{10}T_{1/2}$ $T_{1/2}$ in s	$log_{10}T_{1/2}^{Om}$ $T_{1/2}$ in s
^{268}Rg	^{264}Mt	12.03	-5.26	–	^{300}Rg	^{296}Mt	7.82	6.78	–
^{269}Rg	^{265}Mt	11.68	-4.54	–	^{301}Rg	^{297}Mt	7.66	7.49	–
^{270}Rg	^{266}Mt	11.38	-3.86	–	^{302}Rg	^{298}Mt	7.46	8.36	–
^{271}Rg	^{267}Mt	11.11	-3.23	–	^{303}Rg	^{299}Mt	7.26	9.27	–
^{272}Rg	^{268}Mt	11.00	-2.97	-2.34	^{304}Rg	^{300}Mt	6.93	10.86	–
^{273}Rg	^{269}Mt	10.84	-2.59	–	^{305}Rg	^{301}Mt	6.55	12.84	–
^{274}Rg	^{270}Mt	10.83	-2.59	-2.70	^{306}Rg	^{302}Mt	6.26	14.47	–
^{275}Rg	^{271}Mt	11.3	-3.76	–	^{307}Rg	^{303}Mt	6.13	15.23	–
^{276}Rg	^{272}Mt	11.56	-4.40	-1.43	^{308}Rg	^{304}Mt	6.01	15.89	–
^{277}Rg	^{273}Mt	11.49	-4.25	–	^{309}Rg	^{305}Mt	5.82	17.11	–
^{278}Rg	^{274}Mt	11.26	-3.72	-2.56	^{310}Rg	^{306}Mt	5.56	18.87	–
^{279}Rg	^{275}Mt	10.79	-2.57	-1.47	^{311}Rg	^{307}Mt	5.4	20.00	–
^{280}Rg	^{276}Mt	9.97	-0.31	0.15	^{314}Rg	^{310}Mt	5.48	19.37	–
^{281}Rg	^{277}Mt	9.22	1.93	–	^{315}Rg	^{311}Mt	5.57	18.72	–
^{282}Rg	^{278}Mt	8.79	3.37	–	^{316}Rg	^{312}Mt	5.45	19.56	–
^{283}Rg	^{279}Mt	8.58	4.10	–	^{317}Rg	^{313}Mt	5.4	19.91	–
^{284}Rg	^{280}Mt	8.41	4.71	–	**Z=112**				
^{285}Rg	^{281}Mt	8.22	5.42	–	^{262}Cn	^{258}Ds	12.93	-6.69	–
^{286}Rg	^{282}Mt	8.09	5.91	–	^{263}Cn	^{259}Ds	12.81	-6.47	–
^{287}Rg	^{283}Mt	8.15	5.66	–	^{264}Cn	^{260}Ds	12.98	-6.82	–
^{288}Rg	^{284}Mt	8.1	5.84	–	^{265}Cn	^{261}Ds	13.15	-7.17	–
^{289}Rg	^{285}Mt	7.8	7.05	–	^{266}Cn	^{262}Ds	13.13	-7.15	–
^{290}Rg	^{286}Mt	7.33	9.15	–	^{267}Cn	^{263}Ds	12.91	-6.74	–
^{291}Rg	^{287}Mt	7.27	9.42	–	^{268}Cn	^{264}Ds	12.74	-6.43	–
^{292}Rg	^{288}Mt	7.02	10.61	–	^{269}Cn	^{265}Ds	12.45	-5.85	–
^{293}Rg	^{289}Mt	6.94	10.99	–	^{270}Cn	^{266}Ds	12.15	-5.28	–
^{294}Rg	^{290}Mt	6.94	10.97	–	^{271}Cn	^{267}Ds	11.91	-4.76	–
^{295}Rg	^{291}Mt	7.01	10.60	–	^{272}Cn	^{268}Ds	11.67	-4.23	-2.40
^{296}Rg	^{292}Mt	7.94	6.35	–	^{273}Cn	^{269}Ds	11.57	-4.02	-2.20
^{297}Rg	^{293}Mt	8.02	6.01	–	^{274}Cn	^{270}Ds	11.42	-3.68	-1.98
^{298}Rg	^{294}Mt	7.95	6.28	–	^{275}Cn	^{271}Ds	11.56	-4.03	-1.77
^{299}Rg	^{295}Mt	7.95	6.26	–	^{276}Cn	^{272}Ds	11.91	-4.85	-1.53

Table 4.2 continued

Parent nuclei	Daughter nuclei	Q	$\log_{10}T_{1/2}$	$log_{10}T_{1/2}^{Om}$	Parent nuclei	Daughter nuclei	Q	$\log_{10}T_{1/2}$	$log_{10}T_{1/2}^{Om}$
		MeV	$T_{1/2}$ in s	$T_{1/2}$ in s			MeV	$T_{1/2}$ in s	$T_{1/2}$ in s
^{277}Cn	^{273}Ds	12.13	-5.32	–	^{310}Cn	^{306}Ds	6.12	15.71	–
^{278}Cn	^{274}Ds	12.17	-5.42	-0.99	^{311}Cn	^{307}Ds	5.88	17.22	–
^{279}Cn	^{275}Ds	11.65	-4.31	-0.69	^{312}Cn	^{308}Ds	5.76	18.00	–
^{280}Cn	^{276}Ds	11.09	-3.00	–	^{313}Cn	^{309}Ds	5.68	18.53	–
^{281}Cn	^{277}Ds	10.25	-0.75	-1.29	^{314}Cn	^{310}Ds	5.71	18.30	–
^{282}Cn	^{278}Ds	9.43	1.62	–	^{315}Cn	^{311}Ds	5.87	17.22	–
^{283}Cn	^{279}Ds	9.13	2.59	–	^{316}Cn	^{312}Ds	5.97	16.56	–
^{284}Cn	^{280}Ds	8.96	3.15	–	^{317}Cn	^{313}Ds	5.95	16.67	–
^{285}Cn	^{281}Ds	8.79	3.73	1.18	^{318}Cn	^{314}Ds	5.85	17.31	–
^{286}Cn	^{282}Ds	8.62	4.32	–	^{319}Cn	^{315}Ds	5.68	18.44	–
^{287}Cn	^{283}Ds	8.53	4.63	–	^{320}Cn	^{316}Ds	5.43	20.20	–
^{288}Cn	^{284}Ds	8.59	4.40	–	**Z=113**				
^{289}Cn	^{285}Ds	8.49	4.75	–	^{266}Nh	^{262}Rg	13.62	-7.80	–
^{290}Cn	^{286}Ds	8.07	6.35	–	^{267}Nh	^{263}Rg	13.5	-7.57	–
^{291}Cn	^{287}Ds	7.65	8.15	–	^{268}Nh	^{264}Rg	13.3	-7.21	–
^{292}Cn	^{288}Ds	7.57	8.49	–	^{269}Nh	^{265}Rg	13.12	-6.88	–
^{293}Cn	^{289}Ds	7.38	9.33	–	^{270}Nh	^{266}Rg	12.86	-6.39	–
^{294}Cn	^{290}Ds	7.37	9.36	–	^{271}Nh	^{267}Rg	12.6	-5.88	–
^{295}Cn	^{291}Ds	7.35	9.44	–	^{272}Nh	^{268}Rg	12.36	-5.44	–
^{296}Cn	^{292}Ds	7.43	9.05	–	^{273}Nh	^{269}Rg	12.15	-5.00	–
^{297}Cn	^{293}Ds	8.36	5.10	–	^{274}Nh	^{270}Rg	12.07	-4.84	–
^{298}Cn	^{294}Ds	8.41	4.90	–	^{275}Nh	^{271}Rg	11.95	-4.59	–
^{299}Cn	^{295}Ds	8.48	4.61	–	^{276}Nh	^{272}Rg	11.96	-4.63	–
^{300}Cn	^{296}Ds	8.36	5.06	–	^{277}Nh	^{273}Rg	12.24	-5.27	–
^{301}Cn	^{297}Ds	8.23	5.54	–	^{278}Nh	^{274}Rg	12.52	-5.84	-3.59
^{302}Cn	^{298}Ds	8.02	6.36	–	^{279}Nh	^{275}Rg	11.86	-4.46	–
^{303}Cn	^{299}Ds	7.89	6.88	–	^{280}Nh	^{276}Rg	11.45	-3.53	-1.55
^{304}Cn	^{300}Ds	7.68	7.81	–	^{281}Nh	^{277}Rg	10.76	-1.78	–
^{305}Cn	^{301}Ds	7.66	7.87	–	^{282}Nh	^{278}Rg	10.02	0.25	-1.53
^{306}Cn	^{302}Ds	7.47	8.70	–	^{283}Nh	^{279}Rg	9.46	1.90	-0.81
^{308}Cn	^{304}Ds	6.52	13.45	–	^{284}Nh	^{280}Rg	9.27	2.51	-0.38
^{309}Cn	^{305}Ds	6.32	14.58	–	^{285}Nh	^{281}Rg	9.13	2.95	0.14

Table 4.2 continued

Parent nuclei	Daughter nuclei	Q	$\log_{10}T_{1/2}$	$log_{10}T_{1/2}^{Om}$	Parent nuclei	Daughter nuclei	Q	$\log_{10}T_{1/2}$	$log_{10}T_{1/2}^{Om}$
		MeV	$T_{1/2}$ in s	$T_{1/2}$ in s			MeV	$T_{1/2}$ in s	$T_{1/2}$ in s
^{286}Nh	^{282}Rg	8.97	3.48	0.48	^{319}Nh	^{315}Rg	6.31	14.99	–
^{287}Nh	^{283}Rg	8.89	3.75	–	^{320}Nh	^{316}Rg	6.18	15.70	–
^{288}Nh	^{284}Rg	8.84	3.90	–	^{321}Nh	^{317}Rg	5.93	17.27	–
^{289}Nh	^{285}Rg	8.81	4.00	–	^{322}Nh	^{318}Rg	5.74	18.52	–
^{290}Nh	^{286}Rg	8.6	4.74	–	^{323}Nh	^{319}Rg	5.68	18.92	–
^{291}Nh	^{287}Rg	8.22	6.16	–	^{324}Nh	^{320}Rg	5.5	20.18	–
^{292}Nh	^{288}Rg	7.96	7.25	–	**Z=114**				
^{293}Nh	^{289}Rg	7.94	7.32	–	^{269}Fl	^{265}Cn	13.55	-7.39	–
^{294}Nh	^{290}Rg	7.92	7.38	–	^{270}Fl	^{266}Cn	13.4	-7.13	–
^{295}Nh	^{291}Rg	7.92	7.37	–	^{271}Fl	^{267}Cn	13.19	-6.74	–
^{296}Nh	^{292}Rg	7.94	7.27	–	^{272}Fl	^{268}Cn	12.96	-6.31	–
^{297}Nh	^{293}Rg	8.02	6.87	–	^{273}Fl	^{269}Cn	12.76	-5.93	–
^{298}Nh	^{294}Rg	8.9	3.52	–	^{274}Fl	^{270}Cn	12.61	-5.63	–
^{299}Nh	^{295}Rg	8.95	3.33	–	^{275}Fl	^{271}Cn	12.43	-5.31	–
^{300}Nh	^{296}Rg	9.04	3.00	–	^{276}Fl	^{272}Cn	12.43	-5.34	–
^{301}Nh	^{297}Rg	8.91	3.44	–	^{277}Fl	^{273}Cn	12.38	-5.24	–
^{302}Nh	^{298}Rg	8.75	3.99	–	^{278}Fl	^{274}Cn	11.76	-3.88	-2.99
^{303}Nh	^{299}Rg	8.52	4.82	–	^{279}Fl	^{275}Cn	11.6	-3.52	-2.78
^{304}Nh	^{300}Rg	8.42	5.18	–	^{280}Fl	^{276}Cn	11.05	-2.16	-2.58
^{305}Nh	^{301}Rg	8.16	6.17	–	^{281}Fl	^{277}Cn	10.58	-0.94	-2.34
^{306}Nh	^{302}Rg	7.95	7.06	–	^{282}Fl	^{278}Cn	9.96	0.80	-2.09
^{307}Nh	^{303}Rg	7.6	8.56	–	^{283}Fl	^{279}Cn	9.83	1.12	-1.85
^{308}Nh	^{304}Rg	7.63	8.41	–	^{284}Fl	^{280}Cn	9.52	2.09	-1.56
^{309}Nh	^{305}Rg	7.46	9.16	–	^{285}Fl	^{281}Cn	9.44	2.32	-1.27
^{311}Nh	^{307}Rg	6.56	13.68	–	^{286}Fl	^{282}Cn	9.47	2.21	-0.99
^{312}Nh	^{308}Rg	6.32	15.04	–	^{287}Fl	^{283}Cn	9.4	2.42	-0.61
^{313}Nh	^{309}Rg	6.18	15.81	–	^{288}Fl	^{284}Cn	9.17	3.17	-0.44
^{314}Nh	^{310}Rg	6.13	16.10	–	^{289}Fl	^{285}Cn	9.06	3.52	-0.67
^{315}Nh	^{311}Rg	6.15	15.96	–	^{290}Fl	^{286}Cn	8.84	4.28	–
^{316}Nh	^{312}Rg	6.34	14.86	–	^{291}Fl	^{287}Cn	8.77	4.51	–
^{317}Nh	^{313}Rg	6.42	14.37	–	^{292}Fl	^{288}Cn	8.32	6.18	–
^{318}Nh	^{314}Rg	6.37	14.65	–	^{293}Fl	^{289}Cn	8.27	6.36	–

Table 4.2 continued

Parent nuclei	Daughter nuclei	Q MeV	$\log_{10}T_{1/2}$ $T_{1/2}$ in s	$log_{10}T_{1/2}^{Om}$ $T_{1/2}$ in s	Parent nuclei	Daughter nuclei	Q MeV	$\log_{10}T_{1/2}$ $T_{1/2}$ in s	$log_{10}T_{1/2}^{Om}$ $T_{1/2}$ in s
^{294}Fl	^{290}Cn	8.44	5.68	–	^{327}Fl	^{323}Cn	5.57	20.18	–
^{295}Fl	^{291}Cn	8.44	5.67	–	**Z=115**				
^{296}Fl	^{292}Cn	8.47	5.54	–	^{272}Mc	^{268}Nh	13.34	-6.74	–
^{297}Fl	^{293}Cn	8.58	5.11	–	^{273}Mc	^{269}Nh	13.23	-6.55	–
^{298}Fl	^{294}Cn	8.66	4.79	–	^{274}Mc	^{270}Nh	13.11	-6.33	–
^{299}Fl	^{295}Cn	9.55	1.73	–	^{275}Mc	^{271}Nh	12.94	-6.01	–
^{300}Fl	^{296}Cn	9.57	1.65	–	^{276}Mc	^{272}Nh	12.84	-5.83	–
^{301}Fl	^{297}Cn	9.71	1.19	–	^{277}Mc	^{273}Nh	12.75	-5.66	–
^{302}Fl	^{298}Cn	9.54	1.72	–	^{278}Mc	^{274}Nh	12.45	-5.09	–
^{303}Fl	^{299}Cn	9.3	2.48	–	^{279}Mc	^{275}Nh	11.91	-3.91	–
^{304}Fl	^{300}Cn	9.1	3.14	–	^{280}Mc	^{276}Nh	11.86	-3.81	–
^{305}Fl	^{301}Cn	8.89	3.85	–	^{281}Mc	^{277}Nh	11.48	-2.94	–
^{306}Fl	^{302}Cn	8.62	4.81	–	^{282}Mc	^{278}Nh	10.95	-1.58	–
^{307}Fl	^{303}Cn	8.51	5.21	–	^{283}Mc	^{279}Nh	10.83	-1.28	–
^{308}Fl	^{304}Cn	8.01	7.22	–	^{284}Mc	^{280}Nh	10.38	-0.08	–
^{309}Fl	^{305}Cn	7.73	8.40	–	^{285}Mc	^{281}Nh	10.3	0.13	–
^{310}Fl	^{306}Cn	7.37	10.02	–	^{286}Mc	^{282}Nh	10.21	0.38	-2.09
^{311}Fl	^{307}Cn	6.9	12.33	–	^{287}Mc	^{283}Nh	10.22	0.32	-1.69
^{313}Fl	^{309}Cn	6.79	12.88	–	^{288}Mc	^{284}Nh	10.14	0.54	-1.39
^{314}Fl	^{310}Cn	6.66	13.57	–	^{289}Mc	^{285}Nh	10.09	0.67	-1.01
^{315}Fl	^{311}Cn	6.57	14.05	–	^{290}Mc	^{286}Nh	10.04	0.80	-0.61
^{316}Fl	^{312}Cn	6.58	13.98	–	^{291}Mc	^{287}Nh	9.74	1.65	-0.55
^{317}Fl	^{313}Cn	6.76	12.97	–	^{292}Mc	^{288}Nh	9.6	2.07	–
^{318}Fl	^{314}Cn	6.9	12.22	–	^{293}Mc	^{289}Nh	9.44	2.57	–
^{319}Fl	^{315}Cn	6.81	12.68	–	^{294}Mc	^{290}Nh	9.45	2.53	–
^{320}Fl	^{316}Cn	6.76	12.93	–	^{295}Mc	^{291}Nh	9.58	2.09	–
^{321}Fl	^{317}Cn	6.57	13.96	–	^{296}Mc	^{292}Nh	9.59	2.04	–
^{322}Fl	^{318}Cn	6.41	14.85	–	^{297}Mc	^{293}Nh	9.59	2.02	–
^{323}Fl	^{319}Cn	6.22	15.93	–	^{298}Mc	^{294}Nh	9.6	1.97	–
^{324}Fl	^{320}Cn	6.11	16.60	–	^{299}Mc	^{295}Nh	9.69	1.68	–
^{325}Fl	^{321}Cn	5.95	17.60	–	^{300}Mc	^{296}Nh	10.54	-0.79	–
^{326}Fl	^{322}Cn	5.71	19.20	–	^{301}Mc	^{297}Nh	10.56	-0.86	–

Table 4.2 continued

Parent nuclei	Daughter nuclei	Q	$\log_{10}T_{1/2}$	$log_{10}T_{1/2}^{0m}$	Parent nuclei	Daughter nuclei	Q	$\log_{10}T_{1/2}$	$log_{10}T_{1/2}^{0m}$
		MeV	$T_{1/2}$ in s	$T_{1/2}$ in s			MeV	$T_{1/2}$ in s	$T_{1/2}$ in s
^{302}Mc	^{298}Nh	10.65	-1.13	–	^{280}Lv	^{276}Fl	12.06	-3.94	–
^{303}Mc	^{299}Nh	10.53	-0.81	–	^{281}Lv	^{277}Fl	12.09	-4.03	–
^{304}Mc	^{300}Nh	10.32	-0.24	–	^{282}Lv	^{278}Fl	12.62	-5.19	–
^{305}Mc	^{301}Nh	10.06	0.49	–	^{283}Lv	^{279}Fl	12.29	-4.51	–
^{306}Mc	^{302}Nh	9.68	1.59	–	^{284}Lv	^{280}Fl	12.22	-4.37	–
^{307}Mc	^{303}Nh	9.37	2.57	–	^{285}Lv	^{281}Fl	11.85	-3.55	–
^{308}Mc	^{304}Nh	8.83	4.42	–	^{286}Lv	^{282}Fl	11.68	-3.17	–
^{309}Mc	^{305}Nh	8.48	5.70	–	^{287}Lv	^{283}Fl	11.2	-1.96	-2.89
^{310}Mc	^{306}Nh	8.2	6.83	–	^{288}Lv	^{284}Fl	11.2	-1.98	-2.63
^{311}Mc	^{307}Nh	7.97	7.77	–	^{289}Lv	^{285}Fl	11.1	-1.74	-2.36
^{314}Mc	^{310}Nh	9.59	1.75	–	^{290}Lv	^{286}Fl	11.07	-1.69	-2.05
^{315}Mc	^{311}Nh	7.01	12.17	–	^{291}Lv	^{287}Fl	11.02	-1.57	-1.98
^{316}Mc	^{312}Nh	6.99	12.26	–	^{292}Lv	^{288}Fl	10.82	-1.06	-1.93
^{317}Mc	^{313}Nh	6.98	12.30	–	^{293}Lv	^{289}Fl	10.78	-0.97	-1.49
^{318}Mc	^{314}Nh	7.18	11.27	–	^{294}Lv	^{290}Fl	10.91	-1.34	–
^{319}Mc	^{315}Nh	7.33	10.53	–	^{295}Lv	^{291}Fl	10.87	-1.25	–
^{320}Mc	^{316}Nh	7.26	10.85	–	^{296}Lv	^{292}Fl	11.18	-2.07	–
^{321}Mc	^{317}Nh	7.23	10.98	–	^{297}Lv	^{293}Fl	11.12	-1.94	–
^{322}Mc	^{318}Nh	7.00	12.12	–	^{298}Lv	^{294}Fl	11.14	-2.00	–
^{323}Mc	^{319}Nh	6.86	12.83	–	^{299}Lv	^{295}Fl	11.18	-2.12	–
^{324}Mc	^{320}Nh	6.73	13.51	–	^{300}Lv	^{296}Fl	11.26	-2.34	–
^{325}Mc	^{321}Nh	6.56	14.45	–	^{301}Lv	^{297}Fl	12.06	-4.30	–
^{326}Mc	^{322}Nh	6.4	15.31	–	^{302}Lv	^{298}Fl	12.08	-4.36	–
^{327}Mc	^{323}Nh	6.00	17.77	–	^{303}Lv	^{299}Fl	12.18	-4.60	–
^{328}Mc	^{324}Nh	5.88	18.55	–	^{304}Lv	^{300}Fl	12.03	-4.28	–
^{329}Mc	^{325}Nh	5.62	20.34	–	^{305}Lv	^{301}Fl	11.71	-3.55	–
Z=116					^{306}Lv	^{302}Fl	11.56	-3.22	–
^{275}Lv	^{271}Fl	13.55	-6.89	–	^{307}Lv	^{303}Fl	11.09	-2.02	–
^{276}Lv	^{272}Fl	13.37	-6.57	–	^{308}Lv	^{304}Fl	10.53	-0.54	–
^{277}Lv	^{273}Fl	13.24	-6.33	–	^{309}Lv	^{305}Fl	9.76	1.67	–
^{278}Lv	^{274}Fl	12.74	-5.38	–	^{310}Lv	^{306}Fl	9.44	2.68	–
^{279}Lv	^{275}Fl	12.64	-5.19	–	^{311}Lv	^{307}Fl	8.96	4.30	–

Table 4.2 continued

Parent nuclei	Daughter nuclei	Q	$\log_{10}T_{1/2}$	$log_{10}T_{1/2}^{Om}$	Parent nuclei	Daughter nuclei	Q	$\log_{10}T_{1/2}$	$log_{10}T_{1/2}^{Om}$
		MeV	$T_{1/2}$ in s	$T_{1/2}$ in s			MeV	$T_{1/2}$ in s	$T_{1/2}$ in s
^{312}Lv	^{308}Fl	8.83	4.76	–	^{289}Ts	^{285}Mc	11.98	-3.59	–
^{313}Lv	^{309}Fl	8.48	6.05	–	^{290}Ts	^{286}Mc	11.85	-3.31	–
^{314}Lv	^{310}Fl	8.23	7.08	–	^{291}Ts	^{287}Mc	11.75	-3.06	–
^{315}Lv	^{311}Fl	7.59	9.82	–	^{292}Ts	^{288}Mc	11.71	-2.98	-2.61
^{316}Lv	^{312}Fl	9.91	1.10	–	^{293}Ts	^{289}Mc	11.4	-2.23	-2.16
^{317}Lv	^{313}Fl	7.38	10.77	–	^{294}Ts	^{290}Mc	11.3	-2.00	-1.58
^{318}Lv	^{314}Fl	7.35	10.90	–	^{295}Ts	^{291}Mc	11.54	-2.61	–
^{319}Lv	^{315}Fl	7.54	9.99	–	^{296}Ts	^{292}Mc	11.64	-2.87	–
^{320}Lv	^{316}Fl	7.73	9.11	–	^{297}Ts	^{293}Mc	11.77	-3.24	–
^{321}Lv	^{317}Fl	7.71	9.19	–	^{298}Ts	^{294}Mc	11.86	-3.47	–
^{322}Lv	^{318}Fl	7.62	9.58	–	^{299}Ts	^{295}Mc	11.86	-3.48	–
^{323}Lv	^{319}Fl	7.42	10.49	–	^{300}Ts	^{296}Mc	11.88	-3.54	–
^{324}Lv	^{320}Fl	7.26	11.25	–	^{301}Ts	^{297}Mc	11.94	-3.70	–
^{325}Lv	^{321}Fl	7.1	12.03	–	^{302}Ts	^{298}Mc	12.75	-5.50	–
^{326}Lv	^{322}Fl	6.94	12.84	–	^{303}Ts	^{299}Mc	12.73	-5.47	–
^{327}Lv	^{323}Fl	6.71	14.06	–	^{304}Ts	^{300}Mc	12.82	-5.68	–
^{328}Lv	^{324}Fl	6.47	15.37	–	^{305}Ts	^{301}Mc	12.69	-5.42	–
^{329}Lv	^{325}Fl	6.34	16.12	–	^{306}Ts	^{302}Mc	12.41	-4.83	–
^{330}Lv	^{326}Fl	5.98	18.38	–	^{307}Ts	^{303}Mc	12.24	-4.47	–
^{331}Lv	^{327}Fl	5.79	19.65	–	^{308}Ts	^{304}Mc	11.41	-2.51	–
Z=117					^{309}Ts	^{305}Mc	10.79	-0.91	–
^{278}Ts	^{274}Mc	13.34	-6.24	–	^{310}Ts	^{306}Mc	10.37	0.24	–
^{279}Ts	^{275}Mc	12.97	-5.56	–	^{311}Ts	^{307}Mc	10.15	0.82	–
^{280}Ts	^{276}Mc	12.78	-5.18	–	^{312}Ts	^{308}Mc	9.78	1.94	–
^{281}Ts	^{277}Mc	12.31	-4.19	–	^{313}Ts	^{309}Mc	9.54	2.69	–
^{282}Ts	^{278}Mc	12.59	-4.82	–	^{316}Ts	^{312}Mc	8.06	8.18	–
^{283}Ts	^{279}Mc	12.97	-5.63	–	^{317}Ts	^{313}Mc	10.36	0.16	–
^{284}Ts	^{280}Mc	12.65	-4.98	–	^{318}Ts	^{314}Mc	7.86	9.01	–
^{285}Ts	^{281}Mc	12.45	-4.57	–	^{319}Ts	^{315}Mc	7.8	9.26	–
^{286}Ts	^{282}Mc	12.18	-3.99	–	^{320}Ts	^{316}Mc	7.95	8.59	–
^{287}Ts	^{283}Mc	12.11	-3.85	–	^{321}Ts	^{317}Mc	8.12	7.85	–
^{288}Ts	^{284}Mc	12.01	-3.64	–	^{322}Ts	^{318}Mc	8.09	7.96	–

Table 4.2 continued

Parent nuclei	Daughter nuclei	Q	$\log_{10}T_{1/2}$	$log_{10}T_{1/2}^{Om}$	Parent nuclei	Daughter nuclei	Q	$\log_{10}T_{1/2}$	$log_{10}T_{1/2}^{Om}$
		MeV	$T_{1/2}$ in s	$T_{1/2}$ in s			MeV	$T_{1/2}$ in s	$T_{1/2}$ in s
^{323}Ts	^{319}Mc	9.32	3.27	–	^{300}Og	^{296}Lv	12.51	-4.64	-3.85
^{324}Ts	^{320}Mc	7.85	8.96	–	^{301}Og	^{297}Lv	12.56	-4.76	-3.99
^{325}Ts	^{321}Mc	7.67	9.75	–	^{302}Og	^{298}Lv	12.62	-4.91	-4.03
^{326}Ts	^{322}Mc	7.52	10.43	–	^{303}Og	^{299}Lv	13.38	-6.45	-5.21
^{327}Ts	^{323}Mc	7.31	11.42	–	^{304}Og	^{300}Lv	13.4	-6.50	-6.23
^{328}Ts	^{324}Mc	7.05	12.71	–	^{305}Og	^{301}Lv	13.45	-6.61	-5.79
^{329}Ts	^{325}Mc	6.67	14.70	–	^{306}Og	^{302}Lv	13.34	-6.41	-4.89
^{330}Ts	^{326}Mc	6.57	15.25	–	^{307}Og	^{303}Lv	12.53	-4.79	-3.63
^{331}Ts	^{327}Mc	6.02	18.63	–	^{308}Og	^{304}Lv	12.1	-3.86	-4.20
^{332}Ts	^{328}Mc	6.08	18.22	–	^{309}Og	^{305}Lv	11.07	-1.31	–
^{333}Ts	^{329}Mc	5.92	19.26	–	^{310}Og	^{306}Lv	10.75	-0.46	–
^{334}Ts	^{330}Mc	5.89	19.45	–	^{311}Og	^{307}Lv	9.97	1.74	–
Z=118					^{312}Og	^{308}Lv	10.04	1.51	–
^{281}Og	^{277}Lv	13.16	-5.67	-5.95	^{313}Og	^{309}Lv	9.73	2.46	–
^{282}Og	^{278}Lv	13.12	-5.60	-5.61	^{314}Og	^{310}Lv	9.54	3.06	–
^{283}Og	^{279}Lv	13.2	-5.78	-5.45	^{318}Og	^{314}Lv	7.46	11.29	–
^{284}Og	^{280}Lv	13.57	-6.49	-5.39	^{319}Og	^{315}Lv	10.85	-0.88	–
^{285}Og	^{281}Lv	13.23	-5.88	-5.21	^{320}Og	^{316}Lv	8.22	7.87	–
^{286}Og	^{282}Lv	13.05	-5.53	-5.03	^{321}Og	^{317}Lv	8.41	7.09	–
^{287}Og	^{283}Lv	12.96	-5.36	-4.90	^{322}Og	^{318}Lv	8.56	6.48	–
^{288}Og	^{284}Lv	12.86	-5.17	-4.64	^{323}Og	^{319}Lv	9.9	1.77	–
^{289}Og	^{285}Lv	12.76	-4.98	-4.67	^{324}Og	^{320}Lv	9.62	2.64	–
^{290}Og	^{286}Lv	12.67	-4.81	-4.78	^{325}Og	^{321}Lv	9.27	3.80	–
^{291}Og	^{287}Lv	12.55	-4.57	-4.78	^{326}Og	^{322}Lv	9.03	4.62	–
^{292}Og	^{288}Lv	12.39	-4.24	-4.17	^{327}Og	^{323}Lv	7.9	9.13	–
^{293}Og	^{289}Lv	12.34	-4.15	-3.37	^{328}Og	^{324}Lv	7.79	9.60	–
^{294}Og	^{290}Lv	12.37	-4.23	-3.37	^{329}Og	^{325}Lv	7.47	11.07	–
^{295}Og	^{291}Lv	11.93	-3.25	-2.85	^{330}Og	^{326}Lv	7.17	12.53	–
^{296}Og	^{292}Lv	12.28	-4.06	3.29	^{331}Og	^{327}Lv	5.97	19.49	–
^{297}Og	^{293}Lv	12.39	-4.32	-4.11	^{332}Og	^{328}Lv	5.88	20.08	–
^{298}Og	^{294}Lv	12.49	-4.56	-4.31	^{333}Og	^{329}Lv	5.94	19.66	–
^{299}Og	^{295}Lv	12.51	-4.62	-4.04	^{334}Og	^{330}Lv	6.16	18.19	–

Table 4.2 continued

Parent nuclei	Daughter nuclei	Q MeV	$\log_{10}T_{1/2}$ $T_{1/2}$ in s	$log_{10}T_{1/2}^{Om}$ $T_{1/2}$ in s	Parent nuclei	Daughter nuclei	Q MeV	$\log_{10}T_{1/2}$ $T_{1/2}$ in s	$log_{10}T_{1/2}^{Om}$ $T_{1/2}$ in s
^{335}Og	^{331}Lv	6.35	16.99	–	^{312}119	^{308}Ts	9.9	2.32	–
^{336}Og	^{332}Lv	6.2	17.91	–	^{313}119	^{309}Ts	10.06	1.81	–
^{337}Og	^{333}Lv	5.88	20.01	–	^{314}119	^{310}Ts	9.55	3.41	–
Z=119					^{315}119	^{311}Ts	9.36	4.03	–
^{284}119	^{280}Ts	13.67	-6.37	-5.57	^{316}119	^{312}Ts	9.2	4.57	–
^{285}119	^{281}Ts	14.06	-7.12	-5.78	^{317}119	^{313}Ts	9.07	5.02	–
^{286}119	^{282}Ts	13.75	-6.56	-5.58	^{318}119	^{314}Ts	12.69	-4.99	–
^{287}119	^{283}Ts	13.37	-5.89	-5.42	^{319}119	^{315}Ts	12.74	-5.11	–
^{288}119	^{284}Ts	13.57	-6.26	-5.44	^{320}119	^{316}Ts	12.58	-4.79	–
^{289}119	^{285}Ts	13.47	-6.08	-5.41	^{321}119	^{317}Ts	10.17	1.34	–
^{290}119	^{286}Ts	13.31	-5.82	-5.33	^{322}119	^{318}Ts	10.17	1.33	–
^{291}119	^{287}Ts	13.24	-5.70	-5.39	^{323}119	^{319}Ts	10.24	1.10	–
^{292}119	^{288}Ts	13.08	-5.39	-5.18	^{324}119	^{320}Ts	10.05	1.66	–
^{293}119	^{289}Ts	12.92	-5.08	-4.89	^{325}119	^{321}Ts	9.79	2.46	–
^{294}119	^{290}Ts	12.85	-4.94	-4.89	^{326}119	^{322}Ts	9.43	3.62	–
^{295}119	^{291}Ts	12.94	-5.15	–	^{327}119	^{323}Ts	7.87	9.70	–
^{296}119	^{292}Ts	12.98	-5.25	–	^{328}119	^{324}Ts	9.12	4.67	–
^{297}119	^{293}Ts	12.9	-5.10	–	^{329}119	^{325}Ts	8.12	8.58	–
^{298}119	^{294}Ts	13.09	-5.52	–	^{330}119	^{326}Ts	7.93	9.39	–
^{299}119	^{295}Ts	13.08	-5.51	–	^{331}119	^{327}Ts	6.16	18.76	–
^{300}119	^{296}Ts	13.03	-5.42	–	^{332}119	^{328}Ts	6.11	19.07	–
^{301}119	^{297}Ts	13.08	-5.55	–	^{333}119	^{329}Ts	6.21	18.41	–
^{302}119	^{298}Ts	13.05	-5.49	–	^{334}119	^{330}Ts	6.2	18.45	–
^{303}119	^{299}Ts	13.11	-5.64	–	^{335}119	^{331}Ts	6.65	15.71	–
^{304}119	^{300}Ts	13.86	-7.08	-5.68	^{336}119	^{332}Ts	6.5	16.57	–
^{305}119	^{301}Ts	13.86	-7.10	-6.61	^{337}119	^{333}Ts	6.6	15.96	–
^{306}119	^{302}Ts	13.93	-7.25	-6.17	^{338}119	^{334}Ts	6.29	17.82	–
^{307}119	^{303}Ts	13.39	-6.23	-5.32	^{339}119	^{335}Ts	6.15	18.70	–
^{308}119	^{304}Ts	12.16	-3.67	-3.75	**Z=120**				
^{309}119	^{305}Ts	11.7	-2.56	-2.10	^{287}120	^{283}Og	13.96	-6.68	-6.03
^{310}119	^{306}Ts	10.67	0.11	–	^{288}120	^{284}Og	13.85	-6.49	-5.94
^{311}119	^{307}Ts	10.32	1.05	–	^{289}120	^{285}Og	13.75	-6.32	-6.03

Table 4.2 continued

Parent nuclei	Daughter nuclei	Q MeV	$\log_{10}T_{1/2}$ $T_{1/2}$ in s	$log_{10}T_{1/2}^{Om}$ $T_{1/2}$ in s	Parent nuclei	Daughter nuclei	Q MeV	$\log_{10}T_{1/2}$ $T_{1/2}$ in s	$log_{10}T_{1/2}^{Om}$ $T_{1/2}$ in s
$^{290}120$	^{286}Og	13.75	-6.34	-6.12	$^{322}120$	^{318}Og	10.48	0.78	–
$^{291}120$	^{287}Og	13.87	-6.58	-5.88	$^{323}120$	^{319}Og	10.54	0.59	–
$^{292}120$	^{288}Og	13.78	-6.43	-5.91	$^{324}120$	^{320}Og	10.78	-0.07	–
$^{293}120$	^{289}Og	13.65	-6.20	-5.87	$^{325}120$	^{321}Og	10.4	0.96	–
$^{294}120$	^{290}Og	13.49	-5.94	-5.64	$^{326}120$	^{322}Og	10.28	1.30	–
$^{295}120$	^{291}Og	13.46	-5.90	-5.78	$^{327}120$	^{323}Og	8.48	7.55	–
$^{296}120$	^{292}Og	13.59	-6.14	-5.98	$^{328}120$	^{324}Og	8.4	7.86	–
$^{297}120$	^{293}Og	13.65	-6.27	-5.66	$^{329}120$	^{325}Og	8.26	8.42	–
$^{298}120$	^{294}Og	13.24	-5.51	-5.46	$^{330}120$	^{326}Og	7.99	9.56	–
$^{299}120$	^{295}Og	13.73	-6.46	-5.99	$^{331}120$	^{327}Og	6.87	15.01	–
$^{300}120$	^{296}Og	13.7	-6.41	-6.15	$^{332}120$	^{328}Og	6.5	17.13	–
$^{301}120$	^{297}Og	13.62	-6.28	-5.68	$^{333}120$	^{329}Og	6.5	17.12	–
$^{302}120$	^{298}Og	13.55	-6.16	-5.36	$^{334}120$	^{330}Og	6.47	17.28	–
$^{303}120$	^{299}Og	13.51	-6.10	-5.22	$^{335}120$	^{331}Og	7.56	11.45	–
$^{304}120$	^{300}Og	13.55	-6.19	-5.12	$^{336}120$	^{332}Og	7.45	11.97	–
$^{305}120$	^{301}Og	14.26	-7.54	-6.16	$^{337}120$	^{333}Og	7.25	12.95	–
$^{306}120$	^{302}Og	14.28	-7.60	-7.10	$^{338}120$	^{334}Og	7.03	14.03	–
$^{307}120$	^{303}Og	13.62	-6.37	-6.59	$^{339}120$	^{335}Og	6.77	15.45	–
$^{308}120$	^{304}Og	12.96	-5.10	-5.51	**Z=121**				
$^{309}120$	^{305}Og	11.77	-2.39	-3.78	$^{290}121$	$^{286}119$	14.17	-6.82	-6.98
$^{310}120$	^{306}Og	11.29	-1.20	-2.21	$^{291}121$	$^{287}119$	14.35	-7.18	-7.06
$^{311}120$	^{307}Og	10.76	0.20	–	$^{292}121$	$^{288}119$	14.01	-6.57	-7.02
$^{312}120$	^{308}Og	10.71	0.27	–	$^{293}121$	$^{289}119$	14.06	-6.68	-6.77
$^{313}120$	^{309}Og	10.5	0.86	–	$^{294}121$	$^{290}119$	14.42	-7.35	-6.87
$^{314}120$	^{310}Og	10.33	1.35	–	$^{295}121$	$^{291}119$	14.3	-7.15	-6.74
$^{315}120$	^{311}Og	10.16	1.84	–	$^{296}121$	$^{292}119$	14.3	-7.17	-6.88
$^{316}120$	^{312}Og	9.94	2.50	–	$^{297}121$	$^{293}119$	14.47	-7.49	-7.15
$^{317}120$	^{313}Og	9.82	2.87	–	$^{298}121$	$^{294}119$	14.52	-7.60	-6.81
$^{318}120$	^{314}Og	9.66	3.37	–	$^{299}121$	$^{295}119$	14.16	-6.96	-6.44
$^{319}120$	^{315}Og	13.15	-5.66	–	$^{300}121$	$^{296}119$	13.95	-6.60	-6.78
$^{320}120$	^{316}Og	13.15	-5.68	–	$^{301}121$	$^{297}119$	14.25	-7.17	-6.85
$^{321}120$	^{317}Og	13.08	-5.55	–	$^{302}121$	$^{298}119$	14.06	-6.84	-6.28

Table 4.2 continued

Parent nuclei	Daughter nuclei	Q	$\log_{10}T_{1/2}$	$log_{10}T_{1/2}^{Om}$	Parent nuclei	Daughter nuclei	Q	$\log_{10}T_{1/2}$	$log_{10}T_{1/2}^{Om}$
		MeV	$T_{1/2}$ in s	$T_{1/2}$ in s			MeV	$T_{1/2}$ in s	$T_{1/2}$ in s
$^{303}121$	$^{299}119$	14.11	-6.94	-5.96	$^{335}121$	$^{331}119$	8.22	8.93	–
$^{304}121$	$^{300}119$	14.1	-6.94	-5.93	$^{336}121$	$^{332}119$	8.11	9.38	–
$^{305}121$	$^{301}119$	14.11	-6.98	-5.93	$^{337}121$	$^{333}119$	7.94	10.11	–
$^{306}121$	$^{302}119$	14.78	-8.23	-6.95	$^{338}121$	$^{334}119$	7.81	10.68	–
$^{307}121$	$^{303}119$	14.81	-8.30	-7.88	$^{339}121$	$^{335}119$	7.6	11.65	–
$^{308}121$	$^{304}119$	13.74	-6.32	-7.41	**Z=122**				
$^{309}121$	$^{305}119$	13.06	-5.02	-5.90	$^{294}122$	$^{290}120$	14.52	-7.24	–
$^{310}121$	$^{306}119$	11.87	-2.31	-4.24	$^{295}122$	$^{291}120$	14.49	-7.20	-6.38
$^{311}121$	$^{307}119$	11.82	-2.21	-2.75	$^{296}122$	$^{292}120$	14.94	-8.02	-5.98
$^{312}121$	$^{308}119$	11.74	-2.03	–	$^{297}122$	$^{293}120$	14.93	-8.01	-6.01
$^{313}121$	$^{309}119$	11.65	-1.83	–	$^{298}122$	$^{294}120$	15.16	-8.46	-6.05
$^{314}121$	$^{310}119$	11.46	-1.36	–	$^{299}122$	$^{295}120$	14.63	-7.52	-5.74
$^{315}121$	$^{311}119$	11.27	-0.89	–	$^{300}122$	$^{296}120$	14.72	-7.70	-5.16
$^{316}121$	$^{312}119$	11.08	-0.40	–	$^{301}122$	$^{297}120$	14.47	-7.27	-5.28
$^{317}121$	$^{313}119$	10.87	0.15	–	$^{302}122$	$^{298}120$	14.77	-7.82	-5.51
$^{318}121$	$^{314}119$	10.74	0.45	–	$^{303}122$	$^{299}120$	14.57	-7.49	-5.02
$^{319}121$	$^{315}119$	10.49	1.16	–	$^{304}122$	$^{300}120$	14.58	-7.52	4.60
$^{320}121$	$^{316}119$	10.34	1.59	–	$^{305}122$	$^{301}120$	14.55	-7.48	-5.03
$^{321}121$	$^{317}119$	10.16	2.11	–	$^{306}122$	$^{302}120$	14.62	-7.62	-5.32
$^{322}121$	$^{318}119$	9.98	2.65	–	$^{307}122$	$^{303}120$	15.27	-8.80	-6.78
$^{323}121$	$^{319}119$	9.76	3.34	–	$^{308}122$	$^{304}120$	15.29	-8.85	-8.24
$^{324}121$	$^{320}119$	9.87	2.97	–	$^{309}122$	$^{305}120$	13.8	-6.21	-7.30
$^{325}121$	$^{321}119$	9.64	3.70	–	$^{310}122$	$^{306}120$	13.11	-4.82	-5.95
$^{326}121$	$^{322}119$	9.47	4.26	–	$^{311}122$	$^{307}120$	12.68	-3.93	–
$^{327}121$	$^{323}119$	9.24	5.04	–	$^{312}122$	$^{308}120$	12.74	-4.07	–
$^{328}121$	$^{324}119$	9.09	5.61	–	$^{313}122$	$^{309}120$	12.67	-3.94	–
$^{329}121$	$^{325}119$	8.8	6.68	–	$^{314}122$	$^{310}120$	12.57	-3.72	–
$^{330}121$	$^{326}119$	8.66	7.21	–	$^{315}122$	$^{311}120$	12.43	-3.39	–
$^{331}121$	$^{327}119$	6.69	16.52	–	$^{316}122$	$^{312}120$	12.19	-2.85	–
$^{332}121$	$^{328}119$	6.37	18.43	–	$^{317}122$	$^{313}120$	12.05	-2.54	–
$^{333}121$	$^{329}119$	6.91	15.24	–	$^{318}122$	$^{314}120$	11.78	-1.89	–
$^{334}121$	$^{330}119$	6.8	15.84	–	$^{319}122$	$^{315}120$	11.67	-1.64	–

Table 4.2 continued

Parent nuclei	Daughter nuclei	Q (MeV)	$\log_{10}T_{1/2}$ $T_{1/2}$ in s	$log_{10}T_{1/2}^{Om}$ $T_{1/2}$ in s	Parent nuclei	Daughter nuclei	Q (MeV)	$\log_{10}T_{1/2}$ $T_{1/2}$ in s	$log_{10}T_{1/2}^{Om}$ $T_{1/2}$ in s
$^{320}122$	$^{316}120$	11.47	-1.15	–	$^{308}123$	$^{304}121$	15.8	-9.39	-8.43
$^{321}122$	$^{317}120$	11.27	-0.64	–	$^{309}123$	$^{305}121$	15.82	-9.45	-9.23
$^{322}122$	$^{318}120$	10.88	0.35	–	$^{310}123$	$^{306}121$	14.07	-6.40	-8.00
$^{323}122$	$^{319}120$	10.47	1.52	–	$^{311}123$	$^{307}121$	13.36	-5.05	-6.44
$^{324}122$	$^{320}120$	10.35	1.86	–	$^{312}123$	$^{308}121$	13.34	-5.02	–
$^{325}122$	$^{321}120$	8.9	6.77	–	$^{313}123$	$^{309}121$	13.41	-5.18	–
$^{326}122$	$^{322}120$	10.12	2.52	–	$^{314}123$	$^{310}121$	13.32	-5.02	–
$^{327}122$	$^{323}120$	9.96	3.01	–	$^{315}123$	$^{311}121$	13.21	-4.81	–
$^{328}122$	$^{324}120$	9.77	3.61	–	$^{316}123$	$^{312}121$	13.03	-4.44	–
$^{329}122$	$^{325}120$	9.58	4.23	–	$^{317}123$	$^{313}121$	12.81	-3.99	–
$^{330}122$	$^{326}120$	9.33	5.07	–	$^{318}123$	$^{314}121$	12.61	-3.52	–
$^{331}122$	$^{327}120$	8.82	6.98	–	$^{319}123$	$^{315}121$	12.38	-3.01	–
$^{332}122$	$^{328}120$	7.25	13.91	–	$^{320}123$	$^{316}121$	12.27	-2.77	–
$^{333}122$	$^{329}120$	7.18	14.26	–	$^{321}123$	$^{317}121$	12.06	-2.29	–
$^{334}122$	$^{330}120$	7.07	14.83	–	$^{322}123$	$^{318}121$	11.86	-1.82	–
$^{335}122$	$^{331}120$	8.85	6.80	–	$^{323}123$	$^{319}121$	11.47	-0.85	–
$^{336}122$	$^{332}120$	8.73	7.26	–	$^{324}123$	$^{320}121$	10.99	0.37	–
$^{337}122$	$^{333}120$	8.62	7.67	–	$^{325}123$	$^{321}121$	10.75	1.03	–
$^{338}122$	$^{334}120$	8.44	8.38	–	$^{326}123$	$^{322}121$	10.46	1.86	–
$^{339}122$	$^{335}120$	8.31	8.91	–	$^{327}123$	$^{323}121$	10.39	2.05	–
Z=123					$^{328}123$	$^{324}121$	10.26	2.43	–
$^{297}123$	$^{293}121$	15.16	-8.12	–	$^{329}123$	$^{325}121$	10.12	2.85	–
$^{298}123$	$^{294}121$	14.9	-7.69	–	$^{330}123$	$^{326}121$	9.87	3.63	–
$^{299}123$	$^{295}121$	14.99	-7.87	–	$^{331}123$	$^{327}121$	9.44	5.10	–
$^{300}123$	$^{296}121$	14.98	-7.87	-7.74	$^{332}123$	$^{328}121$	9.32	5.51	–
$^{301}123$	$^{297}121$	15	-7.92	-7.35	$^{333}123$	$^{329}121$	9.61	4.45	–
$^{302}123$	$^{298}121$	14.85	-7.68	-7.57	$^{334}123$	$^{330}121$	7.84	11.49	–
$^{303}123$	$^{299}121$	15.05	-8.04	-7.75	$^{335}123$	$^{331}121$	9.41	5.15	–
$^{304}123$	$^{300}121$	15.11	-8.16	-7.46	$^{336}123$	$^{332}121$	9.28	5.60	–
$^{305}123$	$^{301}121$	15.13	-8.21	-7.31	$^{337}123$	$^{333}121$	9.11	6.20	–
$^{306}123$	$^{302}121$	15.17	-8.34	-7.41	$^{338}123$	$^{334}121$	9	6.60	–
$^{307}123$	$^{303}121$	15.18	-8.37	-7.47	$^{339}123$	$^{335}121$	8.84	7.19	–

Table 4.2 continued

Parent nuclei	Daughter nuclei	Q MeV	$\log_{10}T_{1/2}$ $T_{1/2}$ in s	$log_{10}T_{1/2}^{Om}$ $T_{1/2}$ in s	Parent nuclei	Daughter nuclei	Q MeV	$\log_{10}T_{1/2}$ $T_{1/2}$ in s	$log_{10}T_{1/2}^{Om}$ $T_{1/2}$ in s
Z=124									
^{300}124	^{296}122	14.99	-7.60	–	^{331}124	^{327}122	9.73	4.45	–
^{301}124	^{297}122	14.87	-7.41	-8.00	^{332}124	^{328}122	9.58	4.99	–
^{302}124	^{298}122	14.48	-6.73	-7.75	^{333}124	^{329}122	9.64	4.72	–
^{303}124	^{299}122	15.00	-7.67	-7.95	^{334}124	^{330}122	9.56	5.03	–
^{304}124	^{300}122	15.56	-8.68	-8.23	^{335}124	^{331}122	8.61	8.57	–
^{305}124	^{301}122	15.61	-8.77	-8.10	^{336}124	^{332}122	9.81	4.11	–
^{306}124	^{302}122	15.61	-8.79	-8.04	^{337}124	^{333}122	11.19	-0.03	–
^{307}124	^{303}122	15.67	-8.91	-8.04	^{338}124	^{334}122	9.51	5.14	–
^{308}124	^{304}122	15.72	-8.99	-8.05	^{339}124	^{335}122	9.4	5.52	–
^{309}124	^{305}122	15.21	-8.13	-8.95	**Z=125**				
^{310}124	^{306}122	15.15	-8.05	-9.30	^{303}125	^{299}123	14.74	-6.93	–
^{311}124	^{307}122	14.1	-6.21	-8.08	^{304}125	^{300}123	14.77	-7.01	–
^{312}124	^{308}122	13.38	-4.81	-6.54	^{305}125	^{301}123	14.67	-6.84	–
^{313}124	^{309}122	10.23	3.14	–	^{306}125	^{302}123	15.05	-7.53	–
^{314}124	^{310}122	10.25	3.05	–	^{307}125	^{303}123	15.12	-7.67	–
^{315}124	^{311}122	10.25	3.04	–	^{308}125	^{304}123	16.31	-9.66	–
^{316}124	^{312}122	13.7	-5.52	–	^{309}125	^{305}123	16.35	-9.73	–
^{317}124	^{313}122	13.52	-5.17	–	^{310}125	^{306}123	11.35	0.31	-9.69
^{318}124	^{314}122	13.34	-4.82	–	^{311}125	^{307}123	10.91	1.52	-9.62
^{319}124	^{315}122	13.09	-4.31	–	^{312}125	^{308}123	9.86	4.76	-8.45
^{320}124	^{316}122	12.9	-3.92	–	^{313}125	^{309}123	9.24	6.92	-7.12
^{321}124	^{317}122	7.29	14.82	–	^{314}125	^{310}123	9.8	4.93	-6.59
^{322}124	^{318}122	12.4	-2.79	–	^{315}125	^{311}123	9.82	4.84	-6.20
^{323}124	^{319}122	11.89	-1.59	–	^{316}125	^{312}123	9.79	4.93	-6.10
^{324}124	^{320}122	11.55	-0.74	–	^{317}125	^{313}123	9.8	4.88	-6.00
^{325}124	^{321}122	11.09	0.42	–	^{318}125	^{314}123	9.89	4.51	-5.30
^{326}124	^{322}122	9.5	5.36	–	^{319}125	^{315}123	13.7	-5.26	-4.34
^{327}124	^{323}122	9.58	5.07	–	^{320}125	^{316}123	13.54	-4.95	-3.48
^{328}124	^{324}122	9.56	5.12	–	^{321}125	^{317}123	7.45	14.45	–
^{329}124	^{325}122	11.05	0.47	–	^{322}125	^{318}123	7.14	16.07	–
^{330}124	^{326}122	9.74	4.44	–	^{323}125	^{319}123	12.67	-3.10	–

Table 4.2 continued

Parent nuclei	Daughter nuclei	Q MeV	$\log_{10}T_{1/2}$ $T_{1/2}$ in s	$log_{10}T_{1/2}^{Om}$ $T_{1/2}$ in s	Parent nuclei	Daughter nuclei	Q MeV	$\log_{10}T_{1/2}$ $T_{1/2}$ in s	$log_{10}T_{1/2}^{Om}$ $T_{1/2}$ in s
^{324}125	^{320}123	12.1	-1.78	–	^{332}125	^{328}123	10.08	3.67	–
^{325}125	^{321}123	11.73	-0.88	–	^{333}125	^{329}123	10.11	3.55	–
^{326}125	^{322}123	11.3	0.18	–	^{334}125	^{330}123	10.11	3.54	–
^{327}125	^{323}123	11.3	0.17	–	^{335}125	^{331}123	10.38	2.68	–
^{328}125	^{324}123	9.8	4.65	–	^{336}125	^{332}123	10.22	3.16	–
^{329}125	^{325}123	9.94	4.17	–	^{337}125	^{333}123	9.84	4.37	–
^{330}125	^{326}123	10.08	3.70	–	^{338}125	^{334}123	10.05	3.67	–
^{331}125	^{327}123	10.17	3.39	–	^{339}125	^{335}123	12.2	-2.25	–

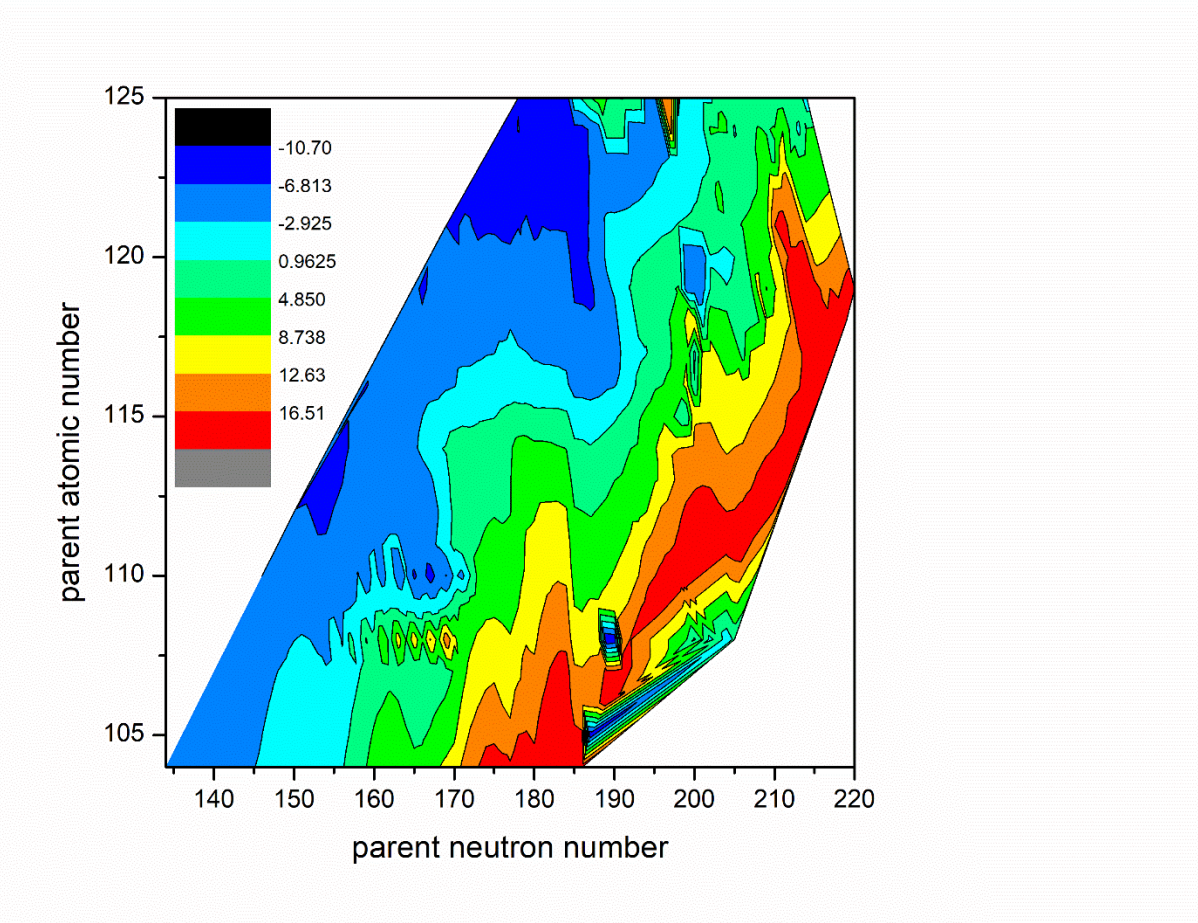

Fig.4.34 Contour representation of $log_{10}T_{1/2}$experimentally synthesized superheavy nuclei with the atomic number ranges from 104 ≤ Z ≤ 125 with the mass number ranges from 238 ≤ A ≤ 331.

CHAPTER V

SUMMARY AND CONCLUSION

Alpha particles have a significant role in the development of atomic structure as well as the development of the field nuclear physics. Present study aimed at finding the half-lives of alpha decay of heavy and superheavy nuclei. Preformation probability (P_0) means the probability of formation of an alpha particle inside the mother nucleus. While doing so, it's value reveals the structure of the mother/daughter nucleus through magic number, which is confirmed through the present study. P_0 values are high at neutron number N=152, 162 and 184. Half-lives calculated matches with experimental half-lives in heavy nuclei. The half-lives of heavy nuclei of 106 cases ranges from 9.13×10^{-8} s to 2.20×10^{19}s. In case of superheavy nuclei, the predicted half-lives for isotopes of Z = 104 to 125, they are compared with other works. For nearly 1140 cases of superheavy nuclei, contour representation of half-lives is given. The half-lives of superheavy nuclei with $104 \leq Z \leq 125$ varies from 2.08×10^{-11} s to 2.18×10^{20}s.

REFERENCES

[1] D.C. Tayal, Nuclear Physics, 68, Himalaya publishing house, (1997).

[2] S.N.Ghosal, Nuclear Physics,39-44, 59, S.Chand & Company Ltd, eighteenth edition(2008).

[3] S.B. Patel, Nuclear Physics An Introduction, 59, New age international publications, First edition (1991).

[4]https://thefactfactor.com/facts/pure_science/chemistry/modern-chemistry/nuclear-stability/15030/

[5] R.Murugesan and Sivaprasath Kiruthika, Modern Physics, 327, S.Chand & Company Ltd ,eighteenth edition, (2017).

[6] https://www.vedantu.com/question-answer/factors-determine-nuclear-stability-class-11-chemistry-cbse-608ac8fff4e14b3491af5330.

[7] https://www.vedantu.com/physics/magic-number.

[8] Glenn F. Knoll, Radiation Detection and Measurement, 2, John Wiley & Sons, Inc,3rd edition (2013).

[9] https://www.brainkart.com/article/Artificial-radioactivity_2961/

[10] Keneth S Crane, Introductory to Nuclear Physics, 160, John Wiley & Sons, (1987).

[11] Shatendra Sharma, Atomic and Nuclear Physics, 160, Pearson education, (2008).

[12] https://winnerscience.com/10-properties-alpha-particles/

[13] Nanda Karmaker, Kazi M. Maraz, Farhana Islam, Md. Marjanul Haque, Md. Razzak, M.Z.I. Mollah, M. R. I. Faruque and Ruhul A. Khan, GSC Advanced Research and Reviews, **07 (01)** , 064–072, (2021).

[14] Morlat T, Fernandes AC, Felizardo M, Kling A, Girard TA, Marques JG, Carvalho FP. **180 (1-4)**, 230-234, (2018).

[15] Perrett GM, Maxwell JA, Campbell JL. **46(3)**, 171-179, (2017).

[16] Guerra Liberal FD, O'Sullivan JM, McMahon SJ, Prise KM, **35(6)**, 404-417, (2020).

[17] Song Luo, Yang-Yang Xu, De-Xing Zhu, Biao He, Peng-Cheng Chu,a, Xiao-Hua Li, Eur. Phys. J. A. **58**, 244, (2022).

[18] L. Vasanthi and N. S. Rajeswari, Int. J. Mod. Phys E. **30**, 8 (2021)

[19] Akhilesh Yadav, A.Shykla and V.Kumar, Pramana – J. Phys. **97**,48, (2023).

[20] D D.N.Poenaru, H.Stocker, and R.A.Gherghescu, Romanian Reports in Physics **75**, 201 (2023).

[21] V. Zanganeh, S.S. Hosseini and A.M. Izadpanah, Nucl. Phys. A,122561, (2023).

[22] Chen-Qi Li, Chao-Nan Tong, Hong-Jing Du, and Long-Gang Pang, Phys. Rev. C. **105**, 064306 (2022).

[23] Mayan Ibraheem Khalil and Firas Mohamed Ali, Egypt. J. Phy. **50**, pp. 99 -108 (2022).

[24] Song Luo, Yang-Yang Xu, De-Xing Zhu, Biao He, Peng-Cheng Chu, Xiao-Hua L, Eur. Phys. J. A **58**, 244, (2022).

[25] N. S. Rajeswari and L. Vasanthi, Int. J. Mod. Phys E. **30**, 8, 2150071, (2021).

[26] F. Koyuncu, Nucl. Phys. A **1012**,122211, (2021).

[27] Jun-Gang Deng and Hong-Fei Zhang, Phys. Lett. B **816**, 136247, (2021).

[28] W. A. Surdoval and D. A. Berry, "A New Approach for Calculating the Alpha-Decay Half-Life for the Heavy and Super-heavy Elements and an Exact A Priori Result for Beryllium-8".

[29] Omar Nagib, Phys. Rev. C **101**, 014610 (2020).

[30] Jun-Gang Deng, Hong-Fei Zhang and G. Royer, Phys. Rev. C **101**, 034307 (2020).

[31] O. N. Ghodsi and M. Hassanzad, Phys. Rev. C 101, 034606 (2020).

[32] Hong-Ming Liu, You-Tian Zou, Xiao Pan, Xiao-Jun Bao, Xiao-Hua Li, Chin. Phys. C **44**, No. 9 ,094106, (2020).

[33] Aladdin Abdul-latif and Omar Nagib, Phys. Rev. C **100**, 024601, (2019).

[34] Dashty T. Akrawy and Ali H. Ahmed, Phys. Rev. C **100**, 044618, (2019).

[35] Sivasankaran B.R., Christas Mony A., Aarthi K.V., Larny Mary Jayan, Nucl. Phys. A **989,** 246–256, (2019).

[36] D. N. Poenaru and R. A. Gherghescu, Phys. Rev. C 97, 044621 (2018).

[37] K.P. Santhosh and C. Nithya, At. Data Nucl. Data Tables, 121-122, 216-255 (2017).

[38] S. S. Hosseini and H. Hassanabadi, Chin. Phys. C, Vol. 41, No. 6, 064101 (2017).

[39] S. S. Hosseini, H. Hassanabadi and S. Zarrinkamar, Int. J. Mod. Phys. E, Vol. 26, 1750024 (2017).

[40] D. T. Akrawy and D. N. Poenaru, J. Phys. G: Nucl. Part. Phys, **44**, 105105 (2017).

[41] C. Nithya and K. P. Santhosh, IOSR J. Appl. Phys. (IOSR-JAP), e-ISSN: 2278-4861, 92-97, (2017).

[42] Shan Zhang, Yanli Zhang, Jianpo Cui and Yanzhao Wang, Phys. Rev. C **95**, 014311 (2017).

[43] M. Ismail, A. M. Abdul Magead and Samar Gamal, IOSR J. Appl. Phys. (IOSR-JAP) e-ISSN: 2278 - 4861. **9**, (2017).

[44] H.C. Manjunatha and K.N. Sridhar, Eur. Phys. J. A **53**, 7, 156 (2017).

[45] B. Gillis Carlssona, Daniel E. Ward and Sven Aberg, EPJ. Web. Conf. **131**, 08002 (2016).

[46] K. P. Santhosh and C. Nithya, Phys. Rev. C **94**, 054621 (2016).

[47] Xiao-Dong Sun, Ping Guo, and Xiao-Hua Li, Phys. Rev. C **93**, 034316 (2016).

[48] X J Bao, S Q Guo, H F Zhang, Y Z Xing, J M Dong and J Q Li, J. Phys. G: Nucl. Part. Phys. **42**, 085101, (2015).

[49] Y. Z. Wang, S. J. Wang, Z. Y. Hou and J. Z. Gu, Phys. Rev. C **92**, 064301 (2015).

[50] Yibin Qian and Zhongzhou Ren, Phys. Rev. C **90**, 064308 (2014).

[51] N. S. Rajeswari and M. Balasubramaniam, J. Phys. G: Nucl. Part. Phys. **40** ,035104 (2013).

[52] Ren Yuejiao and Ren Zhongzhou, Nuclear Science and Techniques **24**, 050518 (2013).

[53] Yuejiao Ren and Zhongzhou Ren, Phys. Rev. C **85**, 044608 (2012).

[54] D. N. Poenaru, R. A. Gherghescu and W. Greiner, Phys. Rev. C **83**, 014601 (2011).

[55] Yibin Qian, Zhongzhou Ren and Dongdong Ni, Phys. Rev. C **83**, 044317 (2011).

[56] G. Royer and H.F. Zhang, Phys. Rev. C **77**, 037602 (2008).

[57] Zhongzhou Ren and Chang Xu, IOP Publishing, J. Phys, Conf Series **111**, 012040 (2008).

[58] D. N. Poenaru, R. A. Gherghescu, I. H. plonski and W. Greiner, Int. J. Mod. Phys. E, **16,**. 4, 995-1007 (2007).

[59] H. F. Zhang, G. Royer, Y. J. Wang, J. M. Dong, W. Zuo, and J. Q. L, Phys. Rev. C **80**, 057301 (2009).

[60] G. Royer and H.F. Zhang, Phys. Rev. C **77**, 037602 (2008)

[61] Zhongzhou Ren, Phys. Rev. C, **65**, 051304 (2002).

[62] D. N. Poenaru and M. Ivascu, J. Phys. **44 (7),** 791-796, (1983).

[63] D. N. Poenaru, R. A. Gherghescu, I. H. plonski and W. Greiner, Int. J. Mod. Phys. E, **16**, 4, 995-1007 (2007).

[64] Chang Xu and Zhongzhou Ren, Phys. Rev. C **75**, 044301 (2007)

[65] Chang Xu and Zhongzhou Ren, Phys. Rev. C **76**, 027303 (2007).

[66] Chang Xu and Zhongzhou Ren, Phys. Rev. C **78**, 057302 (2008).

[67] Chang Xu and Zhongzhou Ren, Phys. Rev. C **73**, 041301(R) (2006).

[68] Chang Xu and Zhongzhou Ren, Phys. Rev. C **74**, 014304 (2006).

[69] Chang Xu and Zhongzhou Ren, Phys. Rev. C **74**, 037302 (2006)

[70] M. M. Sharma and A. R. Farhan, Phys. Rev. C **71**, 054310 (2005)

[71] V. Yu. Denisov and H. Ikezoe, Phys. Rev. C **72**, 064613 (2005).

[72] Chang Xu, Zhongzhou Ren, Nucl. Phys. A **760,** 303–316, (2005).

[73] Y. K. Gambhir, A. Bhagwat,and M. Gupta, Phys. Rev. C **71** , 037301 (2005)

[74] D. S. Delion, A. Sandulescu, W. Greiner, Phys. Rev. C **69**, 044318 (2004).

[75] Zhongzhou Ren, Phys. Rev. C, **65**, 051304 (2002).

[76] G Royer, J. Phys. G: Nucl. Part. Phys. **26**, 1149–1170, (2000).

[77] D. N. Poenaru and M. Ivascu, J. Physique **44** 791-796, (1983).

[78] D N Poenaru, M Ivaycuj and A SSndulescu, J. Phys. G: Nucl. Phys., **5**, 10, (1979).

[79] D. N. Poenaru and M. Ivascu, J. Phys. **44 (7),** 791-796, (1983).

[80] S. Wuenschel, K. Hagel, M. Barbui, J. Gauthier, X. G. Cao, R. Wada, E. J. Kim, Z. Majka, R. Planeta, Z. Sosin, A. Wieloch, K. Zelga, S. Kowalski, K. Schmidt, C. Ma, G. Zhang and J.B. Natowitzl, Phys. Rev. C **97**, 064602 (2018).

[81] Vladimir Utyonkov, Yuri Oganessian, Sergey Dmitriev, Mikhail Itkiz, Kenton Moody, Mark Stoyer, Dawn Shaughnessy, James Roberto, Krzysztof Rykaczewski and Joseph Hamilton, EPJ Web Conf. **131**, 06003 (2016).

[82] J. M. Gates, Ch. E. Dullmann, M. Schadel, A. Yakushev, A. Turler, K. Eberhardt, J. V. Kratz, D. Ackermann, L.L. Andersson, M. Block, W. Bruchle, J. Dvorak, H. G. Essel, P. A. Ellison, J. Even, U. Forsberg, J. Gellanki, A. Gorshkov, R. Graeger, K. E. Gregorich, W. Hartmann, R.-D. Herzberg, F. P. Heßberger, D. Hild, A. Hubner, E. Jager, J. Khuyagbaatar, B. Kindler, J. Krier, N. Kurz, S. Lahiri, D. Liebe, B. Lommel, M. Maiti, H. Nitsche, J. P. Omtvedt, E. Parr, D. Rudolph, J. Runke, H. Schaffner, B. 76 Schausten, E. Schimpf, A. Semchenkov, J. Steiner, P. Thorle-Pospiech, J. Uusitalo, M. Wegrzecki and N. Wiehl, Phys. Rev. C **83**, 054618 (2011)

[83] Yu. Ts. Oganessian, F. Sh. Abdullin, C. Alexander, J. Binder, R. A. Boll, S. N. Dmitriev, J. Ezold, K. Felker, J. M. Gostic, R. K. Grzywacz, J. H. Hamilton, R. A. Henderson, M. G. Itkis, K. Miernik, D. Miller, K. J. Moody, A. N. Polyakov, A. V. Ramayya, J. B. Roberto, M. A. Ryabinin, K. P. Rykaczewski, R. N. Sagaidak, D. A. Shaughnessy, I. V. Shirokovsky, M. V. Shumeiko, M. A. Stoyer, N. J. Stoyer, V. G. Subbotin, A. M. Sukhov, Yu. S. Tsyganov, V. K. Utyonkov, A. A. Voinov, and G. K. Vostokin, Phys. Rev. C **87**, 054621 (2013).

[84] Yu.Ts. Oganessian, F.Sh. Abdullin, C. Alexander, J. Binder, R.A. Boll, S.N. Dmitriev, J. Ezold, K. Felker, J.M. Gostic, R.K. Grzywacz, J.H. Hamilton, R.A. Henderson, M.G. Itkis, K. Miernik, D. Miller, K.J. Moody, A.N. Polyakov, A.V. Ramayya, J.B. Roberto, M.A. Ryabinin, K.P. Rykaczewski, R.N. Sagaidak, D.A. Shaughnessy, I.V. Shirokovsky, M.V. Shumeiko, M.A. Stoyer, N.J. Stoyer, V.G. Subbotin, A.M. Sukhov, Yu.S. Tsyganov, V.K. Utyonkov, A.A. Voinov, and G.K. Vostokin, Phys. Rev. Lett. **109**, 162501 (2012)

[85] Yu. Ts. Oganessian, F. Sh. Abdullin, P. D. Bailey, D. E. Benker, M. E. Bennett, S. N. Dmitriev, J. G. Ezold, J. H. Hamilton, R. A. Henderson, M. G. Itkis, Yu. V. Lobanov, A. N. Mezentsev, K. J. Moody, S. L. Nelson, A. N. Polyakov, C. E. Porter, A. V. Ramayya, F. D. Riley, J. B. Roberto, M. A. Ryabinin, K. P. Rykaczewski, R. N. Sagaidak, D. A. Shaughnessy,

I. V. Shirokovsky, M. A. Stoyer, V. G. Subbotin, R. Sudowe, A. M. Sukhov, R. Taylor, Yu. S. Tsyganov, V. K. Utyonkov, A. A. Voinov, G. K. Vostokin and P. A. Wilk, Phys. Rev. C **83**, 054315 (2011).

[86] J. M. Gates, Ch. E. Dullmann, M. Schadel, A. Yakushev, A. Turler, K. Eberhardt, J. V. Kratz, D. Ackermann, L.L. Andersson, M. Block, W. Bruchle, J. Dvorak, H. G. Essel, P. A. Ellison, J. Even, U. Forsberg, J. Gellanki, A. Gorshkov, R. Graeger, K. E. Gregorich, W. Hartmann, R.-D. Herzberg, F. P. Heßberger, D. Hild, A. Hubner, E. Jager, J. Khuyagbaatar, B. Kindler, J. Krier, N. Kurz, S. Lahiri, D. Liebe, B. Lommel, M. Maiti, H. Nitsche, J. P. Omtvedt, E. Parr, D. Rudolph, J. Runke, H. Schaffner, B. 76 Schausten, E. Schimpf, A. Semchenkov, J. Steiner, P. Thorle-Pospiech, J. Uusitalo, M. Wegrzecki and N. Wiehl, Phys. Rev. C 83, 054618 (2011).

[87] P. A. Ellison, K. E. Gregorich, J. S. Berryman, D. L. Bleuel, R. M. Clark, I. Dragojevic, J. Dvorak, P. Fallon,2 C. Fineman-Sotomayor, J. M. Gates, O. R. Gothe, I. Y. Lee, W. D. Loveland, J. P. McLaughlin, S. Paschalis, M. Petri, J. Qian, L. Stavsetra, M. Wiedeking, and H. Nitsche,. Rev. Lett. **105**, 182701 (2010).

[88] Yu. Ts. Oganessian, F. Sh. Abdullin, P. D. Bailey, D. E. Benker, M. E. Bennett, S. N. Dmitriev, J. G. Ezold, J. H. Hamilton, R. A. Henderson, M. G. Itkis, Yu. V. Lobanov, A. N. Mezentsev, K. J. Moody, S. L. Nelson, A. N. Polyakov, C. E. Porter, A. V. Ramayya, F. D. Riley, J. B. Roberto, M. A. Ryabinin, K. P. Rykaczewski, R. N. Sagaidak, D. A. Shaughnessy, I. V. Shirokovsky, M. A. Stoyer, V. G. Subbotin, R. Sudowe, A. M. Sukhov, Yu. S. Tsyganov, V. K. Utyonkov, A. A. Voinov, G. K. Vostokin and P. A. Wilk, Phys. Rev. Lett. **104**, 142502 (2010).

[89] H. F. Zhang, G. Royer, Y. J. Wang, J. M. Dong, W. Zuo and J. Q. Li Phys. Rev. C 80, 037307 (2009).

[90] L. Stavsetra, K. E. Gregorich, J. Dvorak, P. A. Ellison, I. Dragojevic, M. A. Garcia and H. Nitsche, Phys. Rev. Lett. **103**, 132502 (2009).

[91] Yu. Ts. Oganessian, V. K. Utyonkov, Yu. V. Lobanov, F. Sh. Abdullin, A. N. Polyakov, R. N. Sagaidak, I. V. Shirokovsky, Yu. S. Tsyganov, A. A. Voinov, G. G. Gulbekian, S. L. Bogomolov, B. N. Gikal, A. N. Mezentsev, V. G. Subbotin, A. M. Sukhov, K. Subotic, V. I. Zagrebaev, G. K. Vostokin, and M. G. Itkis, Phys. Rev. C **76**, 011601(R) (2007).

[92] Yuri Oganessian, Pure Appl Chem. **78**, 5, 889-904 (2006).

[93] P. Roy Chowdhury, C. Samanta and D. N. Basu, Phys. Rev. C **73**, 014612 (2006).

[94] Yu. Ts. Oganessian, V. K. Utyonkoy, Yu. V. Lobanov, F. Sh. Abdullin, A. N. Polyakov, I. V. Shirokovsky, Yu. S. Tsyganov, G. G. Gulbekian, S. L. Bogomolov, A. N. Mezentsev, S. Iliev, V. G. Subbotin, A. M. Sukhov, A. A. Voinov, G. V. Buklanov, K. Subotic, V. I. Zagrebaev, and M. G. Itkis, Phys. Rev. C **69**, 021601(R) (2004).

[95] V. Barci, G. Ardisson, G. Barci-Funel, B. Weiss, O. El Samad and R.K. Sheline, Phys. Rev. C **68**, 034329 (2003).

[96] Yu. Ts. Oganessian, V.K. Utyonkov and K.J. Moody, Phys. At. Nucl, **64**, 1349- 1355 (2001).

[97] S. Hofmann and G. Munzenberg, Rev. Mod. Phys **72**, 3 (2000).

[98] Yu. Ts. Oganessian, V. K. Utyonkov, Yu. V. Lobanov, F. Sh. Abdullin, A. N. Polyakov, I. V. Shirokovsky, Yu. S. Tsyganov, G. G. Gulbekian, S. L. Bogomolov, B. N. Gikal, A. N. Mezentsev, S. Iliev, V. G. Subbotin, A. M. Sukhov, G. V. Buklanov, K. Subotic, and M. G. Itkis, Phys. Rev. Lett, **83**, 16 (1999).

[99] Yu. A. Lazarev, Yu. V. Lobanov, Yu. Ts. Oganessian, Yu. S. Tsyganov, V. K. Utyonkov, F. Sh. Abdullin, S. Iliev, A. N. Polyakov, J. Rigol, I.V. Shirokovsky, V. G. Subbotin, A. M. Sukhov, G. V. Buklanov, B.N. Gikal, V.B. Kutner, A. N. Mezentsev, I.M. Sedykh, and D. V. Vakatov, Phys. Rev. Lett, **75**, 10 (1995).

[100] D. N. Poenaru and W. Greiner, Phys. Scr **44**, 427 (1991).

[101] G. Shanmugam and B. Kamalaharan, Phys. Rev. C **4**, 41, (1990).

[102] N. S. Rajeswari and L.Vasanthi of Int. J. Mod. Phys.E **30**, 8 (2021)

[103] H. J. Krappe, J. R. Nix and A. Sierk, J. Phys. Rev. Lett. **42** (1979); Phys. Rev. C **20,** 992 (1979).

[104] V. Zanganeh, S.S. Hosseini and A.M. Izadpanah, Nucl. Phys. A **1029**, 122561 (2023).

[105] 29. A. Abdul-latif and O. Nagib, Phys. Rev. C **100,** 024601 (2019).

[106] O. Nagib, Phys. Rev. C **101**, (2020).